JOURNAL OF COMPUTATIONAL AND APPLIED MECHANICS

A Publication of the University of Miskolc

VOLUME 2, NUMBER 2 (2001)



MISKOLC UNIVERSITY PRESS

JOURNAL OF COMPUTATIONAL AND APPLIED MECHANICS

A Publication of the University of Miskolc

VOLUME 2, NUMBER 2 (2001)



MISKOLC UNIVERSITY PRESS

EDITORIAL BOARD

- Mechanics, University of Miskolc, 3515 MISKOLC, Hungary, mechpacz@gold.uni-miskolc.hu
- László BARANYI, Department of Fluid and Heat Engineering, University of Miskolc, 3515 MISKOLC, Hungary, arambl@gold.uni-miskolc.hu
- Edgár BERTÓTI, Department of Mechanics, University of Miskolc, 3515 MISKOLC, Hungary, mechber@gold.uni-miskolc.hu
- Tibor CZIBERE, Department of Fluid and Heat Engineering, University of Miskolc, 3515 MISKOLC, Hungary, aramct@gold.uni-miskolc.hu
- Wolfram FRANK, Institut für Fluid- und Thermodynamik, Universität Siegen, Paul-Bonatz-Strasse 9-11, 57076 SIEGEN, Germany, frank@ift.mb.uni-siegen.de
- Ulrich GABBERT, Institut für Mechanik, Otto-von-Guericke-Universität Magdeburg, Universitätsplatz 2, 39106 MAGDEBURG, Germany, ulrich.gabbert@mb.uni-magdeburg.de
- Zsolt GÁSPÁR, Department of Structural Mechanics, Budapest University of Technology and Economics, Műegyetem rkp. 3, 1111 BUDAPEST, Hungary, gaspar@ep-mech.me.bme.hu
- Robert HABER, Department of Theoretical and Applied Mechanics, University of Illinois at Urbana-Champaign, 216 Talbot Lab., 104 S. Wright Str., URBANA, IL 61801, USA, r-haber@uiuc.edu
- Gábor HALÁSZ, Department of Hydraulic Machines, Budapest University of Technology and Economics, Műegyetem rkp. 3, 1111 BUDAPEST, Hungary, HALASZ@vizgep.bme.hu
- Károly JÁRMAI, Department of Materials Handling and Logistics, University of Miskolc, 3515 MISKOLC, Hungary, altjar@gold.uni-miskolc.hu
- László KOLLÁR, Department of Strength of Materials and Structures, Budapest University of Technology and Economics, Műegyetem rkpt. K.II.42., 1521 BUDAPEST, Hungary, lkollar@goliat.eik.bme.hu
- Vladimir KOMPIŠ, Department of Mechanics, Faculty of Mechanical Engineering, University of Žilina, ŽILINA, Slovakia, kompis@fstroj.utc.sk

- István PÁCZELT, Editor in Chief, Department of Imre KOZÁK, Department of Mechanics, University of Miskolc, 3515 MISKOLC, Hungary, mechkoz@gold.uni-miskolc.hu
 - Márta KURUTZ, Department of Structural Mechanics, Budapest University of Technology and Economics, Műegyetem rkp. 3, 1111 BUDAPEST, Hungary, kurutzm@eik.bme.hu
 - R. Ivan LEWIS, Room 2-16 Bruce Building, Newcastle University, NEWCASTLE UPON TYNE, NE1 7RU, UK, R.I.Lewis@NCL.AC.UK
 - Gennadij LVOV, Department of Mechanics, Kharkov Polytechnical Institute, 2 Frunze Str., 310002 KHARKOV, Ukraine, Ivovgi@kpi.kharkov.ua
 - Herbert MANG, Institute for Strength of Materials, University of Technology, Karlsplatz 13, 1040 VI-ENNA, Austria, Herbert.Mang@tuwien.ac.at
 - Zenon MROZ, Polish Academy of Sciences, Institute of Fundamental Technological Research, Swietokrzyska 21, WARSAW, Poland zmroz@ippt.gov.pl
 - Tibor NAGY, Department of Physics, University of Miskolc, 3515 MISKOLC, Hungary, fiznagyt@uni-miskolc.hu
 - Gyula PATKÓ, Department of Machine Tools, University of Miskolc, 3515 MISKOLC, Hungary, mechpgy@uni-miskolc.hu
 - Jan SLADEK, Ústav stavbeníctva a architektúry, Slovenskej akadémie vied, Dubróvska cesta 9, 842 20 BRATISLAVA, Slovakia, usarslad@savba.sk
 - Gábor STÉPÁN, Department of Mechanics, Budapest University of Technology and Economics, Műegyetem rkp. 3, 1111 BUDAPEST, Hungary, stepan@mm.bme.hu
 - Barna SZABO, Center for Computational Mechanics, Washington University, Campus Box 1129, St. LOUIS, MO63130, USA, szabo@ccm.wustl.edu
 - Szilárd SZABÓ, Department of Fluid and Heat Engineering, University of Miskolc, 3515 MISKOLC, Hungary, aram2xsz@uni-miskolc.hu
 - György SZEIDL, Department of Mechanics, University of Miskolc, 3515 MISKOLC, Hungary, Gyorgy.SZEIDL@uni-miskolc.hu

LOCAL EDITORIAL COUNCIL T. CZIBERE, I. KOZÁK, I. PÁCZELT, G. PATKÓ, G. SZEIDL

SUPPRESSION OF KÁRMÁN VORTEX EXCITATION OF A CIRCULAR CYLINDER BY A SECOND CYLINDER SET DOWNSTREAM IN CRUCIFORM ARRANGEMENT

HEON MEEN BAE

National Fisheries Research and Development Institute 408-1 Shirang-Ri, Kijiang-Up, Kijiang-Kun, Pusan, 619-900 Korea

László Baranyi

Department of Fluid and Heat Engineering, University of Miskolc H-3515 Miskolc-Egyetemváros, Hungary

arambl@gold.uni-miskolc.hu

MIZUYASU KOIDE

Department of Mechanical Engineering, Nagaoka University of Technology Kamitomioka, Nagaoka, 940-2188 Japan

orange@stn.nagaokaut.ac.jp

TSUTOMU TAKAHASHI AND MASATAKA SHIRAKASHI
Department of Mechanical Engineering, Nagaoka University of Technology
Kamitomioka, Nagaoka, 940-2188 Japan
ttaka@mech.nagaokaut.ac.jp,kashi@mech.nagaokaut.ac.jp

[Received: July 26, 2001]

Abstract. A new technique for suppressing the Kármán vortex excitation of an elastically supported circular cylinder placed in an otherwise uniform flow is presented in this paper. By placing another cylinder downstream of it in a cruciform arrangement with a gap s between the two cylinders, the oscillation of the upstream cylinder can be virtually eliminated in the range of $\frac{s}{d_1} < 0.4$, where d_1 is the diameter of the upstream cylinder. Compared with conventional techniques, this offers the following advantages: i) it is unnecessary to change the shape of the oscillating body or remodel its supporting structure, and ii) the flow approaching the upstream body is practically undisturbed.

Keywords: Kármán vortex excitation, longitudinal vortex, circular cylinder, cruciform arrangement.

1. Introduction

When a cylindrical bluff body is exposed to a flow, vortices are shed from both sides of the body into the wake. This vortex shedding gives rise to a periodic lift force acting on the body. When the frequency of vortex shedding coincides with the natural frequency of the body, large amplitude oscillation or resonance can occur, Bearman [4]. This phenomenon is known as Kármán vortex excitation. This type of oscillation can be observed in many engineering practices, e.g., structures placed in the flow of air or a liquid, or flow around the tubes of heat exchangers and other

equipment. Due to its practical importance, much effort has been devoted to clarifying the mechanism of vortex excitation. This is of primary importance if one wishes to predict this phenomenon and to develop methods for suppressing or controlling the exciting forces, Sarpkaya [7], Parkinson & Wawzonek [6], Blevins [5].

Application of available techniques for reducing the amplitude of oscillation is limited since they require modifications of the oscillating body or that of its supporting structure. Hence there is a strong demand for a technique for controlling the Kármán vortex excitation without the need for changing the body or its supporting structure.

Inspired by the work of Tomita et al. [11,12] on the acoustic effect of a downstream cylinder, the present authors have found that the Kármán vortex excitation can be suppressed by a cylinder set downstream in cruciform arrangement, Shirakashi et al. [9], Bae et al. [1-3].

The specific aim of this work is to investigate the conditions needed to facilitate this suppression effect and to clarify its mechanism from a fluid dynamical point of view.

Notations

```
\overline{C}_{p}
        time mean pressure coefficient, \left(=\overline{p}/\frac{1}{2}\rho U^2\right)
\overline{C}_{pb}
        time mean base pressure coefficient
d_1
        diameter of the upstream cylinder
d_2
        diameter of the downstream cylinder
f_{nz}
        natural frequency of the elastically supported (upstream) cylinder
        frequency of Kármán vortex shedding
f_{vK}
        frequency of cylinder vibration
f_z
k
        spring constant of the elastically supported (upstream) cylinder
l
        effective length of upstream cylinder (see Figure 1)
        effective mass of upstream cylinder
m
        static pressure
p
Re
        Reynolds number (= Ud_1/v)
        gap between the two cylinders (see Figure 1)
S_p
        linear spectrum of the fluctuating pressure
S_{pp}
        peak value in the linear spectrum of the fluctuating pressure
St
        Strouhal number
S_u
        linear spectrum of the velocity fluctuation
S_{up}
        peak value in the linear spectrum of the fluctuating velocity
U
        free stream velocity
u
        velocity in x direction (see Figure 1)
        root-mean-square value of the displacement of the elastically supported
z_{rms}
        (upstream) cylinder in z direction
        angle measured from upstream stagnation point (see Figures 5 and 6)
\alpha
δ
        logarithmic damping factor
        kinematic viscosity of air
\nu
        density of air
ρ
```

Subscripts

 ∞ for a single cylinder

L left

r resonance

R right

rms root-mean-square value

s separation

Superscript

time mean value

2. Experimental apparatus and procedure

An outline of the experimental apparatus and coordinate system is shown in Figure 1. The wind tunnel is a blowdown type with a square nozzle measuring 350 mm x 350 mm. The maximum attainable velocity is 40 m/s and the turbulence intensity is less than 0.4%. The measuring channel is 320 mm x 320 mm in cross section and 1000 mm in length. The upstream circular cylinder which is supported elastically is set horizontally in the central plane of the test section, and it is allowed to move almost purely in the vertical (z) direction. Another circular cylinder is set vertically downstream of the horizontal cylinder with a gap s between them. The diameters of the upstream and downstream cylinders are d_1 and d_2 , respectively. The aspect ratio of the upstream cylinder l/d_1 is about 12, which corresponds to the spanwise coherent length of a Kármán vortex.

The upstream cylinder passes through slots on the side walls of the test section, and is supported by two identical plate springs outside the side walls, Shirakashi et al. [8]. This setup allows a slight change of attack angle (rotation of the cylinder about its axis) to be superimposed on the z displacement of the cylinder. However, its influence on the oscillation of the circular cylinder is negligible since the length of the plate springs is very large compared with the oscillation amplitude and hence its maximum absolute value is very small. The end plates (shown in Figure 1) are installed in order to avoid flow through the slots. Thus the cylinder displacement is assured to be virtually purely translational in the vertical direction. The characteristics of the oscillating systems used in this experimental study are summarized in Table 1, where the effective mass m, the natural frequency f_{nz} , and the logarithmic damping factor δ are determined through a free damping oscillation in otherwise quiescent air.

The free stream velocity U was measured by a Pitot-static tube. Hot wire probes were used to detect the x component of the fluctuating velocity signals. The displacements at both ends of the upstream cylinder, z_L and z_R , were measured by using non-contacting sensors. Since z_L and z_R were identical under almost all experimental conditions, the motion of the cylinder was assumed to be purely translational. In this paper, the average of z_L and z_R is taken as the translational displacement of the cylinder, and the oscillation amplitude was represented by its root-mean-square value

 z_{rms} .

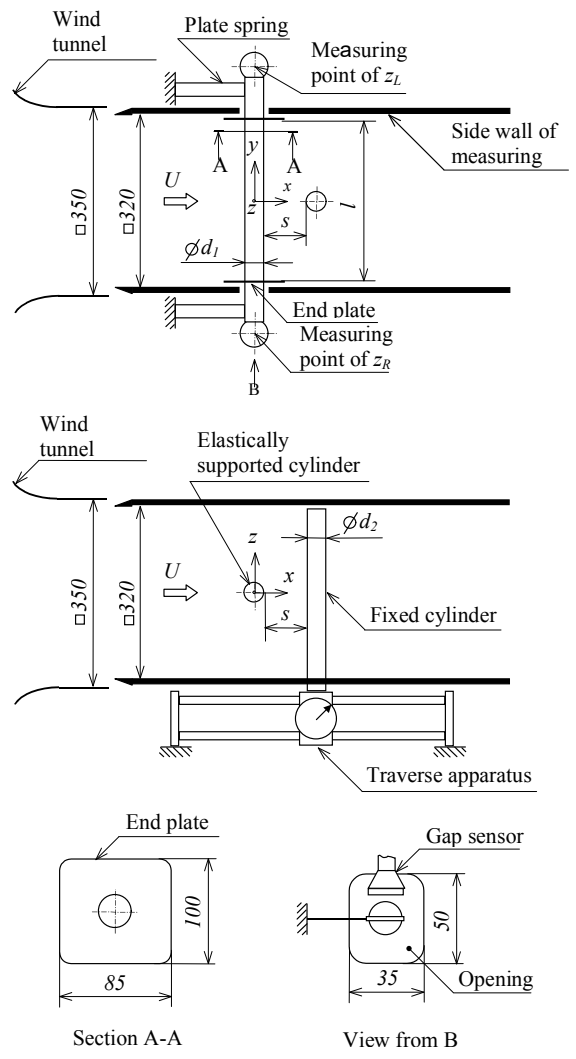


Figure 1. Outline of the apparatus with a coordinate system (unit in mm)

The pressure distribution on the surface of the upstream cylinder was measured with both upstream and downstream cylinders fixed. The geometry of the supporting system and that of the end plates were identical with the one used when the upstream cylinder is allowed to oscillate. The difference of the pressure on the upstream cylinder surface and the static pressure of the free stream was measured by using pressure taps of 0.4 mm in diameter on the surface of a hollow upstream cylinder made of acrylic resin and having a diameter of 26 mm. The hot wire probe was located downstream of the cylinders in a place where the spectrum of the fluctuating velocity signal had a sharp peak. The Kármán vortex shedding frequency f_{vK} was determined as the frequency at which the spectra of the velocity and pressure, S_u and S_p , both have peak values.

	Oscillating system I	Oscillating system II
Upstream cylinder diameter: d_1 (mm)	26.0	26.0
Downstream cylinder diameter: d_2 (mm)	26.0	$18.0\ 26.0\ 32.0$
Effective length: l (mm)	304	304
Effective mass: m (kg)	0.0858	0.0924
Spring constant: k (N/m)	980	2100
Natural frequency: f_{nz} (Hz)	17	24
Logarithmic damping factor: δ (-)	0.0119	0.0166

Table 1. Characteristics of the oscillating systems

In order to visualize the flow pattern on the cylinder surface, the oil-film method was used. A transparent vinyl film of 0.1 mm in thickness was rolled on the surface of the upstream cylinder, and the surface of this film was coated with a mixture of oil and matt-black paint. After having been exposed to the flow, the vinyl film roll was removed, and passing light from below the film made the flow pattern visible.

3. Results and discussion

3.1. Effect of free stream velocity on the vibration of the upstream cylinder. Figure 2 shows the variation of the Kármán vortex shedding frequency f_{vK} , the amplitude z_{rms} , and oscillation frequency of the cylinder f_z versus free stream flow velocity U. In Figure 2 quantities z_{rms} , f_z , and f_{vK} are made dimensionless by diameter d_1 and natural frequency f_{nz} , respectively. The Kármán vortex excitation for the single cylinder is clearly seen in Figure 2(a). However, when the downstream cylinder is added, although the Kármán vortex excitation peak appears at the same velocity, the excitation is substantially suppressed (see Figure 2(b)). It was found that the oscillation frequency coincided with the natural frequency, regardless of flow velocity U. In case of the single cylinder (Figure 2(a)), the amplitude z_{rms} has its maximum in a very small velocity interval at around 2.5 m/s. It is concluded from the results that this vibration is a typical resonance of a system with a small damping factor, i.e., Kármán vortex excitation. The resonance amplitude is denoted by $[z_{rms}]_r$. Narrowing the gap between cylinders reduces the Kármán vortex excitation substantially; in Figure 2(b), where the dimensionless gap $s/d_1 = 0.75$, the amplitude of vibration is reduced to one-fourth of that of the single cylinder.

3.2. Effect of the gap between cylinders on the amplitude of oscillation. Figure 3 shows the relationship between the amplitude of the Kármán vortex excitation $[z_{rms}]_r$ and the dimensionless gap s/d_1 . The vertical bars show the range in oscillation amplitude. Results for downstream cylinders of different diameters are compared in this figure. It was found that $[z_{rms}]_r$ is almost independent of the diameter of the downstream cylinder for dimensionless gap values of $s/d_1 \ge 2$.

By bringing the downstream cylinder closer to the upstream one, the amplitude of oscillation of the two bigger cylinders decreases for $0.4 < s/d_1 < 2$, and it is suppressed completely for $s/d_1 \le 0.4$. The region of s/d_1 with this complete suppression becomes wider with the increase of diameter d_2 . As seen in Figure 3, when the diameter of the

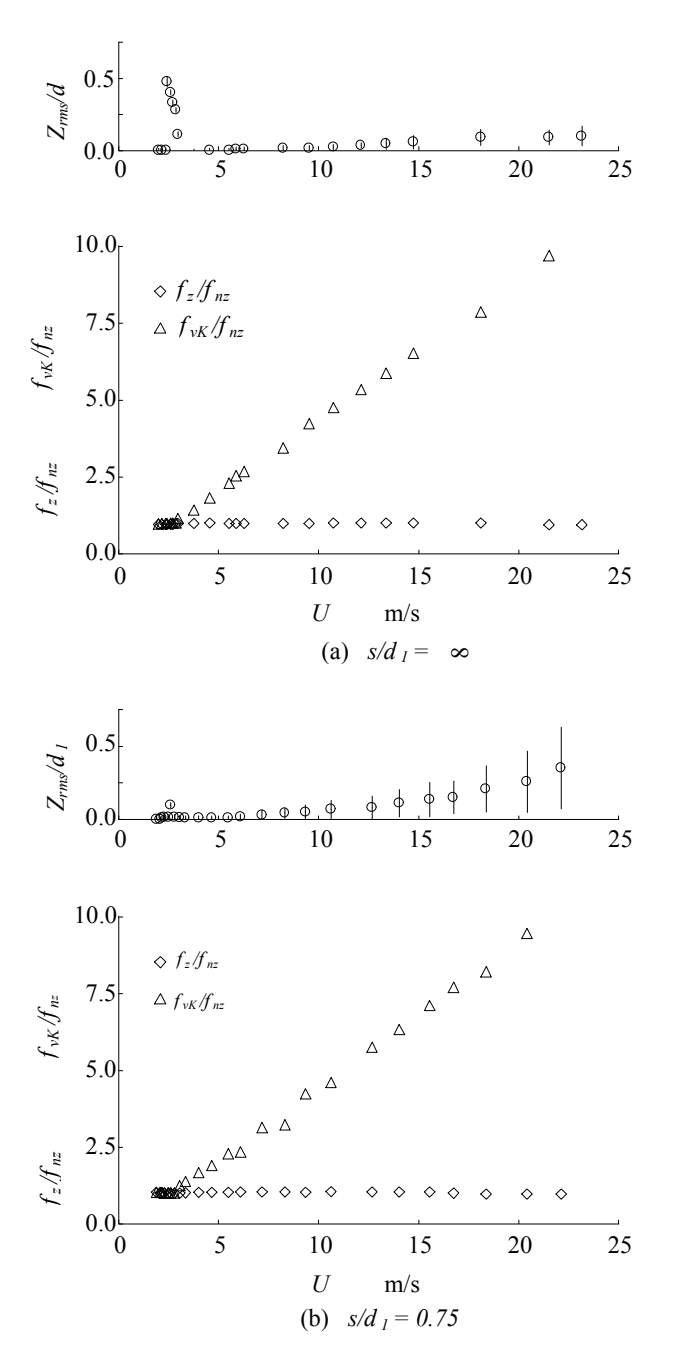


Figure 2. Variation of the nondimensional amplitude and frequency of vibration and the vortex shedding frequency with the freestream velocity (oscillating system I, probe position: $x/d_1 = 2.0$; $y/d_1 = 1.5$; $z/d_1 = 1.0$; $d_1 = d_2 = 26$ mm)

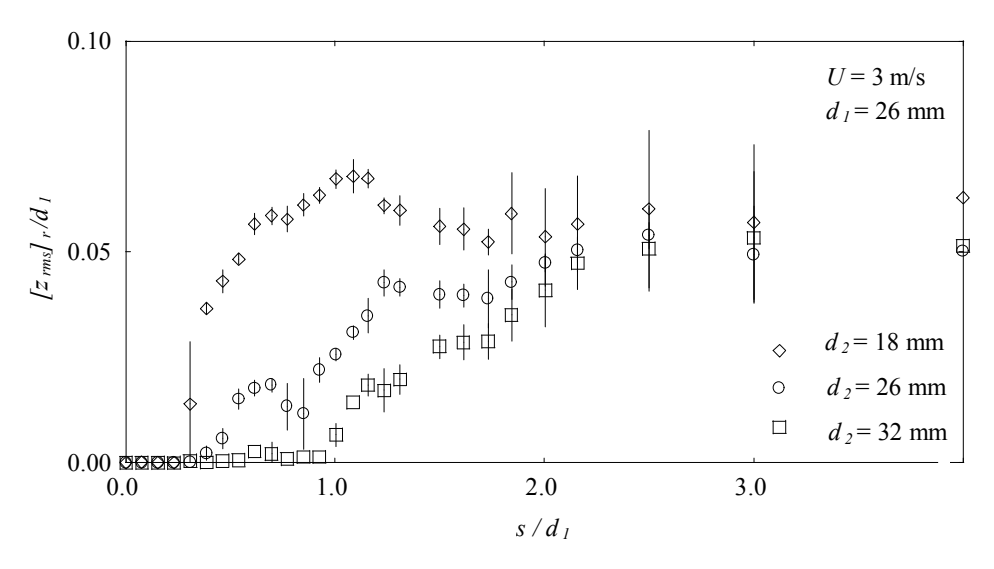


Figure 3. Variation of the vibration amplitude with the gap between two cylinders (oscillating system II)

downstream cylinder is smaller than that of the upstream one, i.e. at $d_2/d_1 = 0.69$, the amplitude of oscillation also becomes nearly zero for small enough gap values. This means that almost complete suppression of oscillation can be achieved for downstream cylinders of smaller diameters as well, but the range of s/d_1 for complete suppression becomes narrower.

3.3. Flow around the upstream cylinder. Flow around the upstream cylinder of the fixed system (i.e. both cylinders are fixed) was investigated to find the mechanism of the suppression of Kármán vortex excitation by the downstream cylinder. Figure 4 shows the flow pattern on the surface of the upstream cylinder visualized by the oil-film method for three different s/d_1 values. In Figure 4(a) which shows the case of $s/d_1 = 0$, the separation lines (indicated by arrows) are distorted into highly curved arcs for $|y/d_1| < 1.0$. The appearance of secondary flow in the wake behind the cylinder makes the oil-film pattern rather complex in this region. The separation lines outside of this region are almost straight lines parallel to the axis of the upstream cylinder. From now on the former region will be referred to as the primary effect region, and the latter as the secondary effect region. The length of the primary effect region along the axis of the cylinder depends on the nondimensional gap s/d_1 ; the region of primary effect scarcely appears on the oil-film for $s/d_1 > 1.0$.

The photographs in Figure 4 can be used for the determination of the relationship between the separation angle α_s (see Figure 5) and the dimensionless distance y/d_1 for different s/d_1 values. These relationships are shown and compared with the results of Tomita et al. [12]. The separation lines in the secondary effect region remain parallel with the axis of the cylinder for $y/d_1 > 4.0$, but the separation angle α_s is

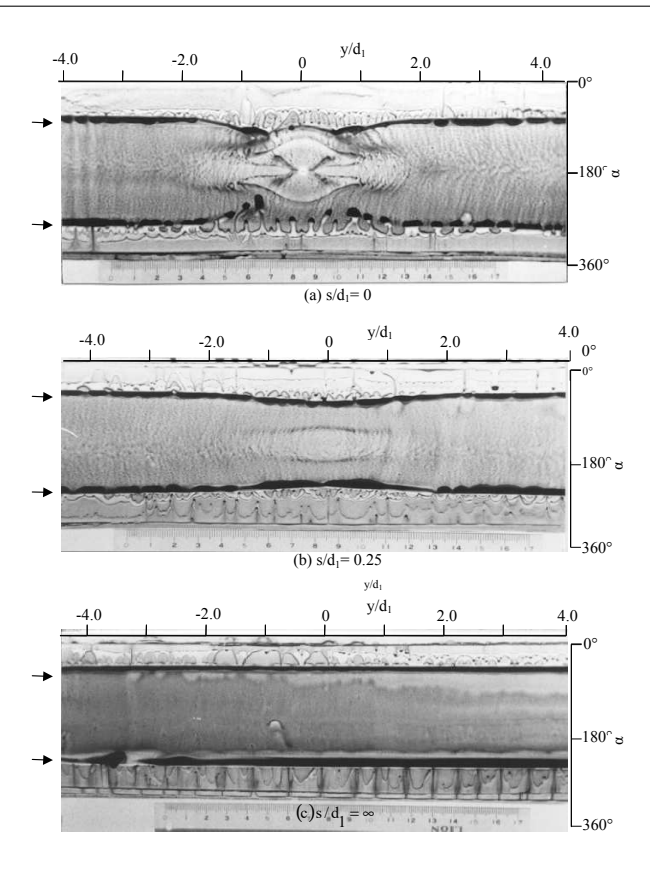


Figure 4. Flow visualisation on the surface of the upstream cylinder by the oil-film method (fixed system $d_1 = d_2 = 26 \ mm$; $U = 8 \ m/s$; Re = 14700; \rightarrow : separation line)

about 5 degrees smaller in this y/d_1 domain than the separation angle for the single cylinder. The distribution of the time mean pressure coefficient \overline{C}_p on the surface of the upstream cylinder is shown in Figure 6 at cross sections, specified by various y/d_1 values. The distribution of \overline{C}_p in the primary effect region of the cylinders in cruciform arrangement is notably different from the distribution around a single cylinder. On the other hand, the pressure distributions are almost the same for the secondary effect region with two cylinders and for the single cylinder. However, the pressure on the rear part of the upstream cylinder surface is a little higher than that on the single cylinder, and the separation line is found to move a little upstream in the former case. The effect of the downstream cylinder on the spectra of the fluctuating velocity and pressure S_u and S_p in the secondary effect region $y/d_1 > 4.0$ is shown in Figure 7. The measuring position was chosen as the one where the fluctuation component due to the Kármán vortices is most definitely observed. When the dimensionless gap $s/d_1 > 2.0$, the spectra S_u and S_p have sharp peaks at the frequency of f = 24 Hz. The Strouhal number for this frequency is St = 0.2, indicating that the sharp peaks

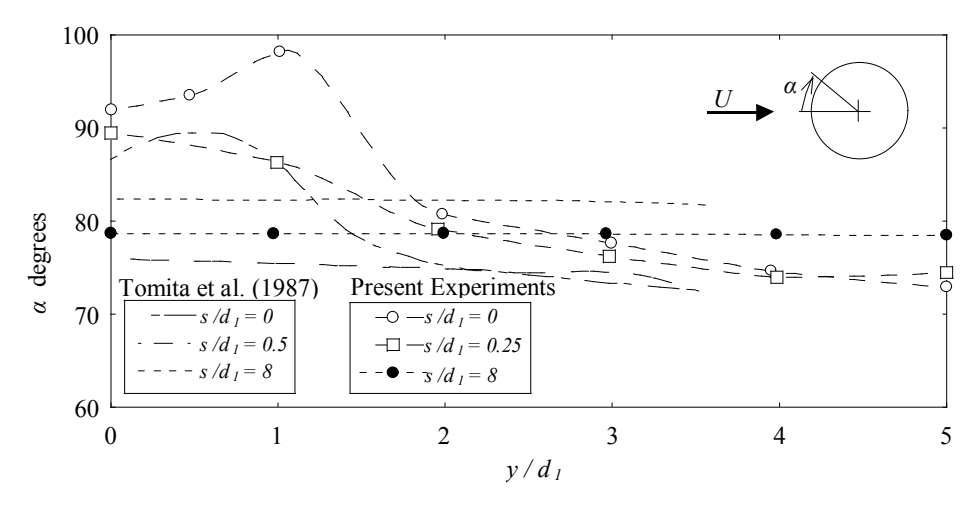


Figure 5. Variation of the separation angle with the spanwise coordinate y for different gap values (fixed system; (a) $d_1 = d_2 = 20 \ mm$; Re = 27000; (b) $d_1 = d_2 = 26 \ mm$; Re = 14700)

are caused by Kármán vortices. Although the decrease of the dimensionless gap s/d_1 reduces the magnitude of the height of spectral peaks S_{up} and S_{pp} , the frequency of Kármán vortex shedding f_{vK} remains unchanged. From the results above, the main features of the two regions for cylinders in cruciform arrangement can be summarized as follows:

- The primary effect region: The mean flow field is very different from that of the single cylinder, and is strongly three-dimensional due to the influence of the downstream cylinder. Kármán vortex shedding is totally suppressed in this region.
- 2. The secondary effect region: The main flow field is basically two-dimensional in this region, and is nearly identical with that of the single cylinder. Nevertheless, the pressure on the rear surface of the upstream cylinder increases a little due to the effect of the downstream cylinder, and the separation lines move slightly upstream. While the fluctuating components of the velocity and pressure signals u and p induced by the shedding of Kármán vortices are reduced with a decreased gap between cylinders, the vortex shedding frequency is unaffected.
- **3.4.** Mechanism for the suppression of Kármán vortex excitation. Considering the results given above, possible factors in the suppression of Kármán vortex excitation by setting a downstream cylinder in the flow can be stated as follows:
 - 1. There is no Kármán vortex shedding in the primary effect region, leading to the reduction of the excitation force acting on the cylinder.
 - 2. The strength of circulation of vortices and the regularity of vortex shedding are reduced in the secondary effect region.
 - The phase of the Kármán vortices, cut into two by the downstream cylinder, can differ on each side.

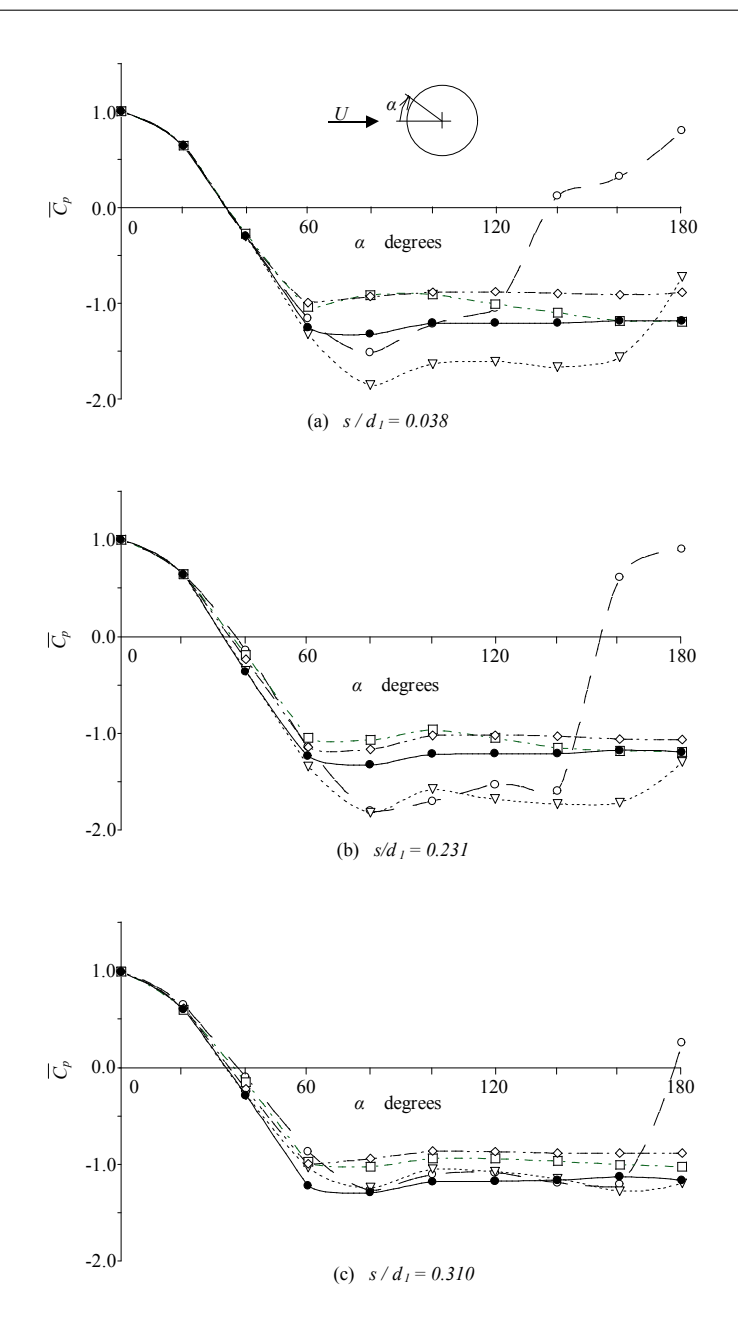
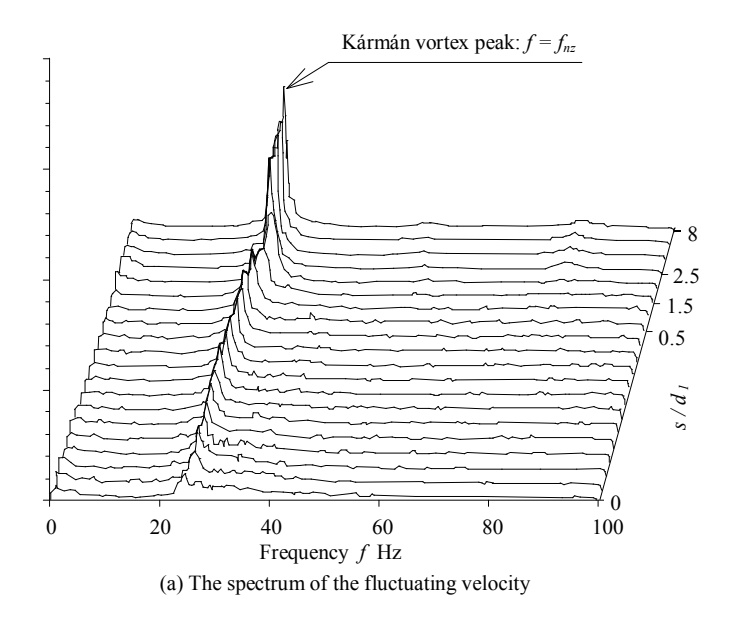


Figure 6. Pressure distribution on the surface of the upstream cylinder (fixed system; $d_1=d_2=26$ mm; Re=14700; (o): $y/d_1=0.0$; (∇): $y/d_1=1.0$; (\square): $y/d_1=2.0$; (\square): $y/d_1=3.0$; (\square):



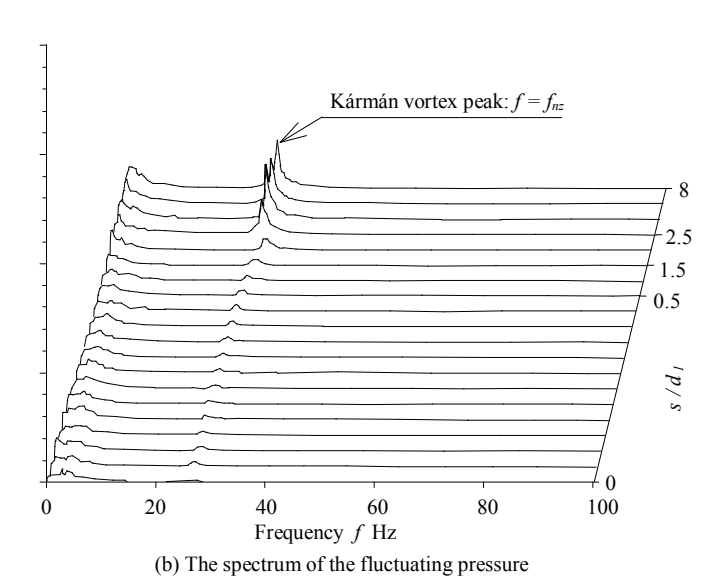


Figure 7. Effect of the gap between the two cylinders on the spectra of the velocity and pressure at the point defined by the following coordinates: $x/d_1 = 2.0$; $y/d_1 = 4.0$; $z/d_1 = 2.0$; (fixed system; $d_1 = d_2 = 26$ mm; Re = 5150; pressure tap position: $\alpha = 80^{\circ}$; $y/d_1 = 4.0$)

It is obvious that the reduction of the excitation force due to factor (1) is proportional to the ratio of the length of the primary effect region l_{sI} to the effective length of the upstream cylinder. The phenomenon, however, cannot be attributed solely to this cause, as it cannot explain why the amplitude of the upstream cylinder oscillation drops to almost zero for $s/d_1 < 0.4$ as found experimentally.

Factor (3) is based on the hypothesis that the correlation of the Kármán vortices, shed from the left and right parts of the horizontal upstream cylinder, becomes weaker since the downstream cylinder breaks the continuity of the Kármán vortex. Although this hypothesis may hold true for fixed upstream cylinders, such phase shift never occurs in an oscillating system because the Kármán vortex shedding synchronizes with the oscillation of the cylinder resulting in zero phase shift. Moreover there is some experimental evidence that even for fixed cylinders the pressure fluctuations due to Kármán vortex shedding in the secondary effect regions are in phase on each side of the downstream cylinder. Hence factor (3) is excluded as a possible cause of the suppression of vibration.

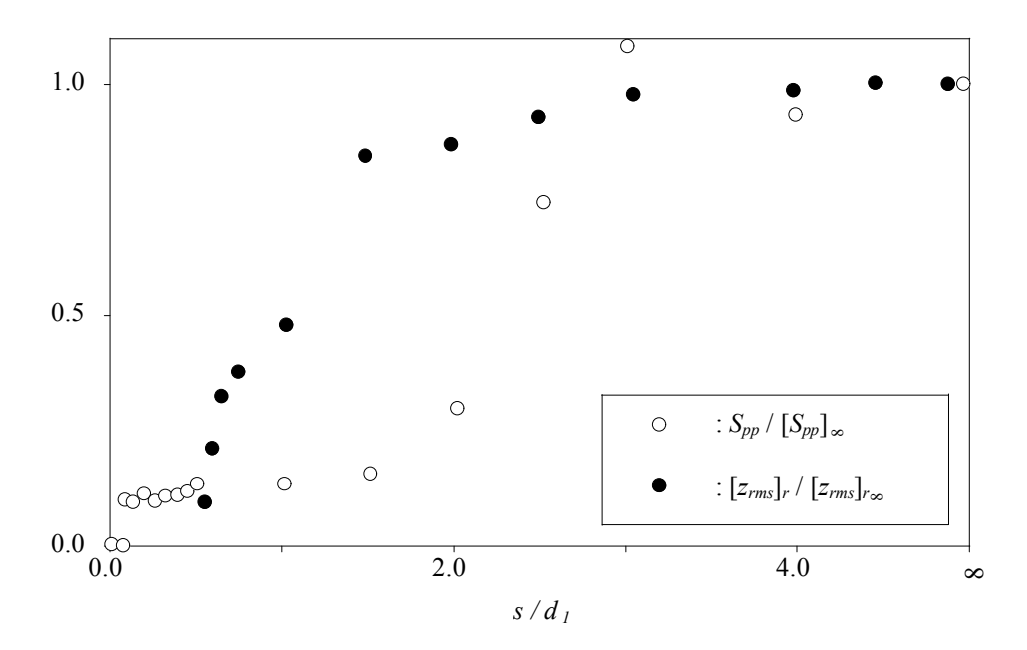


Figure 8. Variation of vibration amplitude and the spectral peak of pressure with the gap between the cylinders (fixed system; $d_1 = d_2 = 26 \text{ mm}$; Re = 5150; pressure tap position: $\alpha = 80^{\circ}$; $y/d_1 = 4.0$)

The role of factor (2) is confirmed by looking into the correlation between the oscillation amplitude and the peak value of spectrum S_{pp} in the secondary region. The relationship between s/d_1 and the peak value S_{pp} of the pressure fluctuation spectrum is shown in Figure 8, and is compared with the Kármán vortex excitation amplitude $[z_{rms}]_r$.

The variables are made nondimensional by the corresponding values belonging to the single cylinder. The relationships between $S_{pp}/[S_{pp}]_{\infty}$ and s/d_1 , further $[z_{rms}]_r/[z_{rms}]_{r\infty}$ and s/d_1 are similar to each other. The fact that S_{pp} is closely related to the fluctuating lift force acting on the cylinder at the frequency of f_{vK} (see Figure 8) suggests that factor (2) is one of the causes of the suppression of vibration.

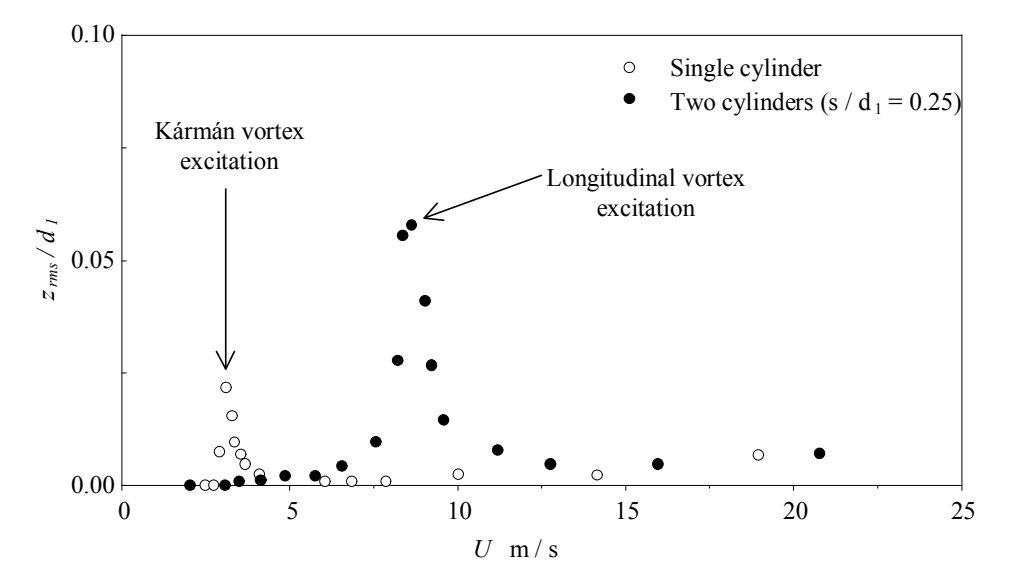


Figure 9. Longitudinal vortex excitation caused by the downstream cylinder

It should be noted that a large oscillation can be induced by the downstream cylinder. As seen in Figure 9, a high oscillation peak appears at a velocity three times higher than that of Kármán vortex excitation.

This oscillation is in resonance with the longitudinal vortices shed periodically near the crossing of the two cylinders, Shirakashi *et al.* [10]. Our investigations on this new excitation have shown that not only the velocity range of its occurrence, but also the phenomenon itself is completely different from those of the Kármán vortex excitation.

4. Conclusions

Kármán vortex excitation of an elastically supported circular cylinder placed in an otherwise uniform crossflow can effectively be suppressed by setting another cylinder downstream to it in a cruciform arrangement. Measurements of pressure on the upstream cylinder surface and velocity near the crossing, together with flow visualization, offer the following explanation for the phenomenon of suppression. Although the shedding frequency of Kármán vortices is unaffected by the downstream cylinder, the strength of circulation of a vortex is reduced and the periodicity of vortex shedding is disturbed along the whole span of the upstream cylinder due to the presence of the

downstream cylinder. In addition, there is no Kármán vortex shedding in the region near to the downstream cylinder.

The advantages of this technique are: i) it requires no modification in the shape of the oscillating body or in its supporting structure, and ii) the flow upstream of the oscillating body is virtually undisturbed.

REFERENCES

- BAE, H.M., ARAI, K., ROSLIN BIN S. and SHIRAKASHI, M.: The influence of a cylinder located downstream on the oscillation of an elastically supported cylinder, Proceedings of the 2nd KSME-JSME Fluids Engineering Conference, Vol. 1, (1990), 72-77.
- BAE, H.M., BARANYI, L., TAKAHASHI, T. and SHIRAKASHI, M.: Suppression of Kármán vortex excitation of circular cylinders, Proceedings of the 11th Conference on Fluid and Heat Machinery and Equipment, Budapest, (1999), on CD ROM, 14/1-11.
- 3. Bae, H.M., Takahashi, T. and Shirakashi, M.: Suppression of Karman vortex excitation of a circular cylinder by another cylinder located downstream in cruciform arrangement. Bulletin of the JSME 59, (557), (1993), 1-7.
- BEARMAN, P.W.: Vortex shedding from oscillating bluff bodies, Annual Review of Fluid Mechanics 16, (1984), 195-222.
- BLEVINS, R.D.: Flow-Induced Vibrations, Van Nostrand Reinhold, 2nd Edition, New York, 1990.
- PARKINSON, G.V. and WAWZONEK, M.A.: Some considerations of combined effects of galloping and vortex resonance, Journal of Wind Engineering 81(1-2), (1981), 135-143.
- SARPKAYA, T.: Vortex induced oscillations, A Selective Review, Journal of Fluid Mechanics 46, (1979), 241-258.
- SHIRAKASHI, M., ISHIDA, Y. and WAKIYA, S.: Higher velocity resonance of circular cylinder in crossflow, Transactions of the ASME, Journal of Fluids Engineering, 108, (1985), 392-396.
- SHIRAKASHI, M., MIZUGUCHI, K. and BAE, H.M.: Flow-induced excitation of an elastically supported cylinder caused by another located downstream in cruciform arrangement, Journal of Fluids and Structures 3, (1989), 595-607.
- SHIRAKASHI, M., BAE, H.M., SANO, M. and TAKAHASHI, T.: Characteristics of periodic vortex shedding from two cylinders in cruciform arrangement, Journal of Fluids and Structures, 8, (1994), 239-256.
- TOMITA, Y., INAGAKI, S., SUZUKI, S. and YOKOYAMA, T.: Acoustic characteristics of two circular cylinders forming a cross in uniform flow (1st Report, Effect on noise reduction), Bulletin of the JSME 29(250), (1986), 1163-1170.
- Tomita, Y., Inagaki, S., Suzuki, S. and Muramatsu, H.: Acoustic characteristics of two circular cylinders forming a cross in uniform flow (Effect on noise reduction and flow around both cylinders), JSME International Journal, 30(265), (1987), 1069-1079.

RELATIONS FOR THE TORSION OF NONHOMOGENEOUS CYLINDRICAL BARS

ISTVÁN ECSEDI
Department of Mechanics, University of Miskolc
3515 Miskolc-Egyetemváros, Hungray
mechecs@uni-miskolc.hu

[Received: September 12, 2001]

Abstract. The present paper refers to the torsion of cylindrical bars, the cross section of which is a simple or multiply connected plane domain. Examples illustrate the application of the Bai-Shield's identity. A lower bound relation is presented for the greatest shearing stress developed in the twisted cylindrical bar and an upper bound relation is proven for the plastic limit torque. Three types of the upper bound formulae are derived for the torsional rigidity of nonhomogeneous isotropic elastic bars.

Mathematical Subject Classification: 74G45, 74K10

Keywords: Cylindrical bar, elastic, inequality, nonhomogeneous, torsional rigidity.

1. Introduction

Consider a bar bounded by a cylindrical surface ("side-surface") and two planes ("end cross sections"), normal to the side surface. For greater generality, it is assumed that the bar under consideration may contain longitudinal cylindrical cavities so that the cross-section of the bar may be multiply connected. Further assumptions are that there are no body forces present, that the side surface of the bar is free from external stresses and that given forces (satisfying the equilibrium conditions of the body as whole) are shearing stresses applied to the end cross sections of the bar. We also suppose that the bar is composed of a material which is homogeneous in the axial direction.

A three-dimensional rectangular Cartesian coordinate system (x, y, z) will be used. The axis Oz is directed parallel to the generators of the side surface and the plane Oxy is chosen to coincide with the "lower" end of the bar. The "upper" end of the bar will then have the coordinate z = L, where L is the length of the bar.

Following Bai and Shield [1], we suppose that τ_{xz} and τ_{yz} are the only nonzero stresses in the whole bar. In this case the equilibrium conditions can be formulated as [5-6, 9]:

$$\frac{\partial \tau_{xz}}{\partial x} + \frac{\partial \tau_{yz}}{\partial y} = 0 \quad \text{in } A \quad , \tag{1.1}$$

$$\tau_{xz}n_x + \tau_{yz}n_y = 0 \quad \text{on } c \quad , \tag{1.2}$$

where A is the cross-section of the cylindrical bar, c is the boundary of A and n_x, n_y

190 I. Ecsedi

are the components of the outward unit normal to the curve c.

It follows from equations (1.1) and (1.2) that [1-2, 5]

$$X = \int_{A} \tau_{xz} dA = 0 \quad \text{and} \quad Y = \int_{A} \tau_{yz} dA = 0, \qquad (1.3)$$

that is, there are no transverse forces on the cross-section of the bar.

The only moment acting on a cross-section is a twisting moment T given by

$$T = \int_{A} (x\tau_{yz} - y\tau_{xz})dA. \qquad (1.4)$$

Bai and Shield proved [1] that each of the rectangular components of shearing stress provides one half of the twisting moment

$$\int_{A} x \tau_{yz} dA = -\int_{A} y \tau_{xz} dA = \frac{T}{2}.$$
(1.5)

Equation (1.5) is valid both for simply connected cross-sections and and for multiply connected ones. It is also independent of any material properties provided that the material properties depend on the cross-sectional coordinates x, y only.

2. Lower bound for the shearing stress

Let τ be the greatest shearing stress in cross-section A of a cylindrical bar subjected to a twisting moment T. We have

$$\tau = \max \sqrt{\tau_{xz}^2 + \tau_{yz}^2} \quad , \quad (x, y) \in \overline{A} = A \cup c \quad . \tag{2.1}$$

Regrading equation (1.5) as a point of departure and using the Schwarz inequality we can write that

$$\int_A x^2 \mathrm{d}A \int_A \tau_{yz}^2 \mathrm{d}A \ge \frac{T^2}{4} \quad \text{and} \quad \int_A y^2 \mathrm{d}A \int_A \tau_{xz}^2 \mathrm{d}A \ge \frac{T^2}{4} \,. \tag{2.2}$$

A combination of inequality

$$\int_{A} (\tau_{xz}^2 + \tau_{yz}^2) dA \le \tau^2 A \tag{2.3}$$

with inequalities $(2.2)_{1,2}$ results in the following lower bound

$$\frac{\tau}{T} \ge \sqrt{\frac{I_x + I_y}{4I_xI_yA}},\tag{2.4}$$

where I_x and I_y are the second moments of the cross-section about the axes x and y, respectively, and A is the area of the cross-section.

3. Upper bound for the limit plastic torque

Let us assume that the material of the cylindrical body is elastic-perfectly plastic. In the case of fully plastic torsion we have

$$\tau_{xz}^2 + \tau_{yz}^2 = \tau_0^2 \quad \text{in } A \cup c,$$
 (3.1)

where $\tau_0 = \tau_0(x, y)$ is the yield stress in pure shear, which may depend on the cross-sectional coordinates x, y. Let T_0 be the plastic torque of the cross section [4,7]. The constant A_0 is defined by

$$A_0 = \int_A \tau_0^2 dA \,. \tag{3.2}$$

Making use of equations $(2.2)_{1,2}$ and the Huber-v. Mises-Hencky yield condition (3.1) we obtain the following upper bound

$$T_0 \le \sqrt{\frac{4I_xI_yA_0}{I_x + I_y}}$$
 (3.3)

Remarks to relations (2.4) and (3.3)

R1. Relation (2.4) is an equality for a thin-walled circular tube with constant thickness.

R2. Relation (3.3) is also an equality for a *homogeneous* thin-walled circular tube with constant thickness.

R3. It can be proved that relation (2.4) leads to the best lower bound for τ_o and formula (3.3) gives the sharpest upper bound for T_o if the axes x, y are principal centroidal axes of the cross-section [3].

4. Upper bound for the torsional rigidity

In this section it is assumed that the material of the twisted bar is inhomogeneous isotropic elastic, the equilibrium state of the bar is the pure torsion according to Saint-Venant's theory [3], [5-6]. A consequence of the nonhomogeneous is that the shear modulus G may depend on x, y that is G = G(x, y).

Once again we regard equation (1.5) as our point of departure and use the Schwarz inequality. We get

$$\frac{T^2}{4} = \left(\int_A x \tau_{yz} dA\right)^2 = \left[\int_A \left(\frac{\tau_{yz}}{\sqrt{G}}\right) \left(x\sqrt{G}\right) dA\right]^2 \le \int_A \frac{\tau_{yz}^2}{G} dA \int_A Gx^2 dA \quad , \quad (4.1a)$$

$$\frac{T^2}{4} = \left(\int_A y \tau_{xz} dA\right)^2 = \left[\int_A \left(\frac{\tau_{xz}}{\sqrt{G}}\right) \left(y\sqrt{G}\right) dA\right]^2 \le \int_A \frac{\tau_{xz}^2}{G} dA \int_A Gy^2 dA \quad . \quad (4.1b)$$

192 I. Ecsedi

The strain energy stored in the unit length of the twisted bar [5-7], [9] is given by

$$U = \int_{A} \frac{\tau_{xz}^{2} + \tau_{yz}^{2}}{2G} dA \quad . \tag{4.2}$$

The torque-twist relation is of the form

$$T = R\vartheta, (4.3)$$

where R is the torsional rigidity of the cross-section and ϑ is the rate of twist [5-6], [9].

We shall consider a unit length of the bar. In this case

$$W = \frac{1}{2}T\vartheta = \frac{T^2}{2R} \tag{4.4}$$

is the work done by the twisting moment T. According to the Clapeyron theorem [9] we can write

$$U = \frac{T^2}{2R}. (4.5)$$

Combination of equations (4.1a,b) with formula (4.2) gives

$$U \ge T^2 \frac{J_x + J_y}{8J_x J_y} \,, \tag{4.6}$$

where

$$J_x = \int_A Gy^2 dA$$
 and $J_y = \int_A Gx^2 dA$ (4.7)

are the G-weighted second moments of the cross-section about the centroidal axes x and y, respectively. Inserting equations (4.1a,b) into inequality (4.6) we obtain the upper bound

$$R \le \frac{4J_x J_y}{J_x + J_y} \,. \tag{4.8}$$

Let J_0 be defined as

$$J_0 = J_x + J_y = \int_A G(x^2 + y^2) dA.$$
 (4.9)

It is clear that

$$(J_x - J_y)^2 = (J_x + J_y)^2 - 4J_x J_y \ge 0$$
(4.10)

from which we get the lower bound

$$J_0 \ge \frac{4J_x J_y}{J_x + J_y} \quad . {(4.11)}$$

Relations (4.8) and (4.11) show that

$$R \le J_0. \tag{4.12}$$

The upper bound (4.12) is weaker than the upper bound (4.8).

Combination of inequalities (4.1a,b) with the lower bounds

$$2U \ge \int_{A} \frac{\tau_{xz}^{2}}{G} dA$$
 and $2U \ge \int_{A} \frac{\tau_{yz}^{2}}{G} dA$

and equation (4.5) yields the Grammer type upper bound

$$R \le \min\{4J_x, 4J_y\} \tag{4.13}$$

for the torsional rigidity of nonhomogeneous cylindrical bars. This estimation is used mainly for narrow rectangular cross-sections [3].

Remarks to relations (4.8), (4.12) and (4.13):

- R1. For a homogeneous bar, estimation (4.8) was first derived by Nicolai [8].
- R2. For a homogeneous bar the upper bound (4.12) was deduced from the theory of Saint-Venant by Diaz and Weinstein [2].
- R3. It can be proved that inequality (4.12) gives the best upper bound if the origin of the cross-sectional coordinate system is chosen in such a way [3] that the equations

$$\int_{A} xG(x,y)dA = 0 \quad \text{and} \quad \int_{A} yG(x,y)dA = 0$$
 (4.14)

hold.

R4. It is proved in [3] that inequalities (4.8) and (4.13) lead to the best upper bound if the origin and the direction of the axes of the cross-sectional coordinate system x, y are chosen in such a way [3] that equations (4.14) and equation

$$\int_{A} xyG(x,y)dA = 0 \tag{4.15}$$

are all satisfied.

R5. Relations (4.8) and (4.12) are equalities if the cross-section is bounded by two concentric circles on which

$$x^2 + y^2 = a_1^2$$
 and $x^2 + y^2 = a_2^2$

and the shear modulus depends only on the radial coordinate $r = \sqrt{(x^2 + y^2)}$. Here, a_1 and a_2 are the radii of the boundary circles.

5. Conclusions

Some applications of the Bai-Shield identity for the torsion of a nonhomogeneous cylindrical bar have been presented. A lower bound is derived for the greatest shearing stress developed in twisted cylindrical bars and an upper bound is set up for the plastic

194 I. Ecsedi

limit torque. Three different upper bounds are derived for the torsional rigidity of nonhomogeneous isotropic elastic bars. It is assumed that the material properties of the bar do not depend on the axial coordinate.

All derivations are based on the Bai-Shield identity and the strength of materials' approach makes it possible to avoid the use of variational methods and the application of the procedures known from higher analysis [3].

The formulas derived are also valid for cases when the bar is a composite one made of different homogeneous materials. These bars are compound bars and reinforced bars. Their discontinuities in the material properties do not affect the validity of the bounding formulas presented here.

REFERENCES

- BAI, Z. and SHIELD, R.T.: Indentities for torsion of cylinders, J. Applied Mechanics, 61, (1994) 499-500.
- DIAZ, J.B. and WEISTEIN, A.: The torsional rigidity and variational methods, American Journal of Mathematics, 70, (1948) 107-116.
- 3. Ecsedi, I.: Supplementary remarks to the theory of torsion of nonhomogeneous bars, Ph. D. Thesis, University of Miskolc, Hungary, 1981. (in Hungarian)
- KALISZKY, S.: Plasticity (Theory and Application), Elsevier Science Publishers, Amsterdam 1989.
- LEKHNITSKII, S.G.: Torsion of anisotropic and nonhomogeneous bars, Nauka, Moscow, 1971. (in Russian)
- LOMAKIN, B.A.: Theory of Nonhomogeneous Elastic Bodies, University of Moscow, Moscow, 1976. (in Russian)
- NADAI, A.: Theory of Flow and Fracture of Solids, Vol. 1., McGraw-Hill, New York, 1950.
- NICOLAI, E.: Über die drillungssteifigkeit zylindrischer Stabe, Z. Angew. Math. Mech., 4, (1924) 181-182.
- SOKOLNIKOFF, I.S.: Mathematical Theory of Elasticity, Second Edition, McGraw-Hill, New York, 1956.

SIMULTANEOUS MOISTURE AND HEAT TRANSFER IN POROUS SYSTEMS

AKBAR KHODAPARAST HAGHI Guilan University P.O. Box 3756, Rasht, Iran Haghi@kadous.gu.ac.ir

[Received: September 18, 2001]

Abstract. Based on an examination of the liquid-vapor equilibra and of the mass and energy transfer processes in porous systems, a theory has been developed. The mathematical model is developed for heat and mass transfer analysis of porous media in a convective dryer. Using the model, the calculated transient temperature of the porous material in the dryer agrees well with the experimental values measured. Variations in temperature and moisture content distribution are solved using the finite difference method. The effects of operation parameters, such as temperature and humidity in the dryer, initial moisture content of the porous material, and heat and mass transfer coefficients are examined using this model. By theoretically simulating the drying process, it is shown that during the falling rate period the evaporation-condensation mechanism is the governing mechanism of drying.

Mathematical Subject Classification: 80A20

Keywords: Convective drying, moisture and heat transfer, porous system

1. Introduction

Convective drying is usually encountered in many industrial fields (food industry, building industry, textile industry etc.). Therefore, the study of this type of problem becomes very important and for several decades now has attracted the attention of several authors [1-11]. From among the several theories so far suggested for explaining migration of moisture in porous media, three have won general recognition: the diffusion theory, the capillary flow theory, and the evaporation-condensation theory.

It is still often assumed that with constant drying conditions, a constant drying rate only occurs when the surface of the drying medium is completely wetted, but for porous media, this is, in general, not true.

Numerous governing equations for heat and mass transfer have been derived by many researchers. Transient state diffusion in hygroscopic textile fibers was first analyzed by Henry [12], who obtained an approximate analytical solution. He showed that moisture diffuses into the porous structure of the fabric and the solid phase of the fabric is hygroscopic. Later, Nordon and David [13] improved Henry's model, and they were able to solve the nonlinear differential equation of moisture transfer using the finite difference method. Farnworth [14] introduced a model to solve transient heat and mass transfer in a multilayered clothing system.

Energy consumption in a convective dryer can be reduced by optimizing the drying process using mathematical analysis of temperature and moisture distribution in the fabric. Thus, development of a suitable mathematical model to predict the accurate performance of the dryer is important for energy conservation in the drying process.

Beard [15] suggested a simplified mathematical model to obtain the temperature and moisture distribution of fabrics in convective dryers. He assumed that a fabric consists of two layers, one dry layer and one wet layer. But his analysis did not describe details of what was going on inside the fabric. Also, he used two experimental constants to fit his data to the experimental results of measured temperature variation inside the dryer.

In this study, the mathematical model developed by Nordon and David to determine the transient temperature and moisture concentration distribution of a fabric in a convective dryer have been modified. Also, distributions of temperature and moisture concentration were calculated using the finite difference method. The advantages of these modifications were the possibilities of analysis of the effects of many operating parameters such as dryer air temperature, humidity, initial moisture content of fabric, fabric characteristics. These have been examined using the model developed in this study.

The discussion is restricted to convective drying of non-shrinking capillary-porous media. Therefore the solid phase is geometrically fixed; the liquid is contained in (assumed relatively large) interconnected interstices (called the pore space); all liquid that leaves the porous medium has to be replaced by air; the vapor pressure above a liquid meniscus in the porous medium is virtually equal to that above a free liquid surface.

2. Notational conventions

 C_A moisture content of air in leather pores, kg/m^3

 C_e moisture content of external air, kg/m^3

 C_F moisture content in leather, kg/m^3

 C_p specific heat, kj/kg K

D diffusion coefficient, m^2/s

G mass flowrate, kg/m^2s

 h_e heat transfer coefficient, W/m^2K

 h_m mass transfer coefficient, m/s

K rate constant, 1/s

k thermal conductivity, W/mK

 \bar{m} mass transfer rate, kg/m^2s

 P_s saturation pressure, kg/m^2

 P_r Prandtl number

q convective heat transfer rate, W/m^2

R gas constant, kj/kgK

 S_c Schmidt number

T temperature, K

 T_e external air temperature, K

t time

 y_A relative humidity of air in pores of leather

 y_F relative humidity of leather

 ε porosity

 λ latent heat of evaporation, kj/kg

 ρ density, kg/m^3

3. Present drying model

The configuration is that of a flat porous slab constituted with a solid phase that is inert and rigid, a liquid phase (pure water) and a gaseous phase which contains both air and water vapor. The theoretical formulation of heat and mass transfer in porous media is usually obtained by a change in scale. Under constant environmental conditions the process of drying can be divided into a "constant rate" and one or two "falling rate" periods. When the initial moisture content is high enough, a considerable amount of moisture leaves the porous medium at a very high, approximately constant rate, which is roughly equal to the rate of evaporation from a continuous water surface under identical environmental conditions. During this initial period the temperature of the system also remains constant and, as a rule, equal to the wet-bulb temperature of the environment.

The mathematical model derived by Nordon is used with small modifications. The modification is explained further in the "solution method".

The resulting differential equations are derived as

$$D\frac{\partial C_A}{\partial x^2} = \frac{\partial C_F}{\partial t} + \varepsilon \frac{\partial C_A}{\partial t} \tag{3.1}$$

and

$$k\frac{\partial^2 T}{\partial x^2} = \rho C_p \frac{\partial T}{\partial t} - \lambda \frac{\partial C_F}{\partial t} \,. \tag{3.2}$$

The boundary conditions for convective heat transfer and mass transfer at the fabric surface are

$$q = h_e \left(T_e - T \right) \tag{3.3}$$

and

$$\bar{m} = h_m (C_e - C_A). \tag{3.4}$$

The deriving force determining the rate of mass transfer inside the fabric is the difference between the relative humidities of the air in the pores and the fabric. The rate of moisture exchange is assumed to be proportional to the relative humidity difference in this study. Thus, the rate equation for mass transfer is

$$\frac{1}{\rho(1-\varepsilon)}\frac{\partial C_F}{\partial t} = K\left(y_A - y_F\right) \tag{3.5}$$

Also, the relative humidities of air and fabric are assumed to be

$$y_A = \frac{C_A RT}{P_s} \tag{3.6}$$

and

$$y_F = \frac{C_p}{\rho(1-\varepsilon)} \,. \tag{3.7}$$

The rate constant in equation (3.5) is an unknown empirical constant and the effect of this constant can be examined. The value of the rate constant was varied from K=0.1 to K=10. The resulting calculated fabric surface temperatures are compared in Figure 1.

When the rate constant is small, the evaporation rate is so small that the moisture content decreases very slowly. Initially, the surface temperature increases rapidly, but later this declines. When K is greater than 1.0, however, the effect of the rate constant on the surface temperature distribution is not significant. This indicates that when the rate constant is greater than 1.0, the evaporation rate is high and the drying process is mainly controlled by the moisture diffusion mechanism inside the fabric. Thus we have assumed the rate constant to be 1.0 in the following calculations.

4. Solution method

Differential equations (3.1) and (3.2) are solved using the explicit-difference method, deriving the finite difference equations and applying the boundary conditions for heat and mass transfer at the fabric surface. It is assumed that heat was transferred from the external hot air to the fabric surface by forced convection, and moisture was transferred from the fabric to the external air. The heat transfer coefficient between the external air and fabric surface is obtained by using a modification of the equation reported by Treybal [16]:

$$h_e = 0.675G^{0.37} (4.1)$$

where G is the mass flow rate of the external air impinging on the fabric surface. The mass transfer coefficient was calculated using the analogy between heat transfer and mass transfer:

$$h_m = \frac{h_e}{\rho C_p} \left(\frac{\Pr}{Sc}\right)^{2/3} \tag{4.2}$$

The temperature and moisture content were calculated using this model. In these calculations, the parameters used for the base condition are shown in Table 1.

•		
Parameter	Unit	Value
Dryer Temp.	K	450
Heat Transfer Coeff.	W/m^2K	70
Mass Transfer Coeff.	m^2/s	0.08
Fabric Thickness	mm	0.7
Porosity	_	0.9
Initial Moisture	%RH	50
Drying Air Moisture	kg/m^3	0.02

Table 1 - Values of parameters for base condition

The convective heat and mass transfer coefficients at the surface are important parameters in drying processes; they are functions of the velocity and physical properties

of the drying medium. The transient fabric temperatures were calculated assuming various values of the rate constant K. The resulting calculated fabric surface temperatures are compared in Figure 1.

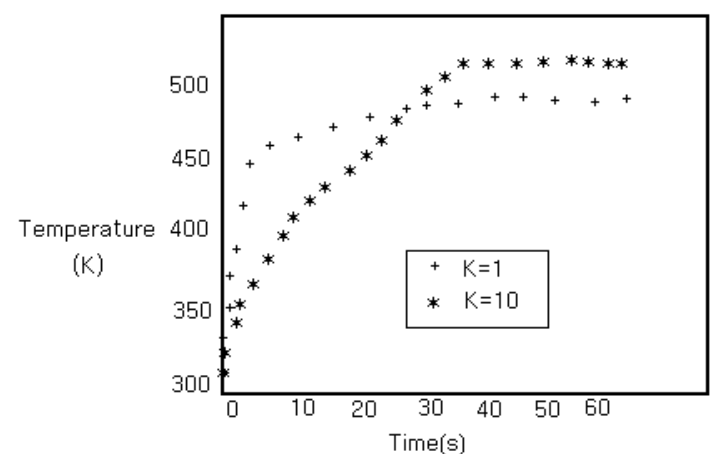


Figure 1. Effect of rate constant on the surface temperature

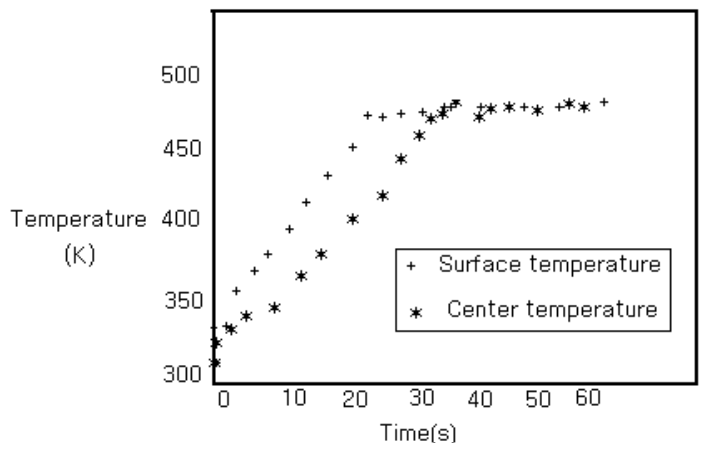


Figure 2. Temperature variation of surface and center

First, the transient temperatures of the surface and center of the fabric using the data shown in Table 1 were calculated. From Figure 2, we see that the surface and center temperatures increase rapidly in the initial stage up to the saturation temperature, at which point the moisture in the fabric starts to evaporate. From that point, the difference between the surface temperature and the center temperature increases due to the different moisture contents of the surface and the center. In this stage, the fabric starts to dry from the surface, and the moisture in the interior is transferred to the fabric surface. Then the moisture content decreases during the drying of the fabric. Thereafter, the surface and center temperatures converge to reach the external air temperature.

The moisture variations of the surface and the center of the fabric were also calculated and are shown in Figure 3.

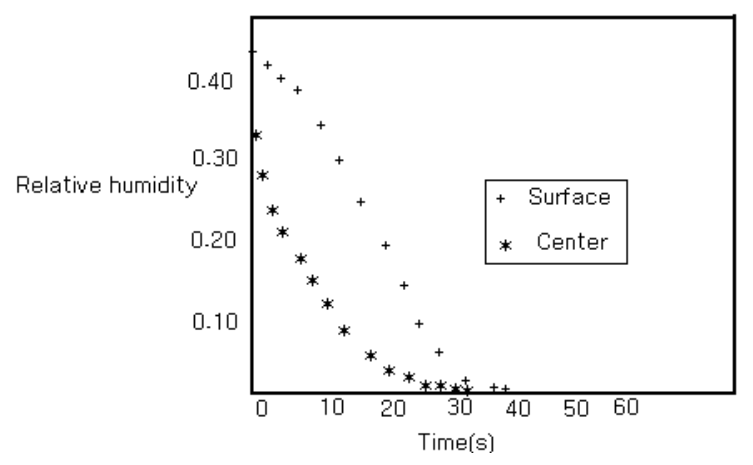


Figure 3. Moisture content of surface and center

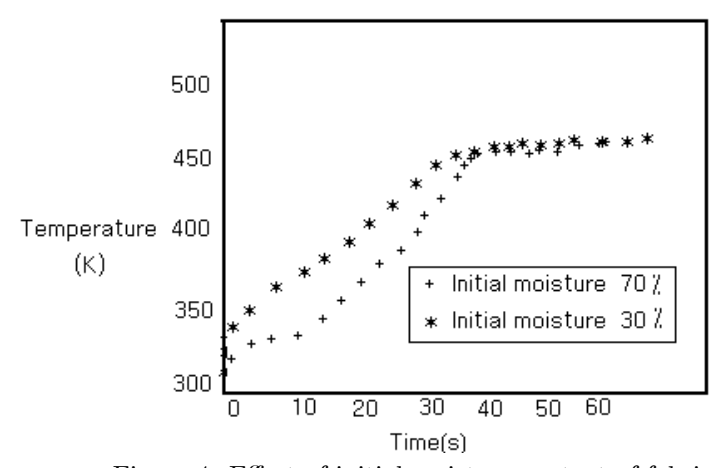


Figure 4. Effect of initial moisture content of fabric

Initially, the surface moisture content decreases rapidly, but later this rate declines because moisture is transferred to the external air from the fabric surface. The center moisture content remains constant for a short time, and then decreases rapidly, because the moisture content difference between the surface and the interior of the fabric becomes large. After drying out, both center and surface moisture contents converge to reach the external air moisture content.

The mathematical model is used to predict the effects of many parameters on the temperature variation of the fabric. These parameters include the operation conditions of the dryer, such as the initial moisture content of the fabric, heat and mass transfer coefficients, drying air moisture content, and dryer air temperature. Figure 4 shows the calculated results of the effect of the fabric initial moisture content. When the initial moisture content is high, the temperature rise is relatively small and drying takes a long time. This may be because the higher moisture content needs much more heat for evaporation from the fabric. Also, the saturation temperature for higher moisture content is lower, and thus the temperature rise in the initial stage is comparatively small.

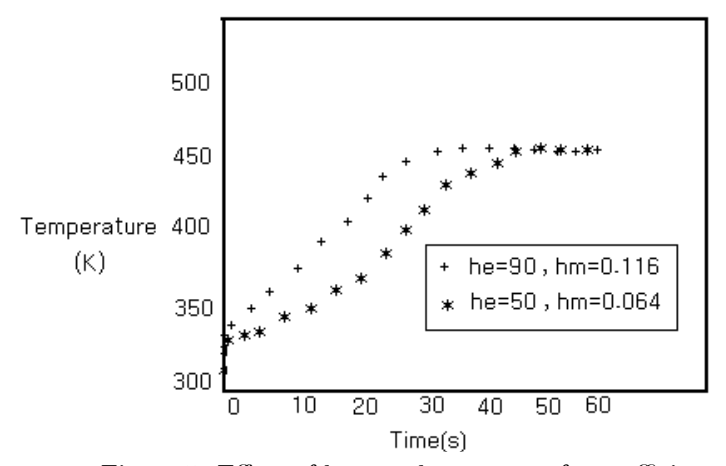


Figure 5. Effect of heat and mass transfer coefficients

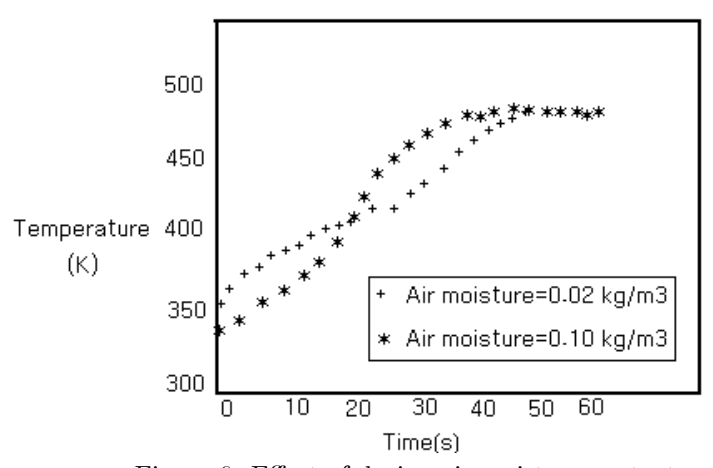


Figure 6. Effect of drying air moisture content

The fabric temperature was calculated to investigate the effects of heat and mass transfer coefficients in the calculation. An analogy was assumed between heat and mass transfer, and so both heat and mass transfer coefficients were determined using this assumption. The calculated results are compared in Figure 5. When the heat and mass transfer coefficients are high, the fabric temperature rise is great and the time required for drying is relatively short.

The effect of drying air moisture content, and the calculated results of the model are shown in Figure 6. When the moisture content is high, the initial temperature rise of the fabric also becomes high. This may be because the saturation temperature in the initial stage largely depends on the drying air moisture content. After the initial temperature rise, however, the temperature increase is relatively small, and thus the time required for complete drying is comparatively long.

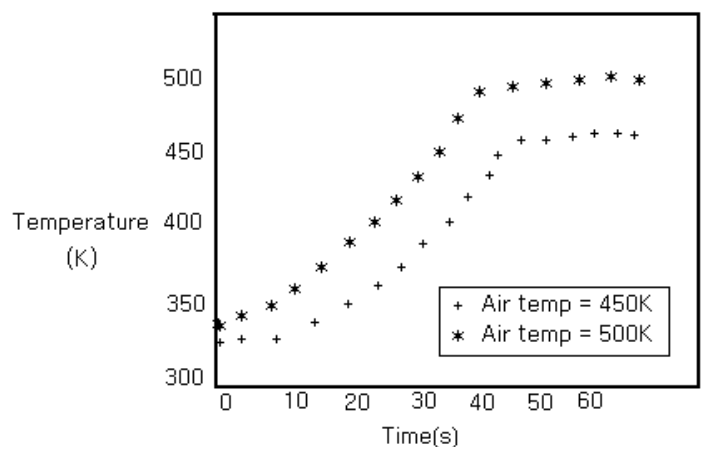


Figure 7. Effect of dryer air temperature

The effect of dryer air temperature was also investigated and the calculation results are shown in Figure 7. When the dryer air temperature is high, the temperature rise of the fabric is great.

When a very wet porous material is dried by a convective medium, three drying rate periods are often observed, the constant rate period, the first falling rate period and the second falling rate period. In the constant rate period and the first falling rate period, the material remains wet, and only the model of the wet region is used. Since evaporation takes place almost entirely at the surface, the drying rate is controlled by the convective heat and mass transfer. If the temperature gradient within the material is negligible, the surface temperature is almost constant and its value is very close to wet bulb temperature of the air flow.

5. Conclusions

The aim of this study is to describe heat and mass transfer in drying by forced convection of porous media. The mathematical model developed in this study is very comprehensive and can be used to predict transient variations in temperature and moisture content distribution of fabrics in the dyer with reasonable accuracy. Simplistic assumptions have been avoided, especially insofar as the effect of gaseous pressure is concerned. The effect of temperature and humidity of the dryer, the initial moisture content of the fabric and the heat and mass transfer coefficients can be predicted for fabrics using the model. With the model predictions, energy consumption may be

reduced by optimizing the drying conditions of the dryer.

On the other hand, for a fully wetted surface, the areas for heat and mass transfer temperature are close to the wet bulb temperature; for a partly wetted surface, the effective area for mass transfer decreases with the surface moisture content.

It was noted that the intercellular spaces, like the voids in porous materials, are interconnected and filled with air and a certain amount of free water. The cells themselves also contain water, which is also defined here as bound water.

Finally, when a porous material is exposed to a convective surface condition, three main mechanisms of internal moisture transfer are assumed to prevail: capillary flow of free water, movement of bound water and vapor transfer. If the initial moisture content of the porous material is high enough, the surface is covered with a continuous layer of free water and evaporation takes place mainly at the surface.

REFERENCES

- 1. Haghi, A. K. and Rondot, D.: Determination des Coefficients de Transfert de Chaleur lors du Sechage de Textiles par Thermographie Infrarouge et Microscopie Thermique a Balayage, Poster presentation, SFT, Paris, 1994, (in French).
- 2. Haghi, A. K. and Rondot, D.: Determination des Coefficient de Transfert de Chaleur lors du Sechage, 2nd DAS Int. Conf. Proc., 189-196, Romania, 1994, (in French).
- 3. Haghi, A. K.: Determination of heat transfer coefficients during the process of through drying of wet textile materials with an optico-mechanical scanning pyrometer & I.R. thermograph, 3rd DAS Int. Conf. Proc., 25-32, 1996, Romania.
- 4. HAGHI, A. K.: Controle de Materiaux par Thermographie Infrarouge: Modelisation et Experiences, 4rth DAS Int. Conf. Proc., 65-76, 1998, Romania, (in French).
- HAGHI, A. K.: A thermal imaging technique for measuring transient temperature field,
 5th DAS Int. Conf. Proc., 80-87, 2000, Romania.
- HAGHI, A. K.: Experimental investigations on drying of porous media using infrared radiation, Acta Polytechnica, 41, (2001), 55-57.
- HAGHI, A. K.: Some aspects of microwave drying, The Annals of Stefan Cel Mare University, 8(14), (2000), 60-65.
- ARMA, C. R. and CORTARY, J.C.: Experimental data and preliminary design of a nonconventional dryer of leather, Sixth Int. Drying Symp., IDS 85, Versailles, France, 1988, 59-63.
- BIENKIEWICZ, K. J.: Physical Chemistry of Leather Making, Robert E. Kriger Publication Co., 1983.
- Tomas, S. and Chou, W.: Drying of porous media, Drying Technology Int. J., 11(6), (1993), 273-278.
- SKANSI, D. and LARSON, G.: Experimental evaluation of the microwave drying of leather, Journal of the Society of Leather Technologists and Chemists, 79, (1993), 171-177.
- 12. Henry, P.S.: Diffusion in absorbing media, Proc. R. Soc., 171A, (1986), 215-655.
- 13. NORDON, P. and DAVID, H. G.: Coupled diffusion of moisture and heat in hygroscopic

- textile materials, Int. J. Heat Mass Trans., 10, (1967), 853-866.
- 14. Farnworth, B.A.: Numerical model of combined diffusion of heat and water vapor through clothing, Textile Res. J., **56**, (1986), 653-655.
- BEARD, J. N.: More efficient tenter frame operations through mathematical modeling, Textile Chem. Colorist, 3, (1976), 47-50.
- 16. TREYBAL, R. E.: Mass Transfer Operation, 2nd edition, McGraw-Hill Book Co., NY., 1968.

TIME RATES OF TENSORS IN CONTINUUM MECHANICS UNDER ARBITRARY TIME DEPENDENT TRANSFORMATIONS PART I. MATERIAL TIME RATES

IMRE KOZÁK
Department of Mechanics, University of Miskolc
3515 Miskolc – Egyetemváros, Hungary
mechkoz@gold.uni-miskolc.hu

[Received: April 16, 2001]

Abstract. The motion of a body and material time rates of tensors are investigated in three coordinate systems: in a fixed and a relative one – the latter is assumed to move arbitrarily with respect to the fixed coordinate system, i.e., it is deformable – and also in the convected coordinate system. Relations have been derived for the material time rates of arbitrary tensors in all three coordinate systems.

Mathematical Subject Classification: 73A05

Keywords: kinematics of continua, moving coordinate systems, relative motion of a body, material time rates of tensors

1. Introduction

1.1. Components of tensors at a point of space can be transformed from one coordinate system into another by making use of the general transformation rules of tensors. If the coordinate systems move with respect to each other, one speaks about time dependent transformations.

If the motion of the coordinate systems relative to each other is arbitrary (one of the coordinate systems is deformed with respect to the other) then the transformation is also referred to as arbitrary, otherwise, i.e., for a rigid body motion as relative motion of the coordinate system, the transformation is an orthogonal one and in both cases time dependent.

From this point of view those tensors (including some time rate of tensors) which can be defined independently of the choice of coordinate systems moving arbitrarily with respect to each other, i.e., which are invariant under any arbitrary and time dependent transformations, will be referred to as physically (or materially) objective, or, for the sake of brevity, objective tensors or objective rates. (We remark that in the literature criteria of physical objectivity are valid mostly for orthogonal transformation only.)

Fulfillment of physical objectivity is a necessary (but not sufficient) condition for

206 I. Kozák

tensors (and time rates of tensors) fulfilling the criterion of material objectivity and disregards the issue of establishing constitutive equations.

1.2. The first objective time rate, the Jaumann stress rate [1] is related to a coordinate system rotating together with the spin tensor of continuum. Later on the Jaumann stress rate was also derived by other authors - for example by Fromm [2], Zaremba [3], Thomas [4], Noll [5] and Hill [6]. These authors have not referred to Jaumann's work. In the literature, however, the Jaumann's stress rate is generally accepted although Atluri [7] associates it with the names Zaremba - Jaumann - Noll.

A detailed description of some objective time rates is presented, among others, by Sedov [8], Prager [9], Naghdi and Wainwright [10], Atluri [7], Masur [11], Dubey [12], Szabó and Balla [13], Haupt and Tsakamakis [14].

There are some famous objective time rates beside the Jaumann stress rate mentioned above. Using convective coordinates objective time rates of tensors with contravariant or covariant components were set up by Oldroyd [15], Trusdell [16], Cotter and Rivlin [17] and with all possible subscripts and superscripts by Sedov [8] and Atluri [7]. Atluri also gave the objective time rates in a fixed coordinate system. The stress rate introduced by Trusdell [16] is that of the II.Piola - Kirchhoff stress tensor. The objective time rates defined by Green and Naghdi [18], Green and McInnis [19], Dienes [20] and Atluri [7] are all regarded in a coordinate system rotating together with the spin tensor of the rotation tensor obtained from the polar decomposition of the deformation gradient. The objective time rate of Sowerby and Chu [21] is related to a coordinate system rotating with the spin tensor taken in the principal axis of the strains in the present configuration.

The objective time rates in [1] an [15]-[21] are all that of the stress tensor and invariance under orthogonal transformation is considered as a criterion for material objectivity.

References [7]-[14] offer not only a survey on the objective time rates but also a sort of systematization. The latter is grounded on the fact that the objective time rates are defined with the aid of a certain movement of the continuum, usually by the mapping of the reference configuration onto the present configuration or by the transformation between the fixed and convected coordinate systems or by the motion of the principal axis of strains. In some cases invariance under orthogonal transformations is a requirement, in the remaining cases, however, it is not.

After a wide mathematical foundation the book [22] by Marsden and Hughes also deals with the physically objective time rates pointing out that "All so called objective rates of second order tensors are in fact Lie derivatives."

1.3. Part I. and Part II. of the present paper are aimed to introduce physically objective time rates on the basis of mechanical (kinematical) considerations only and makes the introduction of the concept independent of the possible motions of continuum.

To accomplish this goal the paper investigates tensors and time rates of tensors in coordinate systems moving arbitrarily with respect to each other or, which is the same thing, in coordinate systems which are deformable. We regard alternatively one of the two coordinate systems as fixed; the other is then in motion with respect to

the fixed one.

1.4. Part I of the present paper investigates the motion of two distinct continua. One of the two continua is the coordinate system moving in the fixed coordinate system as a fictitious purely geometrical continuum. The other is the actual material continuum itself. At the same time the motion of the actual material continuum can be viewed both from the fixed coordinate system and from the one moving with respect to it.

In a particular case the convected coordinate system can also be regarded as a moving coordinate system or a fixed one (see, for example, Section 4). If this is the case, one should keep in mind that the continuum is at a relative rest in the convected coordinate system.

1.5. The next section investigates coordinate systems moving arbitrarily with respect to each other. Metric tensors, velocities, time derivatives of base vectors are also discussed.

Section 3 is devoted to the motion of a continuum in coordinate systems moving arbitrarily with respect to each other.

In Section 4 material time rates are defined in various coordinate systems including the fixed coordinate system, the coordinate system moving arbitrarily with respect to the fixed one and the convected coordinate system. The various time rates of the same tensor are related to each other and the corresponding relations are also presented.

1.6. We shall use both the indicial notations of tensors and the symbolic or direct notational system. The coordinate systems are arbitrary and curvilinear.

In accordance with the general rules of indicial notations - no matter whether the indices are minuscule or majuscule - indices range over the integers 1,2 and 3; summation over repeated indices is implied and the subscripts proceeded by a [comma] {semicolon} denotes [partial] {covariant} differentiation with respect to the corresponding variable. Underscore of indices suspends summation. δ_q^p stands for the Kronecker symbol.

As regards symbolic notations the dot product is denoted in the usual manner, i.e., by a dot placed between the factors, while no operation sign is employed to denote tensor products. If necessary, small asterisks are used to show where the indices stand, for example $\mathbf{A}^*_{\ *} = \hat{a}^k_{\ l} \hat{\mathbf{g}}_k \hat{\mathbf{g}}^l$ in which $\hat{\mathbf{g}}_k$ and $\hat{\mathbf{g}}^l$ are the base vectors. (In the case of indicial notations it is obvious where the indices are.)

The transpose of a tensor is denoted by T. We shall utilize the fact that the covariant derivatives are defined independently of a coordinate system.

Time is common for all sets of variables. At the points of time t_{\circ} and $t > t_{\circ}$ (otherwise t is arbitrary) the state of continuum is referred to as reference configuration and present configuration, respectively.

Further notations and notational conventions are presented at their first occurrence in the text.

2. Arbitrary motion of two coordinate systems with respect to each other

2.1. First let the coordinate system $\{x^p\}$ be the fixed one. The corresponding base vectors and the covariant metric tensor are

$$\mathbf{g}_{p}\left(x^{1}, x^{2}, x^{3}\right) = \frac{\partial \mathbf{r}}{\partial x^{p}}, \quad \mathbf{g}^{q}\left(x^{1}, x^{2}, x^{3}\right) \quad \text{and} \quad g_{pq}\left(x^{1}, x^{2}, x^{3}\right), \quad (2.1)$$

where \mathbf{r} is the position vector of a point P in space.

Let the coordinate system moving arbitrarily with respect to the coordinate system $\{x^p\}$ be denoted by $\{\widehat{x}^k\}$. The motion of the coordinate system $\{\widehat{x}^k\}$ relative to the coordinate system $\{x^p\}$ can be given in the form

$$x^p = {}^{(G)}x^p \left(\widehat{x}^1, \widehat{x}^2, \widehat{x}^3; t\right), \quad \text{where} \quad {}^{(G)}J = \det \frac{\partial^{(G)}x^p}{\partial \widehat{x}^k} \neq 0.$$
 (2.2)

Here and in the sequel a subscript in paranthesis to the left of the variable is of informative nature.

The base vectors in the coordinate system $\{\widehat{x}^k\}$ are of the form

$$\widehat{\mathbf{g}}_{k}\left(\widehat{x}^{1},\widehat{x}^{2},\widehat{x}^{3};t\right) = \frac{\partial \mathbf{r}}{\partial \widehat{x}^{k}} = \frac{\partial \mathbf{r}}{\partial x^{p}} \frac{\partial^{(G)} x^{p}}{\partial \widehat{x}^{k}} = \frac{\partial^{(G)} x^{p}}{\partial \widehat{x}^{k}} \mathbf{g}_{p}, \qquad \widehat{\mathbf{g}}^{l}\left(\widehat{x}^{1},\widehat{x}^{2},\widehat{x}^{3};t\right) = \frac{\partial \widehat{x}^{l}}{\partial^{(G)} x^{q}} \mathbf{g}^{q}. \tag{2.3}$$

The transformation matrices also depend on time and the matrix $\frac{\partial \hat{x}^l}{\partial^{(G)} x^p}$ is the inverse of the matrix $\frac{\partial^{(G)} x^p}{\partial \hat{x}^k}$.

The covariant metric tensor in the coordinate system $\{\hat{x}^k\}$ is

$$\widehat{g}_{kl}\left(\widehat{x}^{1}, \widehat{x}^{2}, \widehat{x}^{3}; t\right) = \frac{\partial^{(G)} x^{p}}{\partial \widehat{x}^{k}} \frac{\partial^{(G)} x^{q}}{\partial \widehat{x}^{l}} g_{pq}, \qquad g_{pq}\left(x^{1}, x^{2}, x^{3}\right). \tag{2.4}$$

As can be seen with ease neither \mathbf{g}_p nor g_{pq} depend on time for an observer being in the coordinate system $\{x^p\}$ while, on the contrary, both $\hat{\mathbf{g}}_k$ and \hat{g}_{kl} are time dependent.

Components of a tensor $\mathbf{A} = a^p_{\ q} \mathbf{g}_p \mathbf{g}^q = \widehat{a}^k_{\ l} \widehat{\mathbf{g}}_k \widehat{\mathbf{g}}^l$ regarded in the coordinate systems $\{x^p\}$ and $\{\widehat{x}^k\}$ obey the transformation rule which follows from (2.3):

$$\widehat{a}^{k}_{l} = \frac{\partial \widehat{x}^{k}}{\partial^{(G)} x^{p}} \frac{\partial^{(G)} x^{q}}{\partial \widehat{x}^{l}} a^{p}_{q}. \tag{2.5}$$

2.2. Secondly let the coordinate system $\{\hat{x}^k\}$ be the fixed one. In this case - for an observer in the coordinate system $\{\hat{x}^k\}$ - neither the base vectors $\hat{\mathbf{g}}_k, \hat{\mathbf{g}}^l$ nor the corresponding metric tensor \hat{g}_{kl} depend on time:

$$\widehat{\mathbf{g}}_{k}\left(\widehat{x}^{1},\widehat{x}^{2},\widehat{x}^{3}\right) = \frac{\partial \mathbf{r}}{\partial \widehat{x}^{k}}, \qquad \widehat{\mathbf{g}}^{l}\left(\widehat{x}^{1},\widehat{x}^{2},\widehat{x}^{3}\right), \qquad \widehat{g}_{kl}\left(\widehat{x}^{1},\widehat{x}^{2},\widehat{x}^{3}\right). \tag{2.6}$$

For the motion of the coordinate system $\{x^p\}$ relative to the coordinate system $\{\hat{x}^k\}$ we can write

$$\widehat{x}^k = {}^{(F)}\widehat{x}^k \left(x^1, x^2, x^3; t\right), \qquad {}^{(F)}J = \det \frac{\partial^{(F)}\widehat{x}^k}{\partial x^p} \neq 0.$$
 (2.7)

In this case the base vectors in the coordinate system $\{x^p\}$ are

$$\mathbf{g}_{p}\left(x^{1}, x^{2}, x^{3}; t\right) = \frac{\partial \mathbf{r}}{\partial x^{p}} = \frac{\partial \mathbf{r}}{\partial \widehat{x}^{k}} \frac{\partial^{(\mathrm{F})} \widehat{x}^{k}}{\partial x^{p}} = \frac{\partial^{(\mathrm{F})} \widehat{x}^{k}}{\partial x^{p}} \widehat{\mathbf{g}}_{k}, \qquad \mathbf{g}^{q}\left(x^{1}, x^{2}, x^{3}; t\right) = \frac{\partial x^{q}}{\partial^{(\mathrm{F})} \widehat{x}^{l}} \widehat{\mathbf{g}}^{l}.$$
(2.8)

The covariant metric tensor in the coordinate system $\{x^p\}$ takes the form

$$g_{pq}\left(x^{1}, x^{2}, x^{3}; t\right) = \frac{\partial^{(F)}\widehat{x}^{k}}{\partial x^{p}} \frac{\partial^{(F)}\widehat{x}^{l}}{\partial x^{q}} \widehat{g}_{kl}, \qquad \widehat{g}_{kl}\left(\widehat{x}^{1}, \widehat{x}^{2}, \widehat{x}^{3}\right). \tag{2.9}$$

The transformation matrices also depend on time and the matrix $\frac{\partial x^p}{\partial^{(F)}\widehat{x}^k}$ is the inverse of the matrix $\frac{\partial^{(F)}\widehat{x}^k}{\partial x^p}$.

The apparent contradiction between the formulae (2.4) and (2.9) giving the metric tensors follows from the fact that time dependence of tensor components depends on which coordinate system is regarded as a fixed one. If the coordinate system $\{x^p\}$ is the fixed one, g_{pq} is independent of time, but \hat{g}_{kl} is time dependent and, on the contrary, if $\{\hat{x}^k\}$ is the fixed coordinate system \hat{g}_{kl} is independent of time while g_{pq} is a function of time.

2.3. In the sequel - unless the opposite is stated - we shall always assume that the coordinate system $\{x^p\}$ is a fixed one while the coordinate system $\{\hat{x}^k\}$, which will be referred to as grid, is the moving one. [Use of the letter "F" (fixed) and "G" (grid) for the motions (2.7) and (2.2) implies this convention tacitly.]

This general convention means no limitation either on the arbitrariness of the motion of coordinate systems relative to each other or on the general validity of the conclusions we hope to come to.

In what follows

- the motion of a material continuum with respect to the fixed coordinate system $\{x^p\}$ will be referred to simply as motion or absolute motion,
- the motion of a material continuum with respect to the coordinate system $\{\hat{x}^k\}$, i.e., to the grid will be referred to as *relative motion*
- and the motion of the coordinate system $\{\hat{x}^k\}$, i.e., that of the grid with respect to the fixed coordinate system $\{x^p\}$ will be called *the motion of grid* or *grid motion*.
- **2.4.** Velocity of a point with coordinates \hat{x}^k of the grid with respect to $\{x^p\}$ follows from the grid motion (2.2):

$${}^{(Gx)}\mathbf{v} = \frac{\partial \mathbf{r}}{\partial t}\bigg|_{(\widehat{x})} = \frac{\partial \mathbf{r}}{\partial x^p} \left. \frac{\partial^{(G)} x^p}{\partial t} \right|_{(\widehat{x})} = {}^{(Gx)} v^p \mathbf{g}_p = {}^{(Gx)} \widehat{v}^k \widehat{\mathbf{g}}_k, \tag{2.10}$$

where
$$^{(Gx)}v^p = \frac{\partial^{(G)}x^p}{\partial t}\Big|_{(\widehat{x})}$$
 and $^{(Gx)}\widehat{v}^k = \frac{\partial \widehat{x}^k}{\partial^{(G)}x^p}{}^{(Gx)}v^p$ (2.11)

are the components of the velocity vector (Gx)**v** in the coordinate systems $\{x^p\}$ and $\{\hat{x}^k\}$. Here and in the sequel a subscript placed to the right of a vertical line – the latter is a right delimiter – refers to the fact that the corresponding coordinates are constants when one determines a time derivative.

With regard to all that has been said about the coordinate systems $\{x^p\}$ and $\{\hat{x}^k\}$ it is obvious that their roles are interchangeable. Comparison of (2.2) and (2.7) yields an identity

$$x^{p} = {}^{(G)}x^{p} \left[{}^{(F)}\widehat{x}^{1} \left(x^{1}, x^{2}, x^{3}; t \right), \widehat{x}^{2} \left(\cdots \right), \widehat{x}^{3} \left(\cdots \right); t \right] = x^{p}$$

which is valid at any point of the grid and from which, taking into account that the points $\{x^p\}$ do not move at all, a further identity follows:

$$\frac{\partial x^{p}}{\partial t}\Big|_{(x)} = 0 = \left. \frac{\partial^{(G)} x^{q}}{\partial t} \right|_{(\widehat{x})} + \left. \frac{\partial^{(G)} x^{p}}{\partial \widehat{x}^{k}} \right. \left. \frac{\partial^{(F)} \widehat{x}^{k}}{\partial t} \right|_{(x)}$$
(2.12)

where
$$\frac{\partial^{(F)}\widehat{x}^k}{\partial t}\Big|_{(x)} = {}^{(F\widehat{x})}\widehat{v}^k.$$
 (2.13)

Let x^p be a point of the coordinate system $\{x^p\}$. After substituting (2.13) and (2.11) into (2.12) we obtain the velocity $^{(F\widehat{x})}\mathbf{v}$ of the point x^p with respect to the grid – that is to the coordinate system $\{\widehat{x}^k\}$:

$$(\widehat{F}\widehat{\mathbf{x}})\widehat{v}^k = -\frac{\partial \widehat{x}^k}{\partial (G)_{x^p}} (G\mathbf{x}) v^p = -(G\mathbf{x})\widehat{v}^k, \quad \text{i.e.,} \quad (\widehat{F}\widehat{\mathbf{x}}) \mathbf{v} = -(G\mathbf{x}) \mathbf{v}.$$
 (2.14)

2.5. From the velocity vector field of the grid (Gx)**v** we can obtain, in the usual manner, the velocity gradient, the strain rate tensor and the spin tensor for the grid motion:

$$^{(Gx)}L = {^{(Gx)}l^p}_q \mathbf{g}_p \mathbf{g}^q = {^{(Gx)}\mathbf{v}\nabla}, {^{(Gx)}l^p}_q = {^{(Gx)}v^p}_{;q},$$
 (2.15)

$${}^{(Gx)}\boldsymbol{D} = {}^{(Gx)}d^{p}_{q}\mathbf{g}_{p}\mathbf{g}^{q} = \frac{1}{2}\left({}^{(Gx)}\boldsymbol{L} + {}^{(Gx)}\boldsymbol{L}^{\mathrm{T}}\right), \quad {}^{(Gx)}d^{p}_{q} = \frac{1}{2}\left({}^{(Gx)}l^{p}_{q} + {}^{(Gx)}l^{p}_{p}\right),$$

$$(2.16)$$

$$^{(Gx)}\boldsymbol{W} = ^{(Gx)}w^{p}_{q}\mathbf{g}_{p}\mathbf{g}^{q} = \frac{1}{2}\begin{pmatrix}^{(Gx)}\boldsymbol{L} - ^{(Gx)}\boldsymbol{L}^{\mathrm{T}}\end{pmatrix}, \quad ^{(Gx)}w^{p}_{q} = \frac{1}{2}\begin{pmatrix}^{(Gx)}l^{p}_{q} - ^{(Gx)}l^{p}_{q}\end{pmatrix}.$$

$$(2.17)$$

By making use of the transformation rule (2.5) we can readily obtain the components ${}^{(Gx)}\hat{l}^p_{q}$, ${}^{(Gx)}\hat{d}^p_{q}$, ${}^{(Gx)}\hat{w}^p_{q}$ as well, i.e., the components of the previous tensors in the coordinate system $\{\hat{x}^k\}$.

Recalling the definition of $^{(Gx)}L$ – see equation (2.15) – , we have

$$\frac{\partial}{\partial t} (d\mathbf{r}) \Big|_{(\widehat{x})} = d \left({}^{(G\mathbf{x})}\mathbf{v} \right) = {}^{(G\mathbf{x})}\mathbf{L} \cdot d\mathbf{r}.$$
 (2.18)

2.6. In accordance with (2.18) it also holds that

$$\frac{\partial \widehat{\mathbf{g}}_k}{\partial t} \bigg|_{(\widehat{\mathbf{x}})} = {}^{(G\mathbf{x})} \mathbf{L} \cdot \widehat{\mathbf{g}}_k, \qquad \frac{\partial \widehat{\mathbf{g}}^l}{\partial t} \bigg|_{(\widehat{\mathbf{x}})} = -\widehat{\mathbf{g}}^l \cdot {}^{(G\mathbf{x})} \mathbf{L}. \qquad (2.19)$$

3. Motion of a body in the absolute coordinate system and the grid

3.1. Let $\{X^K\}$ be the convected coordinate system. Further let the motion of the body with respect to the coordinate system $\{\hat{x}^k\}$ be

$$\widehat{x}^k = {}^{(\mathrm{B})}\widehat{x}^k \left(X^1, X^2, X^3; t \right), \qquad {}^{(\mathrm{B})}J = \det \frac{\partial^{(\mathrm{B})}\widehat{x}^k}{\partial X^K} \neq 0. \tag{3.1}$$

This motion is the relative motion of the body. By

$$x^{p} = {}^{(B)}x^{p} (X^{1}, X^{2}, X^{3}; t), \qquad J = \det \frac{\partial^{(B)}x^{p}}{\partial X^{K}} \neq 0$$
 (3.2)

we denote the motion of the body with respect to $\{x^p\}$ – absolute motion of the body. With the relative motion of the body it follows that

$$x^{p} = {}^{(\mathrm{B})}x^{p} \left(X^{1}, X^{2}, X^{3}; t \right) = {}^{(\mathrm{G})}x^{p} \left[{}^{(\mathrm{B})}\widehat{x}^{1} \left(X^{1}, X^{2}, X^{3}; t \right), {}^{(\mathrm{B})}\widehat{x}^{2} \left(\cdots \right), {}^{(\mathrm{B})}\widehat{x}^{3} \left(\cdots \right); t \right]$$

$$(3.3)$$

$$\text{and} \quad J = \det \frac{\partial^{(\mathrm{B})} x^p}{\partial X^K} = \det \frac{\partial^{(\mathrm{G})} x^p}{\partial \widehat{x}^k} \frac{\partial^{(\mathrm{B})} \widehat{x}^k}{\partial X^K} = \ ^{(\mathrm{G})} J^{\ (\mathrm{B})} J \neq 0.$$

3.2. The base vectors of the coordinate system $\{X^K\}$ assume the form

$$\widehat{\mathbf{G}}_{K} = \frac{\partial \mathbf{r}}{\partial X^{K}} = \frac{\partial \mathbf{r}}{\partial x^{p}} \frac{\partial^{(\mathrm{B})} x^{p}}{\partial X^{K}} = \frac{\partial^{(\mathrm{B})} x^{p}}{\partial X^{K}} \mathbf{g}_{p}, \qquad \widehat{\mathbf{G}}^{L} = \frac{\partial X^{L}}{\partial^{(\mathrm{B})} x^{q}} \mathbf{g}^{q}, \tag{3.4}$$

from which using (2.3) and (3.3) we obtain

$$\widehat{\mathbf{G}}_{K} = \frac{\partial^{(\mathrm{B})} x^{p}}{\partial X^{K}} \frac{\partial \widehat{x}^{k}}{\partial^{(\mathrm{G})} x^{p}} \widehat{\mathbf{g}}_{k} = \frac{\partial^{(\mathrm{G})} x^{p}}{\partial \widehat{x}^{l}} \frac{\partial^{(\mathrm{B})} \widehat{x}^{l}}{\partial X^{K}} \frac{\partial \widehat{x}^{k}}{\partial^{(\mathrm{G})} x^{p}} \widehat{\mathbf{g}}_{k} = \frac{\partial^{(\mathrm{B})} \widehat{x}^{k}}{\partial X^{K}} \widehat{\mathbf{g}}_{k}, \qquad \widehat{\mathbf{G}}^{L} = \frac{\partial X^{L}}{\partial^{(\mathrm{B})} \widehat{x}^{l}} \widehat{\mathbf{g}}^{l}.$$
(3.5)

The transformation matrices are again time dependent and the matrices $\frac{\partial X^L}{\partial^{(B)}x^q}$ and $\frac{\partial X^L}{\partial^{(B)}\hat{x}^l}$ are respectively inverses of the matrices $\frac{\partial^{(B)}x^p}{\partial X^K}$ and $\frac{\partial^{(B)}\hat{x}^k}{\partial X^K}$.

Using (3.4) and (3.5) for the covariant metric tensor of the coordinate system $\{X^K\}$ we can write

$$\widehat{G}_{KL} = \frac{\partial^{(\mathrm{B})} x^p}{\partial X^K} \frac{\partial^{(\mathrm{B})} x^q}{\partial X^L} g_{pq} = \frac{\partial^{(\mathrm{B})} \widehat{x}^k}{\partial X^K} \frac{\partial^{(\mathrm{B})} \widehat{x}^l}{\partial X^L} \widehat{g}_{kl}. \tag{3.6}$$

In view of (3.4) and (3.5) the components of a tensor $\mathbf{A} = a^p_{\ q} \mathbf{g}_p \mathbf{g}^q = \hat{a}^k_{\ l} \hat{\mathbf{g}}_k \hat{\mathbf{g}}^l = \hat{a}^K_{\ L} \hat{\mathbf{G}}_K \hat{\mathbf{G}}^L$, which is regarded in the fixed coordinate system $\{x^p\}$ and the coordinate systems $\{\hat{x}^k\}$ and $\{X^K\}$ each moving with respect to the fixed one, should follow the transformation rules

$$\widehat{\boldsymbol{a}}^{K}{}_{L} = \frac{\partial \boldsymbol{X}^{K}}{\partial^{(\mathrm{B})}\boldsymbol{x}^{p}} \frac{\partial^{(\mathrm{B})}\boldsymbol{x}^{q}}{\partial \boldsymbol{X}^{L}} \boldsymbol{a}^{p}{}_{q} = \frac{\partial \boldsymbol{X}^{K}}{\partial^{(\mathrm{B})}\widehat{\boldsymbol{x}}^{K}} \frac{\partial^{(\mathrm{B})}\widehat{\boldsymbol{x}}^{l}}{\partial \boldsymbol{X}^{L}} \widehat{\boldsymbol{a}}^{k}{}_{l}. \tag{3.7}$$

Without entering into further details, we mention that for the case when the convected coordinate system $\{X^K\}$ is chosen as a fixed one

$$\widehat{\mathbf{G}}_K\left(X^1, X^2, X^3\right) = \frac{\partial \mathbf{r}}{\partial X^K}, \qquad \widehat{\mathbf{G}}^L\left(X^1, X^2, X^3\right). \tag{3.8}$$

are the base vectors observed from the coordinate system itself.

3.3 The quantities we have defined so far are associated with the current configuration and are regarded at the spatial point P. The quantities that are regarded at the points of the reference configuration will be denoted by barred letters (for example $\overline{\mathbf{G}}_K$ or $\mathrm{d}\overline{\mathbf{r}}$).

Motion (3.2) is a mapping of the reference configuration onto the current configuration. The deformation gradient

$$\mathbf{F} = \frac{\partial^{(\mathrm{B})} x^p}{\partial X^L} \mathbf{g}_p \overline{\mathbf{G}}^L$$
 and its inverse $\mathbf{F}^{-1} = \frac{\partial X^K}{\partial^{(\mathrm{B})} x^q} \overline{\mathbf{G}}_K \mathbf{g}^q$ (3.9)

represent a linear mapping and remapping between the line elements $d\mathbf{\bar{r}} = dX^K \mathbf{\bar{G}}_K$ and $d\mathbf{r} = dx^p \mathbf{g}_p$ regarded, respectively, in the reference and current configurations:

$$d\mathbf{r} = \mathbf{F} \cdot d\overline{\mathbf{r}}, \qquad d\overline{\mathbf{r}} = \mathbf{F}^{-1} \cdot d\mathbf{r}.$$
 (3.10)

With the line elements $d\overline{\mathbf{r}} = d\overline{s}\,\overline{\mathbf{e}}$ and $d\mathbf{r} = ds\,\mathbf{e}$, in which $\overline{\mathbf{e}}$ and \mathbf{e} are unit vectors in the reference and current configurations, one can define stretches in the directions $\overline{\mathbf{e}}$ and \mathbf{e} :

$$\lambda_e = \frac{\mathrm{d}s}{\mathrm{d}\overline{s}}, \qquad \lambda_e^2 = \overline{\mathbf{e}} \cdot \mathbf{F}^{\mathrm{T}} \cdot \mathbf{F} \cdot \overline{\mathbf{e}} = \frac{1}{\mathbf{e} \cdot (\mathbf{F}^{-1})^{\mathrm{T}} \cdot \mathbf{F}^{-1} \cdot \mathbf{e}}.$$
 (3.11)

3.4. By using the polar decomposition theorem, the deformation gradient F (det $F = J \neq 0$) can be decomposed into the dot product of the rotation tensor

$$\mathbf{R} = R_K^p \mathbf{g}_p \overline{\mathbf{G}}^K, \qquad \mathbf{R}^{-1} = \mathbf{R}^{\mathrm{T}}$$
 (3.12)

with the right and left stretch tensors

$$\overline{U} = \overline{U}_L^K \overline{\mathbf{G}}_K \overline{\mathbf{G}}^L, \qquad V = V_a^p \mathbf{g}_p \mathbf{g}^q \tag{3.13}$$

in a unique fashion:

$$\mathbf{F} = \mathbf{R} \cdot \overline{\mathbf{U}} = \mathbf{V} \cdot \mathbf{R}. \tag{3.14}$$

Here the tensors \overline{U} and V are defined in the reference and current configurations and are both positive definite and symmetric tensors while the tensor R is orthogonal.

Let $\overline{\mathbf{n}}_p$ and \mathbf{n}_q be orthonormal eigenvectors directed along the principal axes of the stretch tensors $\overline{\boldsymbol{U}}$ and \boldsymbol{V} , respectively. The coordinate systems constituted by the principal axes of the right and left stretch tensors are denoted by $\{\overline{\nu}^p\}$ and $\{\nu^p\}$. It can be shown that

$$\mathbf{n}_p = \mathbf{R} \cdot \overline{\mathbf{n}}_p, \qquad \overline{\mathbf{n}}_p = \mathbf{R}^{\mathrm{T}} \cdot \mathbf{n}_p$$
 (3.15)

The tensors \overline{U} and V have the same eigenvalues (denoted by λ_p). In the coordinate systems $\{\overline{\nu}^p\}$ and $\{\nu^p\}$ we have

$$\overline{\boldsymbol{U}} = \lambda_{\underline{p}} \delta_q^p \overline{\mathbf{n}}_p \overline{\mathbf{n}}^q, \quad \overline{\boldsymbol{U}}^{-1} = \frac{1}{\lambda_{\underline{p}}} \delta_q^p \overline{\mathbf{n}}_p \overline{\mathbf{n}}^q, \qquad \boldsymbol{V} = \lambda_{\underline{p}} \delta_q^p \mathbf{n}_p \mathbf{n}^q, \quad \boldsymbol{V}^{-1} = \frac{1}{\lambda_{\underline{p}}} \delta_q^p \mathbf{n}_p \mathbf{n}^q.$$
(3.16)

In addition we define the *Hencky strain tensor* in the coordinate system $\{\nu^p\}$

$$\ln \mathbf{V} = \ln \lambda_p \delta_q^p \mathbf{n}_p \mathbf{n}^q. \tag{3.17}$$

3.5. The velocity vector of the moving continuum at the point with coordinates X^K observed from the coordinate system $\{x^p\}$ can be obtained from the motion (3.2):

$${}^{(x)}\mathbf{v} = \frac{\partial \mathbf{r}}{\partial t}\Big|_{(X)} = \frac{\partial \mathbf{r}}{\partial x^p} \left. \frac{\partial^{(B)} x^p}{\partial t} \right|_{(X)} = {}^{(x)} v^p \mathbf{g}_p, \qquad {}^{(x)} v^p = \left. \frac{\partial^{(B)} x^p}{\partial t} \right|_{(X)}. \tag{3.18}$$

From the velocity vector field $^{(x)}\mathbf{v}$ of the moving continuum we can derive the velocity gradient, the strain rate tensor and the spin tensor:

$${}^{(\mathbf{x})}\boldsymbol{L} = {}^{(\mathbf{x})}l^p_{\ q}\mathbf{g}_p\mathbf{g}^q = {}^{(\mathbf{x})}\mathbf{v}\nabla, \quad {}^{(\mathbf{x})}l^p_{\ q} = {}^{(\mathbf{x})}v^p_{\ ;q}, \tag{3.19}$$

$${}^{(\mathbf{x})}\boldsymbol{D} = {}^{(\mathbf{x})}d^{p}_{q}\mathbf{g}_{p}\mathbf{g}^{q} = \frac{1}{2}\left({}^{(\mathbf{x})}\boldsymbol{L} + {}^{(\mathbf{x})}\boldsymbol{L}^{\mathrm{T}}\right), \quad {}^{(\mathbf{x})}d^{p}_{q} = \frac{1}{2}\left({}^{(\mathbf{x})}l^{p}_{q} + {}^{(\mathbf{x})}l^{p}_{q}\right), \quad (3.20)$$

$${}^{(x)} \mathbf{W} = {}^{(x)} w^{p}_{q} \mathbf{g}_{p} \mathbf{g}^{q} = \frac{1}{2} \left({}^{(x)} \mathbf{L} - {}^{(x)} \mathbf{L}^{T} \right), \quad {}^{(x)} w^{p}_{q} = \frac{1}{2} \left({}^{(x)} l^{p}_{q} - {}^{(x)} l_{q}^{p} \right). \quad (3.21)$$

The velocity vector at the point with coordinates X^K of the continuum being now observed from the coordinate system $\{\hat{x}^k\}$ (from the grid), i.e., the relative velocity of the continuum follows from the the relative motion (3.1):

$${}^{(\widehat{\mathbf{x}})}\mathbf{v} = \frac{\partial \mathbf{r}}{\partial \widehat{x}^k} \left. \frac{\partial^{(\mathbf{B})} \widehat{x}^k}{\partial t} \right|_{(X)} = {}^{(\widehat{\mathbf{x}})} \widehat{v}^k \widehat{\mathbf{g}}_k, \qquad {}^{(\widehat{\mathbf{x}})} \widehat{v}^k = \left. \frac{\partial \widehat{x}^k}{\partial t} \right|_{(X)}. \tag{3.22}$$

From the relative velocity vector field of the continuum we can obtain the relative velocity gradient, the relative strain rate tensor and the relative spin tensor:

$${}^{(\widehat{\mathbf{x}})}\boldsymbol{L} = {}^{(\widehat{\mathbf{x}})}\widehat{l}^{k}{}_{l}\widehat{\mathbf{g}}_{k}\widehat{\mathbf{g}}^{l} = \frac{\partial}{\partial\widehat{x}^{l}} \left({}^{(\widehat{\mathbf{x}})}\mathbf{v}\right)\widehat{\mathbf{g}}^{l}, \quad {}^{(\widehat{\mathbf{x}})}\widehat{l}^{k}{}_{l} = {}^{(\widehat{\mathbf{x}})}\widehat{v}^{k}{}_{;l}, \tag{3.23}$$

$${}^{(\widehat{\mathbf{x}})}\boldsymbol{D} = {}^{(\widehat{\mathbf{x}})}\widehat{d}^{k}_{\ l}\widehat{\mathbf{g}}_{k}\widehat{\mathbf{g}}^{l} = \frac{1}{2}\left({}^{(\widehat{\mathbf{x}})}\boldsymbol{L} + {}^{(\widehat{\mathbf{x}})}\boldsymbol{L}^{\mathrm{T}}\right), \quad \widehat{d}^{k}_{\ l} = \frac{1}{2}\left({}^{(\widehat{\mathbf{x}})}\widehat{l}^{k}_{\ l} + {}^{(\widehat{\mathbf{x}})}\widehat{l}^{k}_{\ l}\right), \quad (3.24)$$

$$(\widehat{\mathbf{x}}) \mathbf{W} = (\widehat{\mathbf{x}}) \widehat{\mathbf{w}}_{l}^{k} \widehat{\mathbf{g}}_{k} \widehat{\mathbf{g}}^{l} = \frac{1}{2} ((\widehat{\mathbf{x}}) \mathbf{L} - (\widehat{\mathbf{x}}) \mathbf{L}^{\mathrm{T}}), \quad (\widehat{\mathbf{x}}) \widehat{\mathbf{w}}_{l}^{k} = \frac{1}{2} ((\widehat{\mathbf{x}}) \widehat{l}_{l}^{k} - (\widehat{\mathbf{x}}) \widehat{l}_{l}^{k}). \quad (3.25)$$

It follows from the nature of things that the velocity at the point X^K of the continuum with respect to the convected coordinate system $\{X^K\}$ vanishes: $(X^K)\mathbf{v} = \mathbf{0}$, $(X^K)\mathbf{v}^K = \mathbf{0}$.

Similarly, it can be checked with ease that $^{(X)}L = ^{(X)}D = ^{(X)}W = 0$.

3.6. Velocities of the points of continuum defined in the coordinate systems $\{x^p\}$ and $\{\hat{x}^k\}$ can be related to each other by using the motion (2.2) of the grid and the relative motion (3.1) of continuum:

$$\mathbf{v} = \frac{\partial \mathbf{r}}{\partial t}\bigg|_{(X)} = \frac{\partial \mathbf{r}}{\partial x^p} \left(\left. \frac{\partial^{(\mathbf{G})} x^p}{\partial t} \right|_{(\widehat{x})} + \frac{\partial^{(\mathbf{G})} x^p}{\partial \widehat{x}^k} \left. \frac{\partial^{(\mathbf{B})} \widehat{x}^k}{\partial t} \right|_{(X)} \right).$$

Substituting (2.10) and (3.22) we arrive at the result

$${}^{(\mathbf{x})}v^p = {}^{(\mathbf{G}\mathbf{x})}v^p + \frac{\partial^{(\mathbf{G})}x^p}{\partial \widehat{x}^k} {}^{(\widehat{\mathbf{x}})}\widehat{v}^k = {}^{(\mathbf{G}\mathbf{x})}v^p + {}^{(\widehat{\mathbf{x}})}v^p \quad \text{or} \quad {}^{(\mathbf{x})}\mathbf{v} = {}^{(\mathbf{G}\mathbf{x})}\mathbf{v} + {}^{(\widehat{\mathbf{x}})}\mathbf{v}. \quad (3.26)$$

From equation (3.26), which relates the various velocities to each other, taking equations (2.15)-(2.17), (3.19)-(3.21) and (3.23)-(3.25) into account, we can readily establish further equations for the velocity gradients, the strain rate tensors and the spin tensors:

$${}^{(x)}L = {}^{(Gx)}L + {}^{(\widehat{x})}L {}^{(x)}l^p_{\ a} = {}^{(Gx)}l^p_{\ a} + {}^{(\widehat{x})}l^p_{\ a},$$
(3.27)

$${}^{(x)}D = {}^{(Gx)}D + {}^{(\widehat{x})}D, \quad {}^{(x)}d^{p}_{q} = {}^{(Gx)}d^{p}_{q} + {}^{(\widehat{x})}d^{p}_{q}, \tag{3.28}$$

$${}^{(\mathbf{x})} \mathbf{W} = {}^{(\mathbf{G}\mathbf{x})} \mathbf{W} + {}^{(\widehat{\mathbf{x}})} \mathbf{W}, \quad {}^{(\mathbf{x})} w_{q}^{p} = {}^{(\mathbf{G}\mathbf{x})} w_{q}^{p} + {}^{(\widehat{\mathbf{x}})} w_{q}^{p}.$$
(3.29)

The component forms of equations (3.27)-(3.29) can be written not only in the coordinate system $\{x^p\}$, but also in the coordinate system $\{\hat{x}^k\}$ and $\{X^K\}$.

3.7. On the analogy of equation (2.19) we can obtain the time derivatives [measured in the coordinate system $\{x^p\}$] of the base vectors $\hat{\mathbf{G}}_K$ and $\hat{\mathbf{G}}^L$:

$$\stackrel{\text{(x)}}{\vdots} \frac{\partial \widehat{\mathbf{G}}_K}{\partial t} \Big|_{(X)} = \stackrel{\text{(x)}}{\mathbf{L}} \cdot \widehat{\mathbf{G}}_K, \qquad \stackrel{\text{(x)}}{\vdots} \frac{\partial \widehat{\mathbf{G}}^L}{\partial t} \Big|_{(X)} = -\widehat{\mathbf{G}}^L \cdot \stackrel{\text{(x)}}{\mathbf{L}}. \tag{3.30}$$

Similarly, for the time derivatives of the base vectors $\hat{\mathbf{G}}_K$ and $\hat{\mathbf{G}}^L$ [measured in the coordinate system $\{\hat{x}^k\}$] we have:

$$\stackrel{\widehat{(\widehat{\mathbf{x}})}}{\vdots} \frac{\partial \widehat{\mathbf{G}}_K}{\partial t} \Big|_{(X)} = \stackrel{\widehat{(\widehat{\mathbf{x}})}}{\mathbf{L}} \cdot \widehat{\mathbf{G}}_K, \qquad \stackrel{\widehat{(\widehat{\mathbf{x}})}}{\vdots} \frac{\partial \widehat{\mathbf{G}}^L}{\partial t} \Big|_{(X)} = -\widehat{\mathbf{G}}^L \cdot \stackrel{\widehat{(\widehat{\mathbf{x}})}}{\mathbf{L}}. \tag{3.31}$$

4. Material time rates of tensors

4.1. First, we shall separately define material time derivatives in the coordinate systems $\{x^p\}$, $\{\hat{x}^k\}$ and $\{X^K\}$. Then we are seeking relations between the material time derivatives so introduced. Special care will be given to the metric tensor.

Consider the tensor fields

$$\boldsymbol{A} = a_{pq} \mathbf{g}^{p} \mathbf{g}^{q}, \quad \boldsymbol{B} = \widehat{b}_{kl} \widehat{\mathbf{g}}^{k} \mathbf{g}^{l}, \quad \boldsymbol{C} = \widehat{c}_{KL} \widehat{\mathbf{G}}^{K} \widehat{\mathbf{G}}^{L},$$

$$a_{pq} \left(x^{1}, x^{2}, x^{3}; t \right), \quad \mathbf{g}^{p} \left(x^{1}, x^{2}, x^{3} \right),$$

$$\widehat{b}_{kl} \left(\widehat{x}^{1}, \widehat{x}^{2}, \widehat{x}^{3}; t \right), \quad \widehat{\mathbf{g}}^{k} \left(\widehat{x}^{1}, \widehat{x}^{2}, \widehat{x}^{3} \right),$$

$$\widehat{c}_{KL} \left(X^{1}, X^{2}, X^{3}; t \right), \quad \widehat{\mathbf{G}}^{K} \left(X^{1}, X^{2}, X^{3} \right).$$

written in the various coordinate systems as if they were fixed coordinate systems. By material time derivatives defined in the coordinate systems introduced, and for the tensors listed above we mean the time rate of change of the given tensor with respect to the coordinate system in which the tensor is defined and taken at the material point identified by the convected coordinates $\{X^K\}$.

Taking the possibilities one by one

- if $\{x^p\}$ is the defining coordinate system in which the continuum moves according to equation (3.2) and with the velocity (x) given by equation (3.18) then

$${}^{(x)}\boldsymbol{A}^{\cdot} = {}^{(x)}\dot{a}_{pq}\mathbf{g}^{p}\mathbf{g}^{q} = \left. \begin{array}{c} {}^{(x)}\\ \vdots\\ \frac{\partial \boldsymbol{A}}{\partial t} \right|_{(X)} = \frac{\partial a_{pq}}{\partial t} \bigg|_{(x)}\mathbf{g}^{p}\mathbf{g}^{q} + \frac{\partial \boldsymbol{A}}{\partial x^{s}} \bigg|_{(x)} \frac{\partial^{(\mathrm{B})}x^{s}}{\partial t} \bigg|_{(X)}, \quad (4.1)$$

i.e.,
$${}^{(x)}\dot{a}_{pq} = \frac{\partial a_{pq}}{\partial t}\Big|_{(x)} + a_{pq;s} {}^{(x)}v^x,$$
 (4.2)

- if $\{\hat{x}^k\}$ is the defining coordinate system with respect to which the continuum moves according to (3.1) and with the with velocity $^{(\hat{\mathbf{x}})}\mathbf{v}$ given by equation (3.22) then

$${}^{(\widehat{\mathbf{x}})}\boldsymbol{B}^{\cdot} = {}^{(\widehat{\mathbf{x}})}\widehat{b}_{kl}\widehat{\mathbf{g}}^{k}\widehat{\mathbf{g}}^{l} = {}^{(\widehat{\mathbf{x}})}\frac{\partial \boldsymbol{A}}{\partial t}\Big|_{(X)} = \frac{\partial \widehat{b}_{kl}}{\partial t}\Big|_{(\widehat{x})}\widehat{\mathbf{g}}^{k}\widehat{\mathbf{g}}^{l} + \frac{\partial \boldsymbol{B}}{\partial \widehat{x}^{m}}\Big|_{(\widehat{x})}\frac{\partial^{(\mathbf{B})}\widehat{x}^{m}}{\partial t}\Big|_{(X)}, \qquad (4.3)$$

i.e.,
$$\widehat{\hat{y}}\hat{b}_{kl} = \frac{\partial \widehat{b}_{kl}}{\partial t}\Big|_{\widehat{(x)}} + \widehat{b}_{kl;m} \widehat{\hat{y}}^m,$$
 (4.4)

- if $\{X^K\}$ is the defining coordinate system in which the continuum does not move, i.e., the velocity $^{(X)}\mathbf{v} = \mathbf{0}$ then

$${}^{(X)}\boldsymbol{C}^{\cdot} = {}^{(X)}\widehat{\boldsymbol{c}}_{KL}\widehat{\mathbf{G}}^{K}\widehat{\mathbf{G}}^{L} = \left. \begin{array}{c} {}^{(X)}\\ \vdots\\ \partial t \end{array} \right|_{(X)} = \left. \frac{\partial \widehat{\boldsymbol{c}}_{KL}}{\partial t} \right|_{(X)} \widehat{\mathbf{G}}^{K}\widehat{\mathbf{G}}^{L}, \tag{4.5}$$

i.e.,
$${}^{(X)}\hat{c}_{KL} = \frac{\partial \hat{c}_{KL}}{\partial t}\Big|_{(X)}$$
. (4.6)

Making use of the previous results, material time derivatives can be established for second-order tensors with position of indices other than above and for any tensor of higher order.

The material time derivatives obey the derivation rules valid for the sum and product of tensors.

Being real tensors the material time derivatives follow the general transformation laws of tensors. According to (2.5) for example:

$${}^{(\mathbf{x})}\widehat{\dot{a}}_{l}^{k} = \frac{\partial \widehat{x}^{k}}{\partial {}^{(\mathbf{G})}x^{p}} \frac{\partial {}^{(\mathbf{G})}x^{q}}{\partial \widehat{x}^{l}} {}^{(\mathbf{x})}\dot{a}_{q}^{p}. \tag{4.7}$$

4.2 The material time derivatives of the independent tensors A, B and C, which we have defined in a given coordinate system and discussed so far, are also independent of each other.

We are, however, faced with a distinct case when we consider the material time derivatives of the same tensor in various coordinate systems which move with respect to each other, i.e., if the tensor in question is defined independently of a coordinate system since, on the contrary, the material time derivative itself is always defined in a given coordinate system, as is the case, for instance, in respect of the material time derivatives of the tensor

$$\mathbf{A} = a_{pq} \mathbf{g}^p \mathbf{g}^q = \hat{a}_{kl} \hat{\mathbf{g}}^k \hat{\mathbf{g}}^l = \hat{a}_{KL} \hat{\mathbf{G}}^K \hat{\mathbf{G}}^L. \tag{4.8}$$

Depending on what the coordinate system is, the material time derivative of a tensor will be referred to as

- material time derivative if it is defined in the coordinate system $\{x^p\}$,
- relative material time derivative if it is defined in the coordinate system $\{\hat{x}^k\}$,
- convected material time derivative if it is defined in the coordinate system $\{X^K\}$.

In addition, relations can be established between the various material time derivatives.

Assuming that formulae (4.2), (4.4) and (4.6) are valid for the tensor field given by (4.8), we obtain for the tensor \boldsymbol{A} , the material time derivative, the relative material time derivative and the convected material time derivative:

$$^{(\mathbf{x})}\dot{a}_{pq} = \frac{\partial a_{pq}}{\partial t}\Big|_{(x)} + a_{pq;s} ^{(\mathbf{x})} v^{x}, \tag{4.9}$$

$$(\widehat{\mathbf{x}})(\widehat{a}_{kl}) = \frac{\partial \widehat{a}_{kl}}{\partial t} \Big|_{(\widehat{\mathbf{x}})} + \widehat{a}_{kl;m}(\widehat{\mathbf{x}})\widehat{v}^{m}, \tag{4.10}$$

$$(X)(\widehat{a}_{KL}) = \frac{\partial \widehat{a}_{KL}}{\partial t} \bigg|_{(X)}.$$
(4.11)

The preceding equations could be used with minor changes concerning the position of indices for second-order tensors with indices positioned differently and for a tensor of any order.

4.3. Material time derivatives, defined respectively in the coordinate systems $\{x^p\}$ and $\{\hat{x}^k\}$, $\{x^p\}$ and $\{X^K\}$, and finally in the coordinate systems $\{\hat{x}^k\}$ and $\{X^K\}$

can be related to each other by means of the motion of grid and continuum in the coordinate system $\{x^p\}$, provided that the coordinate system $\{x^p\}$ is fixed.

Indeed, the material time derivative of the tensor (4.8) defined independently of the choice of a coordinate system can also be determined in the following manner:

$$(\mathbf{x}) \mathbf{A} = (\mathbf{x}) \left(\mathbf{A} \left(\widehat{x}^{1}, \widehat{x}^{2}, \widehat{x}^{3}; t \right) \right) = \left[\frac{\partial \left(\widehat{a}_{kl} \widehat{\mathbf{g}}^{k} \widehat{\mathbf{g}}^{l} \right)}{\partial t} \right]_{(X)} =$$

$$= \left[\frac{\partial \left(\widehat{a}_{kl} \widehat{\mathbf{g}}^{k} \widehat{\mathbf{g}}^{l} \right)}{\partial t} \right]_{(\widehat{x})} + \frac{\partial \mathbf{A}}{\partial \widehat{x}^{m}} \frac{\partial^{(\mathbf{B})} \widehat{x}^{m}}{\partial t} \right]_{(X)} =$$

$$= \frac{\partial \widehat{a}_{kl}}{\partial t} \Big|_{(\widehat{x})} \widehat{\mathbf{g}}^{k} \widehat{\mathbf{g}}^{l} + \widehat{a}_{kl} \left(\frac{\partial \widehat{\mathbf{g}}^{k}}{\partial t} \right)_{(\widehat{x})} \widehat{\mathbf{g}}^{l} + \widehat{\mathbf{g}}^{k} \left[\frac{\partial \widehat{\mathbf{g}}^{l}}{\partial t} \right]_{(\widehat{x})} + \frac{\partial \mathbf{A}}{\partial \widehat{x}^{m}} \frac{\partial^{(\mathbf{B})} \widehat{x}^{m}}{\partial t} \Big|_{(X)}. \tag{4.12}$$

Substituting equations (4.10) and (2.19) we obtain

$$\mathbf{A}^{\cdot} = \mathbf{A}^{\cdot} = \mathbf{A} \cdot \mathbf{A} \cdot$$

where $^{(Gx)}L$ is the velocity gradient for the motion of grid. The asterisks which indicate the positions of indices, refer to the fact that the relation between the two material time derivatives depends on the positions of indices in the grid coordinate system $\{\hat{x}^k\}$.

We may notice that the difference between (x) A and $(\widehat{x}) A_{**}$ follows from the change of the base vectors $\widehat{\mathbf{g}}^k$ and $\widehat{\mathbf{g}}^l$ of the grid coordinate system $\{\widehat{x}^k\}$ in the fixed coordinate system $\{x^p\}$.

By repeating the above procedure for other positions of indices and gathering then the results we may write

I.
$$(\widehat{\mathbf{x}}) (\mathbf{A}_{**}) = (\widehat{\mathbf{x}}) \mathbf{A} + (\widehat{\mathbf{G}} \widehat{\mathbf{x}}) \mathbf{L}^{\mathrm{T}} \cdot \mathbf{A} + \mathbf{A} \cdot (\widehat{\mathbf{G}} \widehat{\mathbf{x}}) \mathbf{L},$$
 (4.13)

II.
$$(\widehat{\mathbf{x}}) (\mathbf{A}^*) = (\mathbf{x}) \mathbf{A} - (\mathbf{G}\mathbf{x}) \mathbf{L} \cdot \mathbf{A} + \mathbf{A} \cdot (\mathbf{G}\mathbf{x}) \mathbf{L},$$
 (4.14)

III.
$$(\widehat{\mathbf{x}}) (\mathbf{A}_{*}^{*})^{\cdot} = (\mathbf{x}) \mathbf{A}^{\cdot} + (\mathbf{G}\mathbf{x}) \mathbf{L}^{\mathrm{T}} \cdot \mathbf{A} - \mathbf{A} \cdot (\mathbf{G}\mathbf{x}) \mathbf{L}^{\mathrm{T}},$$
 (4.15)

IV.
$$(\widehat{\mathbf{x}}) (\mathbf{A}^{**}) = (\mathbf{x}) \mathbf{A} - (\mathbf{G}\mathbf{x}) \mathbf{L} \cdot \mathbf{A} - \mathbf{A} \cdot (\mathbf{G}\mathbf{x}) \mathbf{L}^{\mathrm{T}}.$$
 (4.16)

In the case $^{(Gx)}D = 0$, i.e., if the grid has a rigid body motion, $^{(Gx)}L = ^{(Gx)}W$, where $^{(Gx)}W$ is the spin tensor of the grid, equations (4.13)-(4.16) lead to the equations

$${}^{(\widehat{\mathbf{x}})}(\boldsymbol{A}_{**})^{\cdot} = {}^{(\widehat{\mathbf{x}})}(\boldsymbol{A}_{*}^{*})^{\cdot} = {}^{(\widehat{\mathbf{x}})}(\boldsymbol{A}_{*}^{*})^{\cdot} = {}^{(\widehat{\mathbf{x}})}(\boldsymbol{A}^{**})^{\cdot} = {}^{(\widehat{\mathbf{x}})}\boldsymbol{A}^{\cdot}, \tag{4.17}$$

$${}^{(\widehat{\mathbf{x}})}\boldsymbol{A}^{\cdot} = {}^{(\mathbf{x})}\boldsymbol{A}^{\cdot} - {}^{(\mathbf{G}\mathbf{x})}\boldsymbol{W} \cdot \boldsymbol{A} + \boldsymbol{A} \cdot {}^{(\mathbf{G}\mathbf{x})}\boldsymbol{W}. \tag{4.18}$$

It is clear that the latter equation, which relates material time derivatives defined in the coordinate systems $\{\hat{x}^k\}$ and $\{x^p\}$, is independent of the position of indices.

4.4. Apply all that has been said above to the metric tensors. In the case when $\{x^p\}$ is the fixed coordinate system then, according to (2.4), g_{pq} does not depend on time but \hat{g}_{kl} does, and conversely, when $\{\hat{x}^k\}$ is the fixed coordinate system, then \hat{g}_{kl} does not depend on time but g_{pq} does. Accordingly if, for instance, $\{x^p\}$ is the fixed coordinate system, then on the basis of equation (4.13) it follows

$$\stackrel{\text{(x)}}{\partial pq} \frac{\partial^{\text{(G)}} x^p}{\partial \widehat{x}^k} \frac{\partial^{\text{(G)}} x^q}{\partial \widehat{x}^l} = 0 = \stackrel{(\widehat{\mathbf{x}})}{(\widehat{g}_{kl})} - \stackrel{\text{(Gx)}}{\widehat{l}^s}_k \widehat{g}_{sl} - \widehat{g}_{ks} \stackrel{\text{(Gx)}}{\widehat{l}^s}_l,$$
i.e.
$$\stackrel{(\widehat{\mathbf{x}})}{(\widehat{g}_{kl})} = \stackrel{\text{(Gx)}}{\widehat{l}_{lk}} + \stackrel{\text{(Gx)}}{\widehat{l}_{kl}} = 2 \stackrel{\text{(Gx)}}{\widehat{d}_{kl}}.$$
(4.19)

Similarly, on the basis of equation (4.16) we have

$$(\widehat{\mathbf{x}}) (\widehat{g}^{kl})^{\cdot} = -2 (G_{\mathbf{x}}) \widehat{d}^{kl}.$$

4.5. Consider now the case of two grids moving arbitrarily with respect to each other. Let $\{\hat{x}^k\}$ and $\{\hat{\xi}^b\}$ be the two grids. Further let $(\xi \hat{x}) L = (\xi x) L - (Gx) L$, where $(\xi x) L$ and (Gx) L are the velocity gradients in the coordinate systems $\{\hat{\xi}^b\}$ and $\{\hat{x}^k\}$ being measured in the coordinate system $\{x^p\}$. In other words $(\xi \hat{x}) L$ is the gradient of the velocity $(\xi \hat{x}) \mathbf{v} = (\xi x) \mathbf{v} - (Gx) \mathbf{v}$, which we measure observing the motion of the coordinate system $\{\hat{\xi}^b\}$ from the coordinate system $\{\hat{x}^k\}$. Writing the equations (4.13)-(4.16) both for the coordinate system $\{\hat{x}^k\}$ and for the coordinate system $\{\hat{\xi}^b\}$ and then subtracting the equations resulting from each other we obtain:

I.
$$(\widehat{\xi}) (\boldsymbol{A}_{**})^{\cdot} = (\widehat{x}) (\boldsymbol{A}_{**})^{\cdot} + (\widehat{\xi}\widehat{x}) \boldsymbol{L}^{\mathrm{T}} \cdot \boldsymbol{A} + \boldsymbol{A} \cdot (\widehat{\xi}\widehat{x}) \boldsymbol{L},$$
 (4.20)

II.
$$(\widehat{\xi}) (\boldsymbol{A}_{*}^{*})^{\cdot} = (\widehat{x}) (\boldsymbol{A}_{*}^{*})^{\cdot} - (\widehat{\xi}\widehat{x}) \boldsymbol{L} \cdot \boldsymbol{A} + \boldsymbol{A} \cdot (\widehat{\xi}\widehat{x}) \boldsymbol{L},$$
 (4.21)

III.
$$(\widehat{\xi})(\boldsymbol{A}_{*}^{*})^{\cdot} = (\widehat{x})(\boldsymbol{A}_{*}^{*})^{\cdot} + (\widehat{\xi}\widehat{x})\boldsymbol{L}^{\mathrm{T}} \cdot \boldsymbol{A} - \boldsymbol{A} \cdot (\widehat{\xi}\widehat{x})\boldsymbol{L}^{\mathrm{T}},$$
 (4.22)

IV.
$$(\widehat{\xi})(A^{**}) = (\widehat{x})(A^{**}) - (\widehat{\xi}\widehat{x})L \cdot A - A \cdot (\widehat{\xi}\widehat{x})L^{\mathrm{T}}.$$
 (4.23)

The results implied in equations (4.13)-(4.16) and (4.20)-(4.23) can be summarized as follows:

If the material time derivative of a tensor defined in a given - say, in the first - coordinate system is known, then the material time derivative of the tensor defined in another - say, the second - coordinate system (moving arbitrarily with respect to the first one) is obtained by adding such an expression to the first material time derivative which is a linear combination of products involving as factors the gradient of the velocity vector field – measured observing the motion of the second coordinate system relative to the first one – and the tensor itself. The terms involved in the linear combination depend on the order of the tensor and the positions of indices.

4.6. On the basis of the above rule it holds for time rate of change of tensors defined in the convected coordinate system (without detailing the equations with

mixed positions of indices) that

I.
$$(\mathbf{X})(\mathbf{A}_{**}) = (\mathbf{X})\mathbf{A} + (\mathbf{X})\mathbf{L}^{\mathrm{T}} \cdot \mathbf{A} + \mathbf{A} \cdot (\mathbf{X})\mathbf{L},$$
 (4.24)

. . .

IV.
$$(X) (A^{**}) = (X) A - (X) L \cdot A - A \cdot (X) L^{T}$$
. (4.25)

where $^{(x)}L$ is the velocity gradient for the velocity vector field $^{(x)}\mathbf{v}$, and

I.
$$(X)(\boldsymbol{A}_{**})^{\cdot} = (\widehat{x})\boldsymbol{A}^{\cdot} + (\widehat{x})\boldsymbol{L}^{\mathrm{T}} \cdot \boldsymbol{A} + \boldsymbol{A} \cdot (\widehat{x})\boldsymbol{L},$$
 (4.26)

. . .

IV.
$$(X) (\boldsymbol{A}^{**}) = (\hat{x}) \boldsymbol{A} - (\hat{x}) \boldsymbol{L} \cdot \boldsymbol{A} - \boldsymbol{A} \cdot (\hat{x}) \boldsymbol{L}^{T}$$
. (4.27)

where ${}^{(\widehat{\mathbf{x}})}\mathbf{L}$ is the velocity gradient for the velocity vector field ${}^{(\widehat{\mathbf{x}})}\mathbf{v}$.

4.7. Relations between the time derivatives can be given, of course, in indicial notations. Considering relation (4.14), for example, we may write

$$(\widehat{\mathbf{x}}) \left(\widehat{a}_{l}^{k}\right)^{\cdot} = \left((\mathbf{x}) \dot{a}_{q}^{p} - (\mathbf{G}\mathbf{x}) l_{s}^{p} a_{q}^{s} + a_{s}^{p} (\mathbf{G}\mathbf{x}) l_{q}^{s} \right) \frac{\partial \widehat{x}^{k}}{\partial (\mathbf{G}) x^{p}} \frac{\partial (\mathbf{G}) x^{q}}{\partial \widehat{x}^{l}} .$$
 (4.28)

The results obtained can also be generalized for a tensor of any order. Considering a third-order tensor $\mathbf{A} = a_p^{\ qr} \mathbf{g}^p \mathbf{g}_q \mathbf{g}_r = \hat{a}_k^{\ lm} \hat{\mathbf{g}}^k \hat{\mathbf{g}}_l \hat{\mathbf{g}}_m$, for example, we shall find

$$^{(\widehat{\mathbf{x}})} \left(\widehat{a}_k^{\ lm}\right)^{\cdot} = \left(^{(\mathbf{x})} \dot{a}_p^{\ qr} + \ ^{(\mathbf{G}\mathbf{x})} l^s_{\ p} a_s^{\ qr} - a_p^{\ sr} \ ^{(\mathbf{G}\mathbf{x})} l^q_{\ s} - a_p^{\ qs} \ ^{(\mathbf{G}\mathbf{x})} l^r_{\ s}\right) \frac{\partial^{(\mathbf{G})} x^p}{\partial \widehat{x}^k} \frac{\partial \widehat{x}^l}{\partial ^{(\mathbf{G})} x^q} \frac{\partial \widehat{x}^m}{\partial ^{(\mathbf{G})} x^q} \frac{\partial \widehat{x}^m}{\partial ^{(\mathbf{G})} x^p} \ .$$

4.8. Dependence of material time derivatives on position of indices can also be shown in indicial notations. For this purpose we write equation (4.28) in the form

$${}^{(\mathbf{x})}\dot{a}^{r}{}_{q} = \frac{\partial^{(\mathbf{G})}x^{r}}{\partial\widehat{x}^{m}}\frac{\partial\widehat{x}^{l}}{\partial^{(\mathbf{G})}x^{q}} \;{}^{(\widehat{\mathbf{x}})}\left(\widehat{a}^{m}{}_{l}\right)^{\cdot} + \;{}^{(\mathbf{G}\mathbf{x})}l^{r}{}_{s}a^{s}{}_{q} - a^{r}{}_{s} \;{}^{(\mathbf{G}\mathbf{x})}l^{s}{}_{q} \;. \label{eq:constraints}$$

Multiplying both sides by g_{pr} and manipulating then the first term on the right side into

$$g_{pr} \frac{\partial^{(\mathbf{G})} x^r}{\partial \widehat{x}^m} \frac{\partial \widehat{x}^l}{\partial^{(\mathbf{G})} x^q} \stackrel{(\widehat{\mathbf{x}})}{(\widehat{\mathbf{g}}^m)} (\widehat{a}^m_l) = \widehat{g}_{km} \frac{\partial \widehat{x}^k}{\partial^{(\mathbf{G})} x^p} \frac{\partial \widehat{x}^l}{\partial^{(\mathbf{G})} x^q} \stackrel{(\widehat{\mathbf{x}})}{(\widehat{\mathbf{g}}^m)} = \frac{\partial \widehat{x}^k}{\partial^{(\mathbf{G})} x^p} \frac{\partial \widehat{x}^l}{\partial^{(\mathbf{G})} x^q} (\widehat{a}^m_l) - (\widehat{a}_{km}) \widehat{a}^m_l,$$

we obtain, also with regard to equation (4.19) that

$${}^{(\mathbf{x})}\dot{a}_{pq} = \frac{\partial \widehat{x}^k}{\partial {}^{(\mathbf{G})}_{r}^{p}} \frac{\partial \widehat{x}^l}{\partial {}^{(\mathbf{G})}_{r}^{q}} {}^{(\widehat{\mathbf{x}})} (\widehat{a}_{kl}) - {}^{(\mathbf{G}\mathbf{x})}l^s_{p} a_{sq} - a_{ps} {}^{(\mathbf{G}\mathbf{x})}l^s_{q}$$

which is identical to equation (4.13).

4.9. Now we shall consider a covariant and a contravariant vector:

$$(\hat{\mathbf{x}})\dot{\mathbf{a}}_* = (\mathbf{x})\dot{\mathbf{a}} + \mathbf{a} \cdot (\mathbf{G}\mathbf{x})\mathbf{L}, \qquad (\hat{\mathbf{x}})\dot{\mathbf{a}}^* = (\mathbf{x})\dot{\mathbf{a}} - (\mathbf{G}\mathbf{x})\mathbf{L} \cdot \mathbf{a}.$$
 (4.30)

4.10. Let $^{(x)}\mathbf{a}$ and $^{(\widehat{\mathbf{x}})}\mathbf{a}^*$ be the accelerations of the point X^K in the coordinate systems $\{x^p\}$ and $\{\widehat{x}^k\}$. For completeness we shall give how these accelerations are related to each other.

By definition

$$^{(x)}\mathbf{a} = ^{(x)} \left(^{(x)}\mathbf{v} \right)^{\cdot} \quad \text{and} \quad ^{(\widehat{x})}\mathbf{a} = ^{(\widehat{x})} \left(^{(\widehat{x})}\mathbf{v} \right)^{\cdot}.$$
 (4.31)

It follows from equation (3.26) that

$$\mathbf{a} = \mathbf{a} = \mathbf{a} \cdot \mathbf{a} \cdot \mathbf{b} \cdot \mathbf{c} = \mathbf{a} \cdot \mathbf{c} \cdot$$

where

$$\begin{array}{ll}
\overset{\text{(x)}}{=} \left(\overset{\text{(x)}}{=} \mathbf{v} \right) \stackrel{\text{(x)}}{=} & \vdots \frac{\partial^{\text{(Gx)}} \mathbf{v}}{\partial t} \Big|_{(X)} = & \vdots \frac{\partial^{\text{(Gx)}} \mathbf{v}}{\partial t} \Big|_{(\widehat{x})} + \frac{\partial^{\text{(Gx)}} \mathbf{v}}{\partial \widehat{x}^k} \frac{\partial^{\text{(B)}} \widehat{x}^k}{\partial t} \Big|_{(X)} = \\
&= & \overset{\text{(Gx)}}{=} \mathbf{a} + \left(\overset{\text{(Gx)}}{=} \mathbf{v} \nabla \right) \cdot \overset{\text{(\widehat{x})}}{=} \mathbf{v}.
\end{array}$$

According to equation (4.30) we have

$$\boldsymbol{f}_{(\boldsymbol{x})} \left(\boldsymbol{f}_{(\boldsymbol{\widehat{x}})} \mathbf{v} \right)^{\boldsymbol{\cdot}} = \boldsymbol{f}_{(\boldsymbol{\widehat{x}})} \left(\boldsymbol{f}_{(\boldsymbol{\widehat{x}})} \mathbf{v} \right)^{\boldsymbol{\cdot}} + \boldsymbol{f}_{(\boldsymbol{G}\boldsymbol{x})} \boldsymbol{L} \cdot \boldsymbol{f}_{(\boldsymbol{\widehat{x}})} \mathbf{v}.$$

On the basis of the above equations we get from equation (4.31)

$${}^{(\mathbf{x})}\mathbf{a} = {}^{(\widehat{\mathbf{x}})}\mathbf{a}^* + {}^{(\mathbf{G}\mathbf{x})}\mathbf{a} + \mathbf{2}^{(\mathbf{G}\mathbf{x})}\boldsymbol{L} \cdot {}^{(\widehat{\mathbf{x}})}\mathbf{v}. \tag{4.32}$$

For our latter considerations we remark that neither the velocity $^{(x)}\mathbf{v}$ nor the acceleration $^{(x)}\mathbf{a}$ are physically objectiv quantities.

REFERENCES

- JAUMANN, G.: Geschlossenes System Physikalischer und Chemischer Differentialgesetze, Sitz. Ber. Akad. Wiss. Wien (IIa), 120, (1911), 385-530.
- FROMM, H.: Stoffgesetze des isotropen Kontinuums insbesondere bei z\u00e4hplastischen Verhalten, Ingenieur-Archiv, 4, (1933), 432-466.
- 3. ZAREMBA, S.: Sur une conception nouvelle des forces interieures dans un fluide en mouvement, Memorial Sci. Math., No.82 Paris (1937), 1-85.
- THOMAS, T.J.: On the structure of stress-strain relations, and combined elastic and Prandtl-Reuss stress-strain relations, Proc. Nat. Acad. U.S.A., 41, (1955), 716-720 and 762-770.
- NOLL, W.: On the continuity of solid and fluid states, Journal Rat. Mech. Analysis, 4, (1955), 3-81.
- Hill, R.: Some basic principles in the mechanics of solids without natural time, Journal Mech. Phys. Solids, 7, (1959), 209-225.
- ATLURI, S.N.: On constitutive relations at finite stress: Hypoelasticity and elasto-plasticity with isotropic or kinematic hardening, Comp. Meth. Appl. Mech. Engng., 43, (1984), 137-171.

- 8. Sedov, L.: Different definition of the rate of change of a tensor, J. Appl. Math. Mech. (PMM), 24, (1960), 393-398 (in Russian).
- PRAGER, W.: An elementary discussion of definition of stress rates, Quart. Appl. Math., XVIII, (1961), 403-407.
- NAGHDI, P.M. and WAINWRIGHT, W.L.: On time derivative of tensors in mechanics of continua, Quart. Appl. Math., XIX, (1961), 95-109.
- 11. Masur, E.F.: On tensor rates in continuum mechanics, ZAMP, 16, (1937), 191-201.
- Dubey R.N.: Choice of tensor rates A methodology, SM Archives, 12/4, (1987), 233-244.
- 13. SZABÓ, L. and Balla, M.: Comparison on stress rates, Int. J. Solids Structures, 25, (1989), 279-297.
- 14. HAUPT, P. and TSAKAMAKIS C.H.: On the application of dual variables in continuum mechanics, In Continuum Mechanics and Thermodynamics I., 1989, 165-196.
- OLDROYD, J.G.: On the formulation of rheological equations of state, Proc. R. Soc. Lond., A220, (1950), 523-541.
- TRUSDELL, C.: The simplest rate theory of pure elasticity, Commun. Pure Appl. Math., 8, (1955), 123-132.
- COTTER, B.A. and RIVLIN P.M.: Tensors associated with time-dependent stress, Quart. Appl. Math., XVIII, (1955), 177-182.
- Green, A.E. and Naghdi, P.M.: A general theory of an elastic-plastic continuum, Ration. Mech. Analysis, 18, (1965), 251-281.
- GREEN, A.E. and McInnis, B.: Generalised hypo-elasticity, Proc. R. Edinb., A57, (1967), 220-230.
- DIENES J.K.: On the analysis of rotation and stress rate in deforming bodies, Acta Mech., 32, (1979), 217-232.
- SOWERBY,R. and CHU, E.: Rotations, stress rates and measures in homogeneous deformation process, Int. J. Solids Structures, 20, (1984), 1037-1048.
- 22. Marsden, E.J. and Hughes, J.R.T.: *Mathematical Foundation of Elasticity*, Prentice-Hall. Inc., Englewood Cliffs New Yersey 07633, 1983.
- 23. Durban, D. and Baruch, M.: Natural stress rate, Quart. Appl. Math., (1977), 55-61.

STRESSES AND DISPLACEMENTS IN A SEMIDIGGER MOULDBOARD AND A PLOUGHSHARE

Enno Saks and Mati Heinloo Department of Mechanics and Machine Design, Estonian Agricultural University Kreutzwaldi 58A, 51014 Tartu, Estonia

mheinloo@eau.ee

[Received: July 21, 2000]

Abstract. The paper investigates stress-strain state in the most important parts of a plough - mouldboard and ploughshare. The mouldboard consists of three layers, while the ploughshare is homogeneous. Two software packets were used to solve the problem. AutoCAD enables us to create the quadrangle curvilinear surfaces of the mouldboard and the ploughshare. It has been achieved by using a special AutoLISP procedure, which must be run under AutoCAD release 15.0. In the environment of ANSYS 5.6 thickness of layers and material properties were added to these quadrangles. The loads according to Goryachev formulae have been added. This way we can find the most dangerous regions where the stress intensity reaches its maximum value. The dependence of displacements on thickness of mouldboard has also been found.

Keywords: Mouldboard, ploughshare, AutoCAD, AutoLISP, ANSYS

1. Symbols used

a – processing depth of a plough

b - grab width of a plough

c – distance between the top working surface of mouldboard and the plane YZ

d – distance between the lower edge of mouldboard and turned soil layer

H – height of working surface at the top nearest to the field unploughed

 Δb – grab width overlap

 $\alpha, \beta, \gamma, \varepsilon$ – angles to set the form of plough body

x - horizontal co-ordinate, perpendicular to furrow

y – horizontal co-ordinate towards the motion of plough

z – vertical co-ordinate

2. Introduction

The textbook by A. Reintam [1] is devoted to the theoretical treatment of the issue how to design mouldboards and ploughshares by making use of graphical methods. These methods are quite troublesome and inaccurate. The main objective of the present paper is to show how to design mouldboards and ploughshares on the screen of a computer. The building process of the virtual models for a mouldboard and a ploughshare in the environment of the Finite Element Package ANSYS is bulky. The

present paper uses an alternative possibility with more flexible modelling possibilities for creating virtual models in the environment provided by the package AutoCAD. The automatic procedure is written in the AutoCAD environment by using the special AutoLISP language for drawing a mesh of the plough body consisting of tetragonal elements.

The parameters are entered through a dialog box on the screen of the computer. Every parameter has its own interval for the numerical values to be entered and the default value is the mean value in this interval.

The plough body is divided into elements which can be used to calculate the strength of the working bodies of a plough. Using ANSYS, which is powerful software based on the finite element method, one can perform these calculations. It is expected that one can make some recommendations to choose the initial parameters for creating a mesh of the plough body. Here it is worthy of mention that the thicknesses of the tetragonal elements in AutoCAD environment are considered to be equal to zero: the thicknesses should be added under ANSYS only. The thickness of an element can either be constant or vary and the elements may consist of several layers.

3. Description of the drawing procedure

To design a mesh for a plough body, the AutoLisp procedure must be loaded and run under AutoCAD. A loaded procedure can be started repeatedly. A procedure can be loaded with aid of various menus or by entering text

(load "plough")

(the brackets here are obligatory; plough is the filename of the corresponding procedure without the extension lsp). To run the procedure we enter PLOUGH (or plough). If the procedure "plough.lsp" should be loaded and/or run repeatedly, it is useful to create an icon under AutoCAD.

Now we describe the procedure *plough.lsp* and demonstrate how it functions. The theoretical base to draw a plough body is described by A. Reintam [1]. However, the graphical methods in the textbook [1] are not suitable for computer aided design, therefore all necessary co-ordinates of a plough body must be calculated prior to drawing.

In addition, the left-hand co-ordinates must be changed to right-hand co-ordinates, because AutoCAD uses only a right-hand co-ordinate system. Another reason is that in the left-hand co-ordinate system some parameters may have opposite signs (so-called pseudo-scalars and pseudo-vectors [2]). To adjust the theory [1] to a right-hand co-ordinate system it is sufficient to interchange the axes X and Y.

The program we have developed for the design of a plough body performs seven steps:

- 1. Constructing the contours of the projection on the plane XZ (a view of the plough body along furrow, as is described in [1] see Figure 8a);
- 2. Formation of the three-dimensional directrix;
- 3. Drawing a set of horizontal straight lines through the points lying in the directrix;

- 4. Finding the intersection points of the lines with the cylinder which is parallel to the axis Y and passes through the contours found in the 1^{st} step);
- 5. Using the points found in the previous step, the contours of the mouldboard and the ploughshare are formed (both closed contours should consist of exactly 4 edges);
- 6. Drawing the curvilinear meshes on these three-dimensional contours;
- 7. Exploding the meshes formed into single quadrangular elements. (The edges and the vertices of the neighboring elements should coincide.)

In fact the first four steps are executed without drawing anything. Only the corresponding calculations are accomplished and the results are saved into the main memory of the computer. However, the contour in the 5^{th} step must be drawn, because without a closed contour AutoCAD cannot execute the 6^{th} step. All steps must be performed both for the mouldboard and for the ploughshare, with a mutual unison in order to avoid a crack between mouldboard and ploughshare.

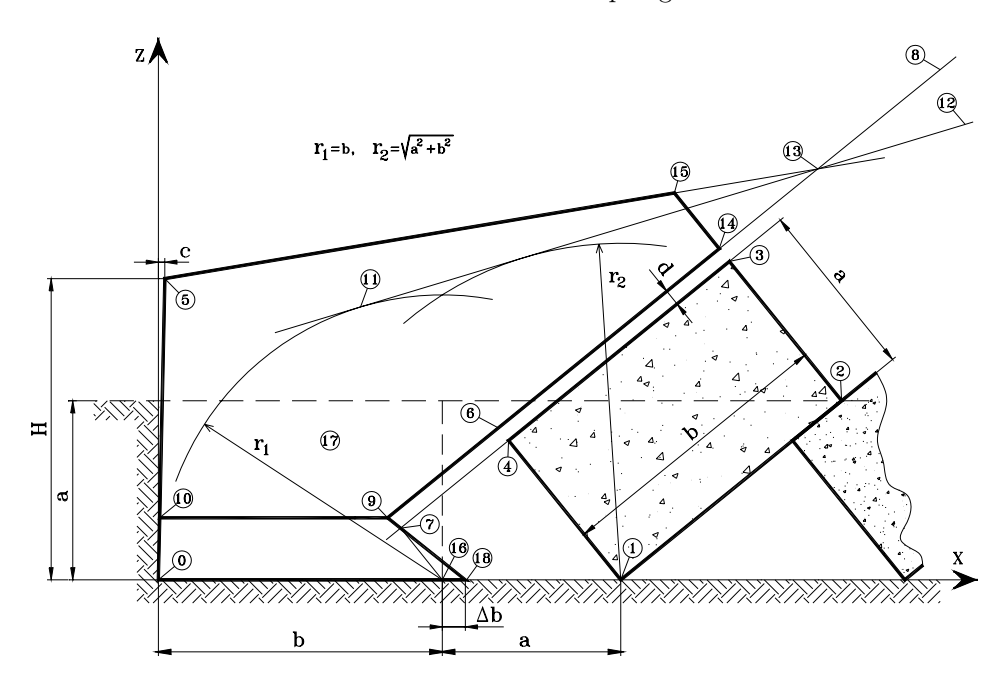


Figure 1. The front view of a plough body and two furrows

Now we discuss these steps in more details. The performance of the 1^{st} step is illustrated in Figure 1. The values of the parameters a, b, c, d, Δb and H are entered by the keyboard input, radii r_1 and r_2 are calculated by the formulae

$$r_1 = b, \quad r_2 = \sqrt{a^2 + b^2}.$$

The closed line that consists of straight segments through points 5, 10, 9, 14 and 15, is the projection of mouldboard on plane XZ. For the ploughshare this line passes through points 0, 18, 9 and 10. The rest of the numbered points in Figure 1 are

auxiliary points for the computation process. The rectangle with vertices 1, 2, 3 and 4 is a turned non-disintegrated furrow (beneath it is a fragment of a previous furrow).

Our AutoLisp procedure uses two standard functions to find the co-ordinates. The standard function

$$(inters p_1 p_2 p_3 p_4 nil)$$

finds the intersection point of two lines, where p_1 and p_2 are the end points of the first line, and p_3 and p_4 are the end points of the second line. If parameter nil exists, then *inters* returns the point where the lines intersect, even if that point is off the end of one or both lines. The standard function

returns the point at a specified angle and distance from a starting-point. Here the angle is measured in radians relative to the axis X, with respect to the current construction plane in the counter-clockwise direction.

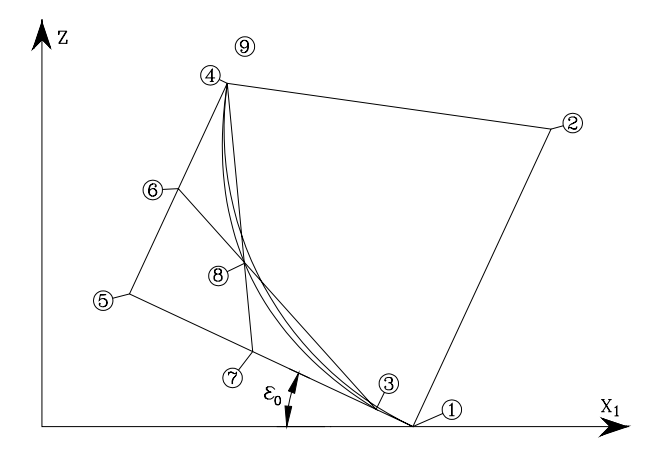


Figure 2. Parabolic directrix

Then the three-dimensional directrix is found, as is in the textbook [1], though the graphical methods are here replaced by appropriate analytical methods. It is known that a parabola is uniquely defined, when three points of the parabola and the slope angle of the axis of symmetry are given. In Figure 2 this angle is equal to ε_0 and the end points of the parabola are points 3 and 4. The intermediate point 8 can be found as the intersection of two lines. One of these lines connects point 3 with the midpoint 6 of the line passing through points 4 and 5; the other line connects point 4 with the midpoint 7 of the line passing through points 3 and 5. If we rotate now the parabola by the angle ε_0 (clockwise), the axis of symmetry of the parabola becomes parallel to the axis X_1 – see Figure 3 – and the equation of the parabola takes the form

$$x_1 = Az^2 + Bz + C,$$

where the coefficients A, B and C should be chosen in such a way that the parabola passes through points 3, 8 and 4. In this way we obtain a system of linear equations with A, B and C as unknowns. After finding A, B and C the parabola is rotated back into the previous position.

It is essential to say that the directrix lies in a vertical plane, the dihedral of this plane and the plane XZ is equal to the known angle γ_0 – see Figure 3. As soon as the directrix has been formed, the horizontal generators are drawn. All the generators pass the directrix at different heights (the heights are measured along the axis Z). Besides, every generator lies under different angle $\gamma = f(z)$ towards the plane YZ. In the case of a semi-digger plough body it is recommended [1] that the angle γ follow the parabolic law

$$f(z) = \frac{(z - z_c)^2}{2p} + \gamma_{min} \,. \tag{3.1}$$

Here z_c is the height where the mouldboard and the plough body contact. The parameters γ_{min} and γ_{max} are then entered; the latter corresponds to the value of γ at the maximum height z_{max} of the mouldboard. These relations allow us to find an appropriate value for the parameter p in equation (3.1).

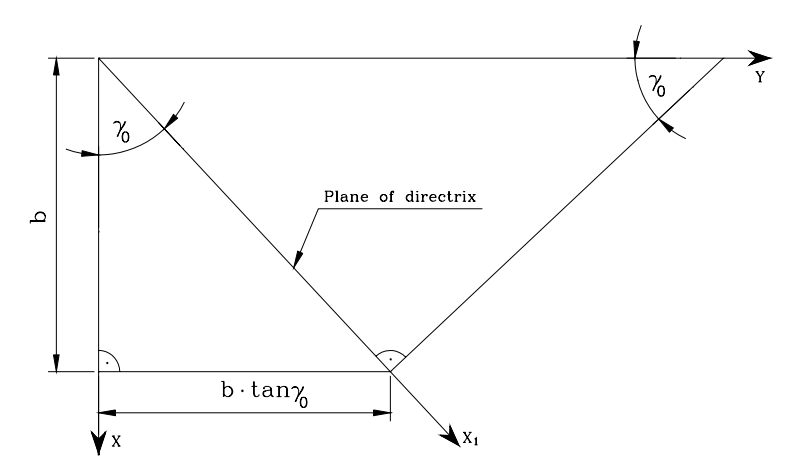


Figure 3. Top view of the directrix

In the next step the intersection points of the horizontal generators and the cylindrical surface (the latter was designed in the 1^{st} step), are found. Since the surface of mouldboard contains five planes each being parallel to axis Y (see Figure 1 for details), every generator has up to five intersection points. However, we should use only those intersection points lying in the closed contour which passes through points 5, 10, 9, 14, 15 and 5, and should disregard the other intersection points (such as the points in the segment between points 15 and 12).

The intersection point of a three-dimensional plane and a line is given by a formula of the handbook [4]. Namely, let us assume, that the plane is given by the equation

$$Ax + By + Cz + D = 0 (3.2)$$

and the line drawn through the points (x_1, y_1, z_1) and (x_2, y_2, z_2) by the equation

$$\frac{x - x_1}{x_2 - x_1} = \frac{y - y_1}{y_2 - y_1} = \frac{z - z_1}{z_2 - z_1}. (3.3)$$

Then the coordinates of the intersection point $(\bar{x}, \bar{y}, \bar{z})$ can be calculated as

$$\bar{x} = x_1 - l\rho$$
, $\bar{y} = y_1 - m\rho$, $\bar{z} = z_1 - n\rho$,

where

$$l = \frac{x_2 - x_1}{d}, \quad m = \frac{y_2 - y_1}{d}, \quad n = \frac{z_2 - z_1}{d}$$

are the direction cosines,

$$d = \sqrt{(x_2 - x_1)^2 + (y_2 - y_1)^2 + (z_2 - z_1)^2}$$

is the distance between two points and

$$\rho = \frac{Ax_1 + By_1 + Cz_1 + D}{Al + Bm + Cn} \tag{3.4}$$

is the distance of the intersection point $(\bar{x}, \bar{y}, \bar{z})$ from the point (x_1, y_1, z_1) .

The intersection point $(\bar{x}, \bar{y}, \bar{z})$ does not exist if the denominator in equation (3.4) is equal to zero. In such a case the plane (3.2) and the line (3.3) are mutually parallel. Incidentally, such is the case for the plane through points 10 and 9 – see Figure 1.

If we have found a sufficient number of intersection points, these must be ordered in such a manner that they form a closed contour consisting of exactly four (curvilinear) edges. It is worthy of mention that for the mouldboard one of these edges connects points 5, 15 and 14 – see again Figure 1.

Now it is necessary to determine the densities of meshes towards two alternative directions. These values must be set by two system variables of AutoCAD: SURFTAB1 and SURFTAB2. The AutoLisp function

(command "EDGESURF"
$$e_1 e_2 e_3 e_4$$
)

constructs a three-dimensional polygon mesh approximating a Coons surface patch mesh from four adjoining edges e_1 , e_2 , e_3 and e_4 . Here e_1 is an edge of the mould-board in vertical direction; and e_2 , e_3 and e_4 are the other three edges. A Coons surface patch mesh is a bicubic surface interpolated between four adjoining edges (which can be general space curves). The Coons surface patch mesh not only meets the corner of the defining edges, but also touches each edge, providing control over the boundaries of the generated surface patch. The same operations must be done for the ploughshare as well. We should ensure that the two densities along the joint edges of the mouldboard and the ploughshare are equal.

After forming the meshes we do not need the edges any more and they can be deleted. As a last step both two-dimensional meshes should be exploded into tetragonal surface elements. The edges and vertices of two neighbouring elements coincide. Exploding does not change the appearance of the mesh, but without exploding the formed mesh cannot be inserted into ANSYS to accomplish the finite element calculations.

In Figures 4 - 6 the same mouldboard and ploughshare are shown in three different views. The view direction in Figure 4 is determined by two angles: the angle in the

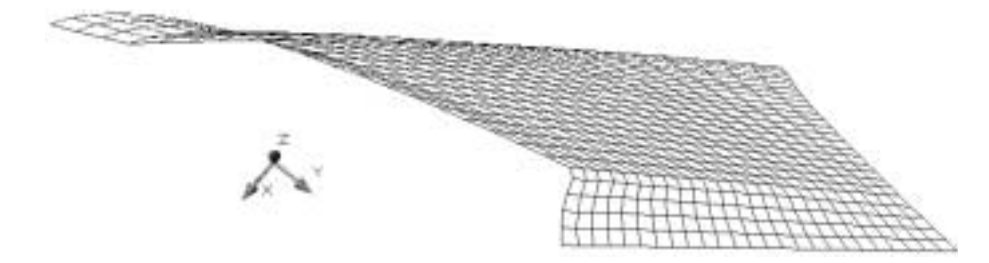


Figure 4. Slanting view of a plough

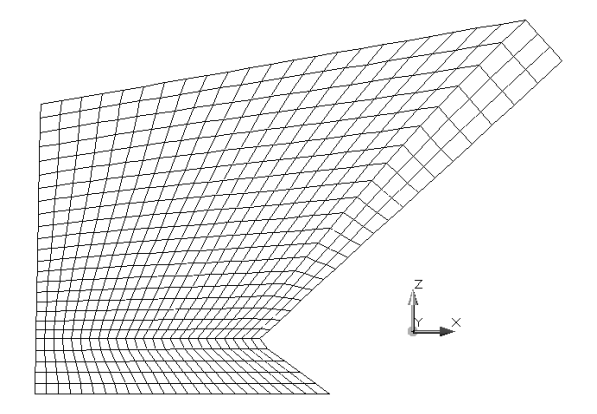


Figure 5. Front view of a plough

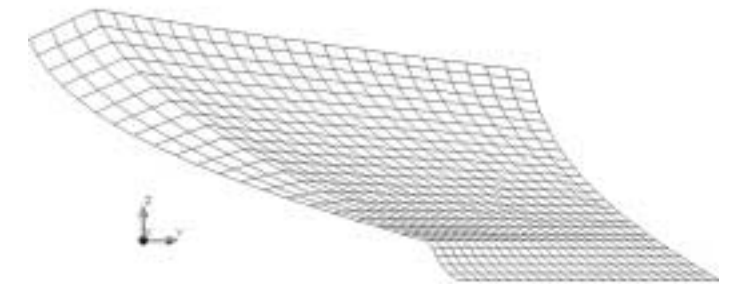


Figure 6. Right view of a plough

plane XY from the axis X is equal to 40° , the angle from the plane XY is equal to 80° . The processing depth a and the grab width b are equal to 36 cm and 22 cm, respectively. The mesh densities in both directions are equal to 25. Consequently we have altogether 625 quadrangle elements.

4. Creation of finite elements

To create a finite element model of the plough body, the ANSYS5.6 linear layered structural shell elements SHELL99 have been used. In these applications up to 100

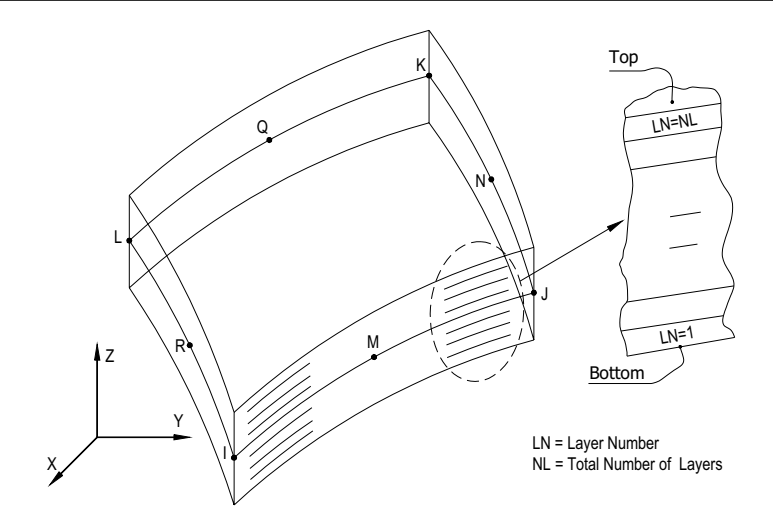


Figure 7. Up to 100-layer shell element SHELL99 with eight nodes

different layers are permitted. Every element has eight nodes: four (I, J, K and L) at the vertices and four (M, N, Q and R) at the midpoints of edges – see Figure 7. Naturally, the neighbouring elements must have common nodes - which insures against the disconnection of the virtual model of element SHELL99. If this property does not exist, the plough body disintegrates into single elements under the loads.

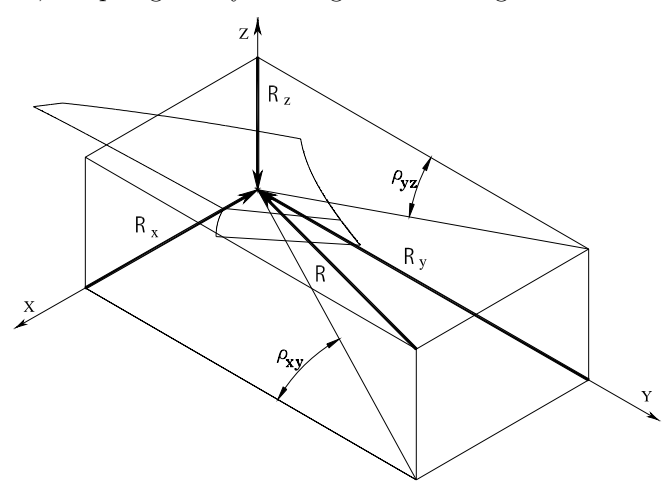


Figure 8. The soil reaction forces acting on the plough body

Every node of the element SHELL99 has six degrees of freedom: three displacements towards the coordinate axes X, Y and Z and three rotations around the same axes. The soil's influence on the plough body has been taken into account by the formulae of Goryachkin. The components of the resultant force \mathbf{R} in the coordinate system (X,Y,Z) – see Figure 8 for details – are given by

$$R_y = fG + (K_\partial + \varepsilon_o \nu_m^2)ab;$$
 $R_x = R_y \tan \rho_{xy};$ $R_z = R_y \tan \rho_{yz}.$ (4.1)

Symbol	Meaning	Unit	Value
K_{∂}	specific resistance to deformation of furrow slice	kPa	35
ε_0	factor, taking into account the form of the plough	${\rm kg/m^3}$	250
	body and the type of soil		
v_m	velocity of moving the plough	m/s	2
a	depth of the furrow	cm	26
b	width of the furrow	cm	40
f	summary friction coefficient		0.5
G	gravity of plough per one plough body	kN	2
ρ_{xy}	inclination angles of the resultant force R (Figure 8)		16
ρ_{yz}	inclination angles of the resultant force it (Figure 8)		13

Table 1. The parameters in the formulae of Goryachkin

The parameters in formula (4.1) are explained in Table 1 and Figure 8 (the plough moves towards the axis Y). The typical values for these parameters are also given there. The permitted values of these parameters can be found in the textbook [1]. We should mention here that these values may change over wide intervals, and it is difficult to get the exact value. Since the forces R_x , R_y and R_z are directed as shown in Figure 8, they are taken with the negative sign. These components should be distributed among the elements of SHELL99. As is well known, forces can be applied at the nodes only. For simplicity we assume that only the vertex nodes I, J, K and L are taken into account (Figure 7). As the actual distributions of the force components (3.1) along the plough body are unknown, we shall consider two possible distributions of the applied forces.

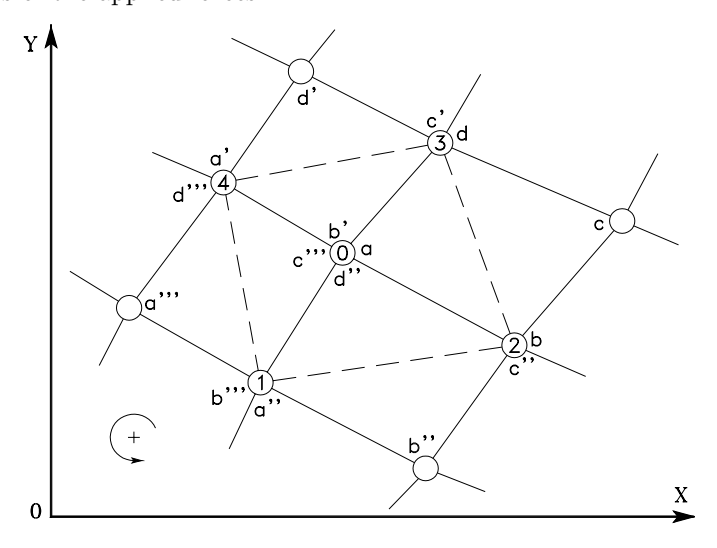


Figure 9. Projections of a quadrangle round a node

First, every force component (4.1) will be distributed uniformly along the projection of the plough body in the plane which is perpendicular to the selected coordinate axis. For instance, the component R_y will be distributed along the projection of the plough body on the plane XZ. As is well known from mathematical statistics,

uniform distribution is the best statistical distribution if the real distribution of some quantity is unknown. In the present case additional justification is given by the fact that real applied forces in a ploughing process are relatively incidental. Therefore, in this case no special cutting forces are applied along the edges of the plough body. This model is the first and best choice for soft soils (e.g. potato fields in autumn).

In the second case we shall try to take the cutting forces also into account. These are distributed along the cutting edge of the ploughshare and along the front edge of the plough body (only beneath the soil surface). At the other nodes the force components (4.1) are distributed uniformly (as in the previous case), although the intensities of the forces are different for these cases. To get a uniform distribution of forces, the weighting function for the force component applied at a node must be proportional to the area of quadrangle surrounding that node. For a node 0 this quadrangle is defined by the vertices 1, 2, 3 and 4 (Figure 9). The projections of the four neighboring elements on the plane XY are also shown (one of these has vertices a, b, c and d), surrounding the node 0. For the projections on coordinate planes YZ and ZX this will be done analogously. The projection of the area of a triangle with vertices 1, 2 and 3 (Figure 9) can be calculated by the formula [4]

$$S_{123} = \frac{1}{2} \left| \begin{array}{ccc} x_1 & y_1 & 1 \\ x_2 & y_2 & 1 \\ x_3 & y_3 & 1 \end{array} \right|.$$

If we add the vertex 4, the last formula yields the projection of the quadrangle area in terms of the coordinates of the vertices 1, 2, 3 and 4:

$$S_0 = \frac{1}{2} \left[(x_1 - x_3) (y_2 - y_4) - (x_2 - x_4) (y_1 - y_3) \right].$$

If the vertices 1, 2, 3 and 4 are oriented towards the positive direction (as shown at the lower left corner in Figure 9), then the calculated area will be positive, otherwise it will be negative (or equal to zero). If the node 0 lays on the edge of the plough body (or at a vertex), one (or two) node(s) 1, 2, 3 or 4 coincide(s) with the central node 0.

The value of edge forces can be found by the following argumentation. In case of uniform distribution of forces based on formulae of theoretical mechanics it is possible to evaluate the centre of the parallel forces. In case of distributed edge forces for the axis X we can use the following formulae

$$\begin{cases}
R'_x + R''_x = R_x \\
R'_x X'_C + R''_x X''_C = R_x X_C,
\end{cases}$$
(4.2)

where the latter corresponds to the weighted average of the centre of forces. Here R'_x and R''_x are resultant edge force and remainder resultant uniform force, X'_C and X''_C are centres of distributed edge forces and remainder uniform forces, and R_x is given by (4.1). According to the textbook [1] the coordinates of the application point of force \mathbf{R} are equal to $X_C = 0.35b$ and $Z_C = 0.33a$. The system of equations (4.2) enables us to find the quantities of R'_x and R''_x . Similar formulae are valid for axis Z. As the textbook [1] does not give Y_C , the distributed edge forces towards the axis Y are not applied.

Figure 10 shows a typical uniform distribution of force projections R_x (horizontal) and R_z (vertical) (a view along the furrow). In the same figure we can see the six bolts where the plough body is fixed to the anchor of the plough [3].

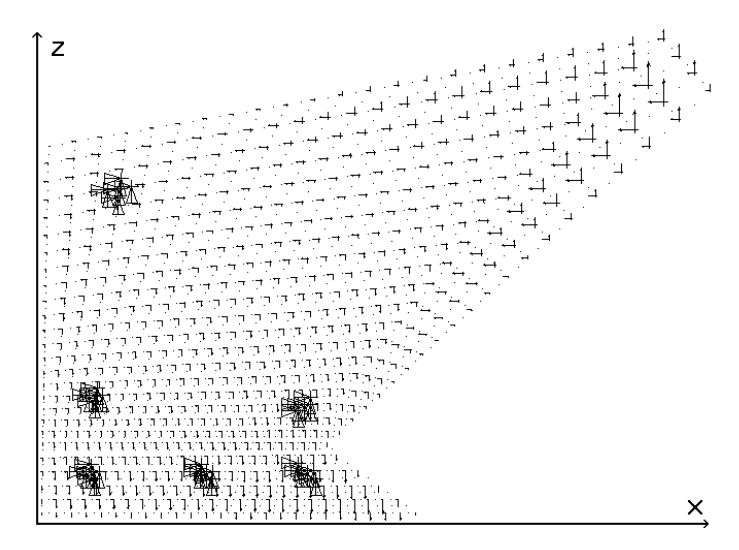


Figure 10. Applied forces and constrained elements (uniform distribution)

At every bolt the five neighboring nodes are fixed so that the number of degrees of freedom is equal to zero, which corresponds to rigid support. An analogous distribution of forces can be obtained for the case of edge forces. Although these two distributions are relatively different, the results of the calculations, as we can see later, are not as different.

5. Results of calculations and conclusions

Stress and displacement distributions were obtained through calculations using AN-SYS 5.6. Due to the limited volume of this paper, we confine ourselves to one set of input parameters (velocity of plough movement and the properties of soil and materials of the plough body). Only the thickness of the mouldboard layers and ploughshare vary.

	Young's	Elastic	Poisson's
Location	modulus	limit	ratio
	(GPa)	(GPa)	
cutting edge of ploughshare	210	0.471	
ploughshare	175	0.373	
bottom layer of mouldboard	200	0.471	0.29
middle layer of mouldboard	170	0.373	
top layer of mouldboard	210	0.471	

Table 2. The parameters of layers

Parameters from Goryachkin formulae (4.1), which correspond to loam as a soil form, have been described in Table 1, properties of different materials in Table 2, and the thicknesses of plough body in the left five columns of Table 3. In reality the thickness of the ploughshare is uneven, but a thick rib behind the cutting edge has been ignored. It is not dangerous because by ignoring this only the calculated stress intensities increase. The model SHELL99 enables us to introduce only ribs with bilateral symmetry, but

Thickness (mm)				$\begin{array}{c} {\rm Displacement} \\ {\rm (mm)} \end{array}$		Stress intensity (GPa)		
cutting	bottom	middle	top	sum	uniform	with	uniform	with
edge	layer	layer	layer	to-	load	edge	load	$_{\mathrm{edge}}$
				tal		loads		loads
0.25	0.25	1.5	0.25	2.0	78.8	77.3	0.606	0.621
0.4	0.5	2.0	0.5	3.0	38.9	38.5	0.339	0.349
0.6	1.0	3.0	1.0	5.0	15.8	15.8	0.155	0.160
0.8	1.5	4.5	1.5	7.5	7.62	7.67	0.0825	0.0852
1.0	2.0	6.0	2.0	10.0	4.48	4.54	0.0529	0.0553

Table 3. Parameters to design the surface of the plough body

the upper rib is clearly inappropriate.

The model SHELL99 (part of ANSYS 5.6) enables us to find the distributions of stress intensities (naturally also that of the stress components) and the displacements (and the rigid body rotations about the coordinate axes) either as numerical values for all (or selected) nodes or in various graphical forms. These parameters can be found for every layer: by selecting the bottom, middle or top surface of a layer.

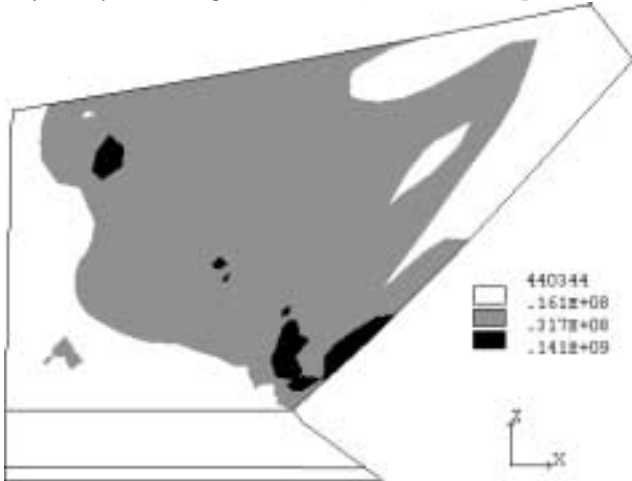


Figure 11. Stress intensities along the bottom surface of the bottom layer

Now we fix the thickness of the plough body at 5 mm (Table 3). Figure 11 illustrates the distribution of stress intensity along the bottom surface of the bottom layer of the plough body under uniform loading. Black areas represent the areas of high stress

intensity (measured in pascals). The most dangerous areas are those surrounding the two fixed points of the mouldboard and the region between them, while the stresses inside the ploughshare are relatively small. Analogous distribution is illustrated in Figure 12. Here along the top surface of the top layer, the dangerous region is at the upper edge of the mouldboard. It appeared that the distributions of the stress components are clearly different from each other and also from the stress intensities. These distributions are not represented in these figures. As the maximum values of stress intensities occur at two fixed points of the mouldboard, it may be useful to increase the thickness of the lower layer of the mouldboard near these regions, or to use a complementary support under the free end of the mouldboard (some plough types have such support).

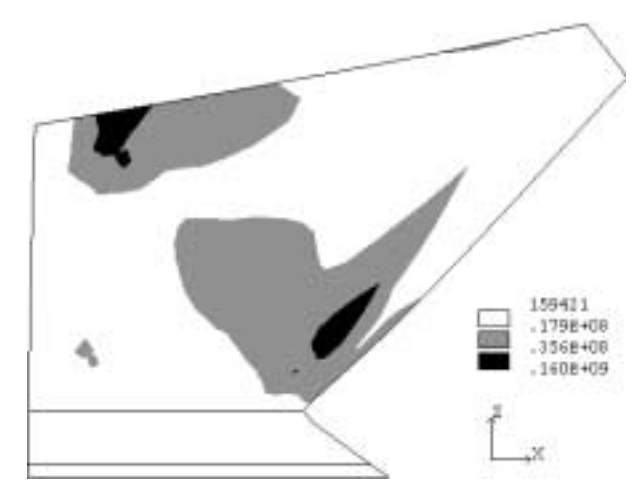


Figure 12. Stress intensities along the top surface of the top layer

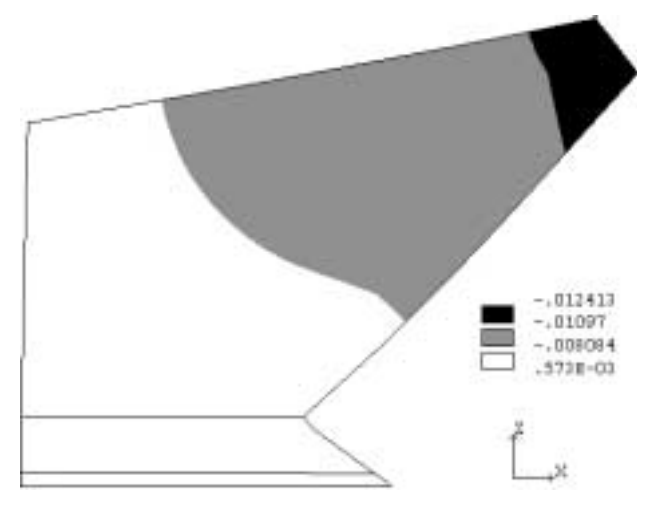


Figure 13. Displacements in the direction X

The distributions of displacements were found in the same manner – see Figure 13.

It is expected that the maximum displacement magnitudes occur at the free end of the mouldboard. Displacements are predominately negative (only vertical displacements towards the axis Z at some nodes may be positive, compared with the distribution of vertical forces in Figure 10).

If we investigate the stress and displacement distribution in the case of distributed edge forces, we obtain similar pictures (see Figures 11 - 13). It is interesting to note that these distributed edge forces are insignificant for the distributions of stress intensities, while the stress components may be more different in comparison with the case where the edge forces are absent.

The four right columns of Table 3 give a numerical comparison of these two load cases. The table shows the maximum displacements and the stress intensities, which take place at the right-most point of the mouldboard (see Figure 13).

Table 3 shows also that if the thickness of the mouldboard is too small, the displacements and stress intensities can be quite large. According to formulae (4.1) the load of a plough body increases with the hardness of soil. Let us remember that our calculations are carried out for loam, which is not a very hard soil. Even though the elastic limit is not exceeded, such large deformations are not proper for a plough. Besides, there exists a risk to exceed the elastic limit, which gives rise to residual deformations. This happens when the total thickness of the mouldboard is equal to 2 mm only (see Table 3). The 3 mm thickness is also dangerous. However, such thin ploughs are not proper for the ploughing process.

Thus the creating of the virtual model in the AutoCAD environment, entering this model into an ANSYS environment for creating the finite element model and carrying the results of computations were successful. This alternative possibility is suitable for AutoCAD users, who wish to use the finite element method.

Acknowledgement. The authors are grateful to the Estonian Science Foundation for their support (grant No. 4098).

REFERENCES

- 1. Reintam, A.: Bases of Theory and Technological Calculations of Farming Machines II. Machines of Soil Cultivation, Tartu, 1969. (in Estonian)
- 2. Kochin, N. E.: Vector Calculus and Bases of Tensor Calculus, Moscow, 1965. (in Russian)
- 3. Reintam, A.: Farming Machines, Tartu, 1997. (in Estonian)
- 4. KORN, G. and KORN, T.: Mathematical Handbook for Scientists and Engineers, Moscow, 1977. (translation into Russian)

BOUNDARY INTEGRAL EQUATIONS FOR PLANE PROBLEMS IN TERMS OF STRESS FUNCTIONS OF ORDER ONE

GYÖRGY SZEIDL
Department of Mechanics, University of Miskolc
3515 Miskolc-Egyetemváros, Hungray
Gyorgy.SZEIDL@uni-miskolc.hu

[Received: October 4, 2001]

Abstract. The present paper is devoted to the plane problem of elastostatics assuming that the governing equations are given in terms of stress functions of order one. After clarifying the conditions of single valuedness we have constructed the fundamental solution for the dual basic equations. Then the integral equations of the direct method have been established. Numerical examples illustrate the applicability of the integral equations.

Mathematical Subject Classification: 74B05, 45A05

Keywords: Boundary integral equations, stress functions of order one, direct method

1. Introduction, Preliminaries

In spite of a great number of publications devoted to plane problems there are only a few dealing with plane problems in terms of stress functions of order one. As regards classical elasticity we refer to the paper [1] and the book [2] by Jaswon and Smith in which the unknown biharmonic function (stress function of order two) is given in terms of two harmonic functions as a single layer potential and the authors set up a pair of integral equations for the unknown source densities.

Application of stress functions of order one was initiated by Frejis de Veubeke in a new complementary energy based finite element procedure [3,4] since the use of C^0 continuous stress functions of order one guarantees continuous surface tractions and makes possible to construct isoparametric elements. Further applications with an emphasis on three dimensional problems and laminated structures are due to Bertóti – see [5,6].

If one uses stress functions of order one calculation of stresses requires determination of first derivatives (in contrast to stress functions of order two from which stresses can be obtained in terms of second derivatives) and this property makes them attractive in boundary element applications though a further equation is needed to ensure that the stresses be symmetric.

As regards the derivation of integral equations for plane problems it is worth citing the papers by Heise [7,8], in which altogether 32 + 16 different integral equations are obtained with the aid of the singularity method. The reader taking an interest in the various formulations made by Heise is referred to these works and the references

238 G. Szeidl

listed therein.

In the present paper we confine ourselves to the direct formulation within the framework of classical elasticity. Our aims are as follows:

- 1. Clarifying the conditions of single valuedness for a class of mixed boundary value problems assuming multiply connected regions.
- 2. Derivation of the fundamental solutions for the stress functions of order one.
- Setting up the dual Somigliana relations (both for inner regions and for outer ones) from which the boundary integral equations of the direct method can be derived.
- 4. Presentation of some results obtained by solving the integral equations of the direct method.

We remark that some results of the paper can be found in the work [9].

2. Dual equations in terms of stress functions of order one

Throughout this paper $x_1 = x$ and $x_2 = y$ are rectangular Cartesian coordinates, referred to an origin O. The totality of $x_1 = x$ and $x_2 = y$ is denoted by x. {Greek}[Latin subscripts] are assumed to have the range $\{(1,2)\}[(1,2,3)]$, summation over repeated subscripts is implied. The triple connected region under consideration is denoted by A_i – inner region – and is bounded by the outer contour

$$\mathcal{L}_0 = \mathcal{L}_{t1} \cup \mathcal{L}_{u2} \cup \mathcal{L}_{t3} \cup \mathcal{L}_{u4}$$

and the inner contours which – partly or wholly – consist of the arcs \mathcal{L}_{t1} , \mathcal{L}_{t3} , \mathcal{L}_{t5} and \mathcal{L}_{u2} , \mathcal{L}_{u4} , \mathcal{L}_{u6} .

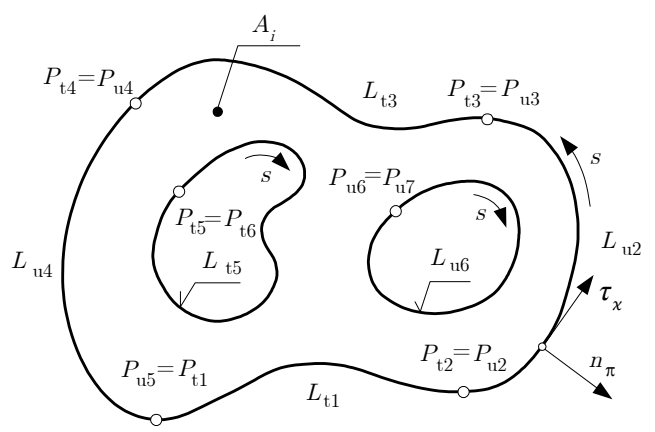


Figure 1

Further the inner contours \mathcal{L}_1 and \mathcal{L}_2 lie wholly in the interior of the outer contour \mathcal{L}_0 and they have no points in common. We stipulate that each contour has a continuously turning unit tangent τ_{κ} and admits a nonsingular parametrization in terms of its arc length s. The outer normal is denoted by n_{π} . In accordance with the notations

introduced $\delta_{\kappa\lambda}$ is the Kronecker symbol, ∂_{α} stands for the derivatives with respect to x_{α} and $\epsilon_{3\kappa\lambda}$ is the permutation symbol. The {symmetric}[skew] part of a tensor, say the tensor $t_{\kappa\lambda}$, is denoted by $\{t_{(\kappa\lambda)}\}[t_{[\kappa\lambda]}]$.

Assuming plane strain, let u_{κ} , $e_{\kappa\lambda}$ and $t_{\kappa\lambda}$ be the displacement field and the in plane components of stress and strain, respectively. The stress functions of order one are denoted by \mathcal{F}_{ρ} .

For homogenous and isotropic material the plane strain problem of classical elasticity in dual system is governed by the dual kinematic equations

$$t_{\kappa\lambda} = \epsilon_{\kappa\rho3} \mathcal{F}_{\lambda} \partial_{\rho} + \stackrel{o}{t}_{\kappa\lambda} \qquad x \in A_i$$
 (2.1)

 $\stackrel{o}{(t_{\kappa\lambda})}$ is the particular solution that belongs to non-zero body forces), the inverse form of Hook's law

$$e_{\kappa\lambda} = \frac{1}{2\mu} \left(t_{(\kappa\lambda)} - \nu t_{\psi\psi} \delta_{\kappa\lambda} \right) \qquad x \in A_i$$
 (2.2)

(μ is the shear modulus of elasticity, ν is the Poisson number), the dual balance equations

$$\epsilon_{\kappa\rho3}e_{\lambda\kappa}\partial_{\rho} + \varphi_3\partial_{\lambda} = \epsilon_{\kappa\rho3}\left(e_{\lambda\kappa} - \epsilon_{\lambda\kappa3}\varphi_3\right)\partial_{\rho} = 0$$
 $x \in A_i$ (2.3)

(equations of compatibility for a simply connected region; φ_3 is the rigid body rotation) and the symmetry condition

$$\epsilon_{3\kappa\lambda}t_{\kappa\lambda} = 0 \qquad x \in A_i$$
 (2.4)

(equation of rotational equilibrium). If this equation is fulfilled, then one of the equations (2.2) can be omitted. In this way we have nine equations for the nine unknowns \mathcal{F}_1 , \mathcal{F}_2 , t_{11} , $t_{12} = t_{21}$, t_{22} , e_{11} , $e_{12} = e_{21}$, e_{22} and φ_3 .

The field equations (2.1), (2.2), (2.3) and (2.4) should be associated with appropriate boundary conditions. If a contour is not divided into parts, then either tractions or displacements are imposed on it. If a contour is divided, then it is assumed to consists of arcs of even number on which displacements and tractions are imposed alternately. In the present case {tractions}[displacements] are given on the arc $\{\mathcal{L}_t = \mathcal{L}_{t1} \cup \mathcal{L}_{t3} \cup \mathcal{L}_{t5}\}[\mathcal{L}_u = \mathcal{L}_{u2} \cup \mathcal{L}_{u4} \cup \mathcal{L}_{u6}]$. We remark that hatted letters stand for the prescribed values.

Upon substitution of the equation (2.1) into the traction boundary condition $n_{\pi}t_{\pi\rho} = \hat{t}_{\rho}$ we arrive at the differential equation

$$\hat{t}_{\rho} - \overset{o}{t}_{\rho} = n_{\kappa} \epsilon_{\kappa \nu 3} \mathcal{F}_{\rho} \partial_{\nu} = \frac{d \mathcal{F}_{\rho}}{ds}$$
(2.5)

where $\overset{o}{t}_{\rho} = n_{\pi}\overset{o}{t}_{\pi\rho}$. One can readily check that the solution on the arcs of \mathcal{L}_{t} assumes the form

$$\hat{\mathcal{F}}_{\rho}(s) = \int_{P_{ti}}^{s} \left[\hat{t}_{\rho}(\sigma) - \overset{o}{t}_{\rho}(\sigma) \right] d\sigma , \qquad s \in \mathcal{L}_{ti} , \qquad i = 1, 3, 5 .$$

240 G. Szeidl

Let the constants $C_{(ti)}^{\rho}$ be that of integration. The condition

$$\mathcal{F}_{\rho}(s) = \hat{\mathcal{F}}_{\rho}(s) + C_{(ti)}^{\rho} \qquad i = 1, 3, 5$$
 (2.6)

is equivalent to the boundary condition (2.5) and conversely.

REMARK 1.: Observe that the number of undetermined constants of integration is two times as much as the number of those arcs on which tractions are imposed.

Since the displacements do not belong to the unknowns of the dual system one has to clarify what boundary conditions can be prescribed on the arcs constituting \mathcal{L}_u . Let

$$\mathcal{K} = \mathcal{K}(t_{\kappa\lambda}, \varphi_3) = -\frac{1}{2} \int_{A_i} t_{\kappa\lambda} e_{\kappa\lambda} \, dA + \int_{\mathcal{L}_u} n_{\kappa} t_{\kappa\lambda} \hat{u}_{\lambda} \, ds - \int_{A_i} t_{\kappa\lambda} \epsilon_{\kappa\lambda 3} \varphi_3 dA \qquad (2.7)$$

be a modified form of the complementary energy functional. (The modification is a must in order to keep up the rotational equilibrium.) Solution to the problem posed can be sought by making use of the stationary condition

$$\delta \mathcal{K} = 0 \tag{2.8}$$

since the latter equation should ensure all the conditions the strains $e_{\kappa\lambda}$ and the rigid body rotation φ_3 are to meet in order to be kinematically admissible. In the functional (2.7) $e_{\kappa\lambda}$ is given in terms of the stresses $t_{\kappa\lambda}$ via Hook's law while the stresses $t_{\kappa\lambda}$ should satisfy the equilibrium equation and the traction boundary condition though it is not necessary for them to be symmetric. Consequently, the variations of stresses can not be arbitrary but should meet the conditions

$$\delta t_{\kappa\lambda} \partial_{\kappa} = 0$$
 $x \in A$ and $n_{\kappa} \delta t_{\kappa\lambda} = 0$ $x \in \mathcal{L}_t$. (2.9)

Both conditions are satisfied if $\delta t_{\kappa\lambda}$ is given in terms of the variations of stress functions

$$\delta t_{\kappa\lambda} = \epsilon_{\kappa\rho3} \delta \mathcal{F}_{\lambda} \partial_{\rho} \tag{2.10}$$

where $\delta \mathcal{F}_{\lambda}$ is arbitrary on A_i . However, with regard to (2.6) it follows that on \mathcal{L}_t

$$\delta \mathcal{F}_{\rho}(s) = \delta \underset{(ti)}{C}_{\rho} \qquad (i = 1, 3, 5) . \tag{2.11}$$

Derivation of the conditions the strains $e_{\kappa\lambda}$ and the rigid body rotation should meet in order to be kinematically admissible requires the transformation of the stationary condition

$$\delta \mathcal{K} = -\int_{A_i} e_{\kappa\lambda} \, \delta t_{\kappa\lambda} \, dA + \int_{\mathcal{L}_u} n_{\kappa} \delta t_{\kappa\lambda} \hat{u}_{\lambda} \, ds - \int_{A_i} \delta t_{\kappa\lambda} \epsilon_{\kappa\lambda3} \varphi^3 dA - \int_{A_i} t_{\kappa\lambda} \epsilon_{\kappa\lambda3} \delta \varphi^3 dA = 0.$$
(2.12)

The main steps of the transformations are as follows:

1. Substitution of the condition (2.10) into the first and second surface integrals and substitution of (2.1) into the third surface integral.

2. Substitution of the relation

$$n_{\kappa} \epsilon_{\kappa \rho 3} \delta \mathcal{F}_{\lambda} \partial_{\rho} = \frac{d \delta \mathcal{F}_{\lambda}}{ds}$$

into the line integral taken on \mathcal{L}_u .

- 3. Application of the Green-Gauss theorem [10] to the first and second surface integrals.
- 4. Performation of partial integrations on the arcs constituting \mathcal{L}_u taking into account the validity of (2.11) at the extremities of the arcs.
- 5. Division of the line integrals obtained by the application of the Green-Gauss theorem by using the relation

$$\int_{\mathcal{L}} \dots = \int_{\mathcal{L}_n} \dots + \int_{\mathcal{L}_t} \dots$$

then substitution of (2.11) into the line integrals taken on \mathcal{L}_t .

6. Transformation of the result making use of the equation

$$n_{\rho}\epsilon_{\kappa\rho3} = -\tau_{\kappa} \ . \tag{2.13}$$

After performing the steps listed above

$$\delta K = \int_{A_i} \left(\epsilon_{\kappa\rho3} e_{\kappa\lambda} \partial_{\rho} + \varphi_3 \partial_{\lambda} \right) \delta \mathcal{F}_{\lambda} dA - \int_{A_i} \left(\mathcal{F}_{\psi} \partial_{\psi} \right) \delta \varphi_3 dA$$

$$+ \sum_{i=2,4,6} \int_{\mathcal{L}_{ui}} \left\{ n_{\pi} \left[\epsilon_{\pi\kappa3} e_{\kappa\lambda} - \delta_{\pi\lambda} \varphi_3 \right] - \frac{d\hat{u}_{\lambda}}{ds} \right\} \delta \mathcal{F}_{\lambda} ds$$

$$+ \sum_{i=1,3,5} \left\{ \int_{\mathcal{L}_{ti}} n_{\pi} \left[\epsilon_{\pi\kappa3} e_{\kappa\lambda} - \delta_{\pi\lambda} \varphi_3 \right] ds - \hat{u}_{\lambda} \Big|_{P_{ti}}^{P_{t,i+1}} \right\} \delta \underset{(ti)}{C}_{\lambda} = 0$$

is the stationary condition. Since the variations are arbitrary from this condition it follows the compatibility condition (2.3), the symmetry condition (2.4) – in the latter $t_{\kappa\lambda}$ is given in terms of \mathcal{F}_{ψ} –, the strain boundary condition

$$\frac{d\hat{u}_{\lambda}}{ds} = n_{\pi} [\epsilon_{\pi\kappa 3} e_{\kappa\lambda} - \delta_{\pi\lambda} \varphi_3] , \qquad (2.14)$$

the compatibility condition in the large

$$\int_{\mathcal{L}_{t5}} n_{\pi} [\epsilon_{\pi\kappa 3} e_{\kappa\lambda} - \delta_{\pi\lambda} \varphi_3] ds = 0$$
(2.15)

and the supplementary condition of single valuedness

$$\int_{C_{\star}} n_{\pi} [\epsilon_{\pi\kappa 3} e_{\kappa\lambda} - \delta_{\pi\lambda} \varphi_3] ds - \hat{u}_{\lambda}|_{P_{ti}}^{P_{t,i+1}} = 0 \qquad (i = 1, 3).$$
 (2.16)

Remark 2.: The strain boundary condition can also be obtained if one regards the primal kinematic equation

$$e_{\kappa\lambda} = \frac{1}{2}(u_{\kappa}\partial_{\lambda} + u_{\lambda}\partial_{\kappa})$$

242 G. Szeidl

on the contour, multiplies it by $n_{\pi}\epsilon_{\pi\kappa3} = \tau_{\kappa}$ taking into account that $u_{[\kappa}\partial_{\lambda]} = -\epsilon_{\kappa\lambda3}\varphi_3$.

REMARK 3.: Both the compatibility condition in the large (2.15) and the supplementary condition of single valuedness (2.16) can be set up by integrating the strain boundary condition (2.14) appropriately.

REMARK 4.: It can be shown that only two of the three conditions (as a matter of fact three times two conditions) (2.15) and (2.16) are independent of each other. In accordance with this, one can set one times two of the three times two undetermined constants of integration $C_{(ti)}^{\rho}$, say $C_{(t1)}^{\rho}$, to zero since there belong no stresses to the stress function $\mathcal{F}_{\rho} = C_{(t1)}^{\rho} = \text{constant}$. In other words, we have as many independent macro conditions of single valuedness as there are undetermined constants of integration.

3. Basic equations and fundamental solutions

Here and in the sequel we shall assume that there are no body forces. Substituting the dual kinematic equation (2.1) into Hook's law (2.2) and the result into the compatibility equations (2.3) we have

$$\frac{1}{2\mu}(1-\nu)\Delta\mathcal{F}_1 - \frac{1}{2\mu}(\frac{1}{2}-\nu)(\mathcal{F}_1\partial_1 + \mathcal{F}_2\partial_2)\partial_1 + \varphi_3\partial_1 = 0, \qquad (3.1a)$$

$$\frac{1}{2\mu}(1-\nu)\Delta\mathcal{F}_2 - \frac{1}{2\mu}(\frac{1}{2}-\nu)(\mathcal{F}_1\partial_1 + \mathcal{F}_2\partial_2)\partial_2 + \varphi_3\partial_2 = 0.$$
 (3.1b)

These equations are associated with the symmetry condition in terms of \mathcal{F}_{ρ} :

$$\mathcal{F}_1 \partial_1 + \mathcal{F}_2 \partial_2 = 0 . \tag{3.1c}$$

Upon substitution of (3.1c) into (3.1a,b) the latter, two equations become much simpler. In spite of that and for the sake of a comparison with the plane orthotropic case, the work on that problem is in progress, we do not change the above equations. Introducing the notations

$$[\mathfrak{D}_{lk}] = \begin{bmatrix} \frac{1}{2\mu} (1-\nu)\Delta - \frac{1}{2\mu} (\frac{1}{2}-\nu)\partial_1\partial_1 & -\frac{1}{2\mu} (\frac{1}{2}-\nu)\partial_1\partial_2 & -\partial_1 \\ -\frac{1}{2\mu} (\frac{1}{2}-\nu)\partial_2\partial_1 & \frac{1}{2\mu} (1-\nu)\Delta - \frac{1}{2\mu} (\frac{1}{2}-\nu)\partial_2\partial_2 & -\partial_2 \\ -\partial_1 & -\partial_2 & 0 \end{bmatrix}$$
(3.2a)

and

$$\mathfrak{u}_k = (\mathcal{F}_1, \mathcal{F}_2, -\varphi_3) \tag{3.2b}$$

the basic equation takes the form

$$\mathfrak{D}_{ik}\mathfrak{u}_k = 0. (3.3)$$

Let D_{kj} be the cofactor of \mathfrak{D}_{jk} :

$$[D_{kl}] = \begin{bmatrix} -\partial_2 \partial_2 & \partial_1 \partial_2 & \frac{1}{2\mu} (1 - \nu) \Delta \partial_1 \\ \partial_2 \partial_1 & -\partial_1 \partial_1 & \frac{1}{2\mu} (1 - \nu) \Delta \partial_2 \\ \frac{1}{2\mu} (1 - \nu) \Delta \partial_1 & \frac{1}{2\mu} (1 - \nu) \Delta \partial_2 & \frac{1}{8\mu^2} (1 - \nu) \Delta \Delta \end{bmatrix}.$$
(3.4)

It is obvious that

$$D_{ik}\mathfrak{D}_{kl} = \mathfrak{D}_{ik}D_{kl} = \det(\mathfrak{D}_{il})\,\delta_{kl} \tag{3.5}$$

where

$$\det(\mathfrak{D}_{jl}) = -\frac{1}{2\mu}(1-\nu)\Delta\Delta \ . \tag{3.6}$$

If we introduce a new unknown χ_l [11], [12] defined by the equation

$$\mathfrak{u}_k = D_{kl}\chi_l \tag{3.7}$$

and substitute it back into the equation (3.3) we have an uncoupled system of differential equations

$$\mathfrak{D}_{ik}\mathfrak{u}_k = \mathfrak{D}_{ik}D_{kl}\chi_l = \det(\mathfrak{D}_{jl})\chi_i = 0. \tag{3.8}$$

Let $Q(\xi_1, \xi_2)$ and $M(x_1, x_2)$ be two points in the plane of strain (the source point and the point of effect). Further let \mathbf{e} with components e_i be a unit vector at Q. We shall assume temporarily that the point Q is fixed. The distance between Q and M is R, the position vector of M relative to Q is r_{κ} . Solution to the differential equation

$$\mathfrak{D}_{ik}\mathfrak{u}_k + \delta(M-Q)e_i = 0$$

is referred to as fundamental solution. It is clear from all that has been said – see (3.7), (3.8) and (3.5) – that the fundamental solution is obtainable from the fundamental solution for the Galorkin functions, i.e., from the solution of the differential equation

$$\det(\mathfrak{D}_{jl})\chi_i + \delta(M - Q)e_i = -\frac{1}{2\mu}(1 - \nu)\Delta\Delta\chi_i + \delta(M - Q)e_i = 0.$$
 (3.9)

Making use of the fundamental solution

$$\chi_i(M,Q) = \frac{\mu}{4\pi(1-\nu)} R^2(\ln R - 1)e_i$$
 (3.10)

valid for the plane biharmonic equation [2] we have

$$\mathfrak{u}_k = \mathfrak{U}_{kl}(M, Q)e_l(Q) \tag{3.11}$$

where

$$\left[\mathfrak{U}_{kl}(M,Q)\right] = \frac{\mu}{4\pi(1-\nu)} \begin{bmatrix} -2\ln R - 3 - 2\frac{r_2r_2}{R^2} & 2\frac{r_1r_2}{R^2} & \frac{2}{\mu}(1-\nu)\frac{r_1}{R^2} \\ 2\frac{r_2r_1}{R^2} & -2\ln R - 3 - 2\frac{r_1r_1}{R^2} & \frac{2}{\mu}(1-\nu)\frac{r_2}{R^2} \\ \frac{2}{\mu}(1-\nu)\frac{r_1}{R^2} & \frac{2}{\mu}(1-\nu)\frac{r_2}{R^2} & 0 \end{bmatrix}.$$

$$(3.12)$$

REMARK 5.: The fundamental solution $\mathfrak{U}_{kl}(M,Q)$ satisfies the symmetry conditions

$$\mathfrak{U}_{kl}(M,Q) = \mathfrak{U}_{lk}(M,Q) = \mathfrak{U}_{kl}(Q,M) = \mathfrak{U}_{lk}(Q,M) . \tag{3.13}$$

Consequently

$$\mathfrak{U}_k = \mathfrak{U}_{kl}(M, Q)e_l(Q) = e_l(Q)\mathfrak{U}_{lk}(M, Q). \tag{3.14}$$

REMARK 6.: Each row and column of $\mathfrak{U}_{kl}(M,Q)$ as a three dimensional vector satisfies the basic equation (3.3) both in M and in Q.

Substituting the columns of $\mathfrak{U}_{kl}(M,Q)$ into (2.1) and recalling that the particular solution for stresses is assumed to be zero, we have the fundamental solution for stresses

$$\begin{bmatrix} t_{11} \\ t_{12} \\ t_{22} \end{bmatrix} = \frac{\mu}{4\pi(1-\nu)R^2} \begin{bmatrix} -6r_2 + 4\frac{r_2^3}{R^2} & 2r_1 - \frac{4r_1r_2^2}{R^2} & -\frac{4}{\mu}(1-\nu)\frac{r_1r_2}{R^2} \\ 2r_1 - \frac{4r_2^2r_1}{R^2} & -2r_2 + \frac{4r_1^2r_2}{R^2} & \frac{2}{\mu}(1-\nu)\frac{r_1^2 - r_2^2}{R^2} \\ -2r_2 + \frac{4r_1^2r_2}{R^2} & 6r_1 - 4\frac{r_1^3}{R^2} & \frac{4}{\mu}(1-\nu)\frac{r_1r_2}{R^2} \end{bmatrix} \begin{bmatrix} e_1 \\ e_2 \\ e_3 \end{bmatrix}.$$
(3.15)

It can be shown that $t_{12} = t_{21}$.

With the aid of Hook's law (2.2) one obtains the fundamental solution for strains

$$\begin{bmatrix} e_{11} \\ e_{12} \\ e_{22} \end{bmatrix} = \frac{\hat{C}}{R^2} \begin{bmatrix} -2(3-2v)r_2 + 4\frac{r_3^2}{R^2} & 2(1-2v)r_1 - 4\frac{r_1r_2^2}{R^2} & -\frac{4}{\mu}(1-\nu)\frac{r_1r_2}{R^2} \\ 2r_1 - \frac{4r_2^2r_1}{R^2} & -2r_2 + \frac{4r_1^2r_2}{R^2} & \frac{2}{\mu}(1-\nu)\frac{r_1^2 - r_2^2}{R^2} \\ -2(1-2v)r_2 + 4\frac{r_1^2r_2}{R^2} & 2(3-2v)r_1 - 4\frac{r_1^3}{R^2} & \frac{4}{\mu}(1-\nu)\frac{r_1r_2}{R^2} \end{bmatrix} \begin{bmatrix} e_1 \\ e_2 \\ e_3 \end{bmatrix},$$
(3.16a)

$$\hat{C} = \frac{1}{8\pi(1-\nu)} \ . \tag{3.16b}$$

For our later considerations we shall introduce the notation

$$\mathfrak{t}_{\lambda} = -\frac{du_{\lambda}}{ds} \tag{3.17}$$

where the vector \mathfrak{t}_{λ} is referred to as displacement derivative. Comparing (2.14), (3.16a,b) and (3.17) for the vector \mathfrak{t}_{λ} from the fundamental solution we get

$$\mathfrak{t}_{\lambda}(\overset{\circ}{M}) = e_{l}(Q)\mathfrak{T}_{l\lambda}(\overset{\circ}{M},Q) \tag{3.18a}$$

where

$$\mathfrak{T}_{l\lambda}(\overset{o}{M},Q) = \frac{\hat{C}}{R^2} \begin{bmatrix} n_1 r_1 \left(4\frac{r_2^2}{R^2} - 2(3 - 2v) \right) & -n_2 r_1 \left(4\frac{r_2^2}{R^2} + 2(1 - 2v) \right) \\ +n_2 r_2 \left(4\frac{r_2^2}{R^2} - 2(3 - 2v) \right) & -n_1 r_2 \left(4\frac{r_1^2}{R^2} - 2(1 - 2v) \right) \\ -n_1 r_2 \left(4\frac{r_1^2}{R^2} + 2(1 - 2v) \right) & n_2 r_2 \left(4\frac{r_1^2}{R^2} - 2(3 - 2v) \right) \\ -n_2 r_1 \left(4\frac{r_2^2}{R^2} - 2(1 - 2v) \right) & +n_1 r_1 \left(4\frac{r_1^2}{R^2} - 2(3 - 2v) \right) \\ -n_1 \frac{2}{\mu} (1 - \nu) \frac{r_1^2 - r_2^2}{R^2} & -n_1 \frac{4}{\mu} (1 - \nu) \frac{r_1 r_2}{R^2} \\ -n_2 \frac{4}{\mu} (1 - \nu) \frac{r_1 r_2}{R^2} & +n_2 \frac{2}{\mu} (1 - \nu) \frac{r_1^2 - r_2^2}{R^2} \end{bmatrix}.$$

$$(3.18b)$$

Here and in the sequel the small circle over the letters M and/or Q has the meaning that the corresponding point is located on the contour. The normal n_{λ} is taken at the point M.

REMARK 7.: Recalling that in the circle of the boundary value problems considered either the stress functions or the derivative of the displacements with respect to the arc coordinate can be prescribed at a point on the contour for our later consideration, it is worth giving the value of the stress functions from the fundamental solution on the boundary:

$$\mathfrak{u}_{\lambda} = e_l(Q)\mathfrak{U}_{l\lambda}(\stackrel{o}{M}, Q) \ . \tag{3.19}$$

The displacement derivative from the fundamental solution is given by (3.18a,b).

4. Somigliana identity and formulae in dual system - inner region

Here and in the sequel it is assumed that the region A_i under consideration is simply connected and lies wholly in finite. The contour \mathcal{L}_0 is divided into arcs of even number on which displacements (or their derivatives with respect to s) and tractions (or stress functions) can be imposed alternately. In Figure 2 the region A_i is divided into four arcs though this fact does not play any role in the transformations.

The functions \mathcal{F}_{ψ} , $t_{\kappa\lambda}$, $e_{\kappa\lambda}$ and φ_3 are referred to as an elastic state of the region A_i provided that they satisfy the field equations (2.1), (2.2), (2.3) and (2.4). Let

$$\mathcal{F}_{\psi}, t_{\kappa\lambda}, e_{\kappa\lambda}, \varphi_3$$
 and $\overset{*}{\mathcal{F}}_{\psi}, \overset{*}{t_{\kappa\lambda}}, \overset{*}{e_{\kappa\lambda}}, \overset{*}{\varphi}_3$

be two elastic states of the region A_i . Applying the Green-Gauss theorem and taking

(2.1) into account (since there are no body forces $\overset{o}{t}_{\kappa\lambda} = 0$) one can write

$$\int_{A_{i}} \left[\epsilon_{\kappa\rho3} e_{\kappa\lambda} \partial_{\rho} + \varphi_{3} \partial_{\lambda} \right] \overset{*}{\mathcal{F}}_{\lambda} dA - \int_{A_{i}} \left(\mathcal{F}_{\psi} \partial_{\psi} \right) \overset{*}{\varphi}_{3} dA =$$

$$= \oint_{\mathcal{L}_{o}} n_{\pi} \left[\epsilon_{\pi\kappa3} e_{\kappa\lambda} - \delta_{\pi\lambda} \varphi_{3} \right] \overset{*}{\mathcal{F}}_{\lambda} ds$$

$$- \int_{A_{i}} \left(\overset{*}{\mathcal{F}}_{\psi} \partial_{\psi} \right) \varphi_{3} dA - \int_{A_{i}} \left(\mathcal{F}_{\psi} \partial_{\psi} \right) \overset{*}{\varphi}_{3} dA .$$

$$(4.1)$$

REMARK 7.: Observe that the first surface integral and the sum of the last two surface integrals on the right side do not depend on the placement of the asterisk which can be put over the first or the second factor of the corresponding products.

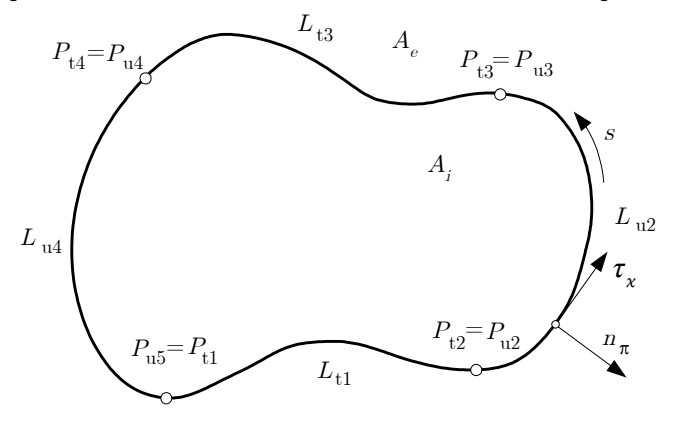


Figure 2

If we replace the asterisk over the letters denoting the first elastic state and subtract (4.1) from the resulting equation, then we get the dual Somigliana identity for plane problems

$$\int_{A_{i}} \left[\epsilon_{\kappa\rho3} \stackrel{*}{e}_{\kappa\lambda} \partial_{\rho} + \stackrel{*}{\varphi}_{3} \partial_{\lambda} \right] \mathcal{F}_{\lambda} dA - \int_{A_{i}} \left(\stackrel{*}{\mathcal{F}}_{\psi} \partial_{\psi} \right) \varphi_{3} dA \qquad (4.2)$$

$$- \int_{A_{i}} \left[\epsilon_{\kappa\rho3} e_{\kappa\lambda} \partial_{\rho} + \varphi_{3} \partial_{\lambda} \right] \stackrel{*}{\mathcal{F}}_{\lambda} dA - \int_{A_{i}} \left(\mathcal{F}_{\psi} \partial_{\psi} \right) \stackrel{*}{\varphi}_{3} dA =$$

$$= \oint_{\mathcal{L}_{o}} n_{\pi} \left[\epsilon_{\pi\kappa3} e_{\kappa\lambda} - \delta_{\pi\lambda} \stackrel{*}{\varphi}_{3} \right] \mathcal{F}_{\lambda} ds - \oint_{\mathcal{L}_{o}} n_{\pi} \left[\epsilon_{\pi\kappa3} e_{\kappa\lambda} - \delta_{\pi\lambda} \varphi_{3} \right] \stackrel{*}{\mathcal{F}}_{\lambda} ds.$$

On the left side we have the integrals of the basic equations. As regards the right side, we have the integrals of those quantities one can prescribe on the boundary. Recalling the relations (3.1a,b,c), (3.2a,b), (3.3) giving the basic equations and the notation (3.17) in which the derivative is given by (2.14), one can cast the Somigliana identity into a form similar to the Green identity [2]

$$\int_{A_i} \left[\mathfrak{u}_k \left(\mathfrak{D}_{kl} \mathfrak{u}_l^* \right) - \mathfrak{u}_k^* \left(\mathfrak{D}_{kl} \mathfrak{u}_l \right) \right] dA = \oint_{\mathcal{L}_o} \left[\mathfrak{u}_{\lambda} \mathfrak{t}_{\lambda}^* - \mathfrak{u}_{\lambda} \mathfrak{t}_{\lambda} \right] ds. \tag{4.3}$$

REMARK 8.: When deriving (4.3) we have never taken into consideration that $\overset{*}{\mathfrak{u}}_k$ and \mathfrak{u}_k are compatible, i.e., fulfill the basic equation (3.3). Consequently, the equation (4.3) is really an identity which is always valid if $\overset{*}{\mathfrak{u}}_k$ and \mathfrak{u}_k are differentiable as many times as required – in other respects both functions can be arbitrary.

In order to establish the dual Somigliana relations it is assumed that u_k^* is an elastic state given by (3.11) and (3.12). Quantities in the line integrals are defined by (3.19) and (3.18a,b).

In what follows we shall utilize that \mathfrak{u}_k is also an elastic state.

Since the state identified by the asterisk is singular at the point Q (at the source point), we distinguish three cases depending on the location of Q with respect to the region A_i .

- 1. If $Q \in A_i$, then the neighborhood of Q with radius R_{ε} , which is denoted by A_{ε} and is assumed to lie in A_i , is removed from A_i and we apply the dual Somigliana identity to the double connected domain $A' = A_i \setminus A_{\varepsilon}$. We remark that the contour $\mathcal{L}_{\varepsilon}$ of A_{ε} and the arc $\mathcal{L}'_{\varepsilon}$ of the contour $\mathcal{L}_{\varepsilon}$ within A_i coincide with each other.
- 2. If $Q = Q \in \partial A_i = \mathcal{L}_o$, then the part $A_i \cap A_{\varepsilon}$ of the neighborhood A_{ε} of Q is removed from A_i and we apply the dual Somigliana identity to the simply connected region $A' = A_i \setminus (A_i \cap A_{\varepsilon})$. If this is the case, the contour of the simply connected region consists of two arcs, the arc \mathcal{L}'_o left from \mathcal{L}_o after the removal of A_{ε} and the arc $\mathcal{L}'_{\varepsilon}$, i.e., the part of $\mathcal{L}_{\varepsilon}$ that lies within A_i .
- 3. If $Q \notin (A_i \cup \mathcal{L}_o)$, we apply the Somigliana identity to the original region A_i . Since both \mathfrak{u}_k and \mathfrak{u}_k are elastic states, the surface integrals in (4.3) are identically equal to zero. In what follows we regard the three cases one by one focusing attention on the line of thought.
 - 1. Making use of all that has been said above for $Q \in A_i$, it follows from (4.3) that

$$\oint_{\mathcal{L}_{o}} \left[\mathfrak{T}_{k\lambda}(\overset{\circ}{M}, Q) \mathfrak{u}_{\lambda}(\overset{\circ}{M}) - \mathfrak{U}_{k\lambda}(\overset{\circ}{M}, Q) \mathfrak{t}_{\lambda}(\overset{\circ}{M}) \right] ds_{\overset{\circ}{M}}$$

$$+ \oint_{\mathcal{L}_{e}} \left[\mathfrak{T}_{k\lambda}(M, Q) \mathfrak{u}_{\lambda}(M) - \mathfrak{U}_{k\lambda}(M, Q) \mathfrak{t}_{\lambda}(M) \right] ds_{M} = 0 .$$
(4.4)

It can be shown that

$$\oint_{\mathcal{L}_{\varepsilon}} \mathfrak{T}_{\kappa\lambda}(M,Q) \, ds_M = \delta_{\kappa\lambda} \,\,, \tag{4.5a}$$

$$\lim_{R_{\varepsilon} \to 0} \oint_{\mathcal{L}_{\varepsilon}} \mathfrak{T}_{\kappa\lambda}(M, Q) \left[\mathfrak{u}_{\lambda}(M) - \mathfrak{u}_{\lambda}(Q) \right] ds_{M} = 0 , \qquad (4.5b)$$

$$\oint_{\mathcal{L}_{\varepsilon}} \mathfrak{T}_{3\lambda}(M,Q) \, ds_M = \frac{1}{4\pi\mu} \frac{1}{R_{\varepsilon}} \int_0^{2\pi} \cos\varphi \, d\varphi = 0 \,, \tag{4.5c}$$

(The latter equation is fulfilled for any $R_{\varepsilon} \neq 0$. Consequently, if $R_{\varepsilon} \to 0$ the

limit of the integral is also zero.)

$$\lim_{R_{\varepsilon}\to 0} \oint_{\mathcal{L}_{\varepsilon}} \mathfrak{T}_{3\lambda}(M,Q) \left[\mathfrak{u}_{\lambda}(M) - \mathfrak{u}_{\lambda}(Q)\right] ds_{M} =$$

$$= \lim_{R_{\varepsilon}\to 0} \left\{ \oint_{\mathcal{L}_{\varepsilon}} \mathfrak{T}_{3\lambda}(M,Q) \left[\left. \frac{\partial \mathfrak{u}_{\lambda}}{\partial x_{1}} \right|_{Q} r_{1} + \left. \frac{\partial \mathfrak{u}_{\lambda}}{\partial x_{2}} \right|_{Q} r_{2} \right] ds_{M} + I_{\varepsilon}(R_{\varepsilon}) \right\} =$$

$$= \frac{1}{4\pi\mu} (t_{21} - t_{12}) + \lim_{R_{\varepsilon}\to 0} I_{\varepsilon}(R_{\varepsilon}) = 0 ,$$

$$(4.5d)$$

(Since $\mathfrak{u}_{\lambda}(M)$ is an elastic state, the stress tensor is symmetric and the expression I_{ε} is homogenous in R_{ε} .)

$$\lim_{R_{\varepsilon} \to 0} \oint_{\mathcal{L}_{\varepsilon}} \mathfrak{U}_{\kappa\lambda}(M, Q) \mathfrak{t}_{\lambda}(M) \, ds_M = 0 \,, \tag{4.5e}$$

(The relation

$$\mathfrak{t}_{\lambda} = -\frac{\partial u_{\lambda}}{\partial s} = -\frac{\partial u_{\lambda}}{\partial x_{1}} \frac{dx_{1}}{ds} - \frac{\partial u_{\lambda}}{\partial x_{2}} \frac{dx_{2}}{ds}$$

has been applied here and it should also be applied in the following transformation. In addition one should take the limit $\lim_{R_{\varepsilon}\to 0} R_{\varepsilon} \ln R_{\varepsilon} = 0$ into consideration.)

$$\lim_{R_{\varepsilon}\to 0} \oint_{\mathcal{L}_{\varepsilon}} \mathfrak{U}_{3\lambda}(M,Q)\mathfrak{t}_{\lambda}(M) \, ds_{M} = \varphi_{3}|_{Q} = -\mathfrak{u}_{3}|_{Q} . \tag{4.5f}$$

If we take the limit of the equation (4.4) as $R_{\varepsilon} \to 0$ and substitute the formulae (4.5a,...,e), we obtain the first dual Somigliana relation:

$$\mathfrak{u}_{k}(Q) = \oint_{\mathcal{L}_{o}} \mathfrak{U}_{k\lambda}(\overset{\circ}{M}, Q) \mathfrak{t}_{\lambda}(\overset{\circ}{M}) \, ds_{\overset{\circ}{M}} - \oint_{\mathcal{L}_{o}} \mathfrak{T}_{k\lambda}(\overset{\circ}{M}, Q) \mathfrak{u}_{\lambda}(\overset{\circ}{M}) \, ds_{\overset{\circ}{M}} \, . \tag{4.6}$$

2. If $Q = \overset{\circ}{Q} \in \partial A = \mathcal{L}_o$, it follows from (4.3) by the steps leading to (4.4) that

$$\int_{\mathcal{L}_{o}^{'}} \left[\mathfrak{T}_{\kappa\lambda}(\overset{o}{M},\overset{o}{Q}) \mathfrak{u}_{\lambda}(\overset{o}{M}) - \mathfrak{U}_{\kappa\lambda}(\overset{o}{M},\overset{o}{Q}) \mathfrak{t}_{\lambda}(\overset{o}{M}) \right] ds_{\overset{o}{M}}$$

$$+ \int_{\mathcal{L}_{\varepsilon}^{'}} \left[\mathfrak{T}_{\kappa\lambda}(M,\overset{o}{Q}) \mathfrak{u}_{\lambda}(M) - \mathfrak{U}_{\kappa\lambda}(M,\overset{o}{Q}) \mathfrak{t}_{\lambda}(M) \right] ds_{M} = 0.$$
(4.7)

It can be shown that

$$\lim_{R_{\varepsilon} \to 0} \int_{\mathcal{L}'_{\varepsilon}} \mathfrak{T}_{\kappa\lambda}(M, \overset{o}{Q}) \, ds_M = c_{\kappa\lambda}(\overset{o}{Q}) \,, \tag{4.8a}$$

where $c_{\kappa\lambda}(\overset{\circ}{Q}) = \delta_{\kappa\lambda}/2$ if the contour \mathcal{L}_o is smooth at the point $\overset{\circ}{Q}$. If the contour is not smooth, then $c_{\kappa\lambda}(\overset{\circ}{Q})$ depends on the angle formed by the tangents to the

contour at $\overset{o}{Q}$.

It can also be proved that

$$\lim_{R_{\varepsilon} \to 0} \int_{\mathcal{L}_{c}^{\prime}} \mathfrak{T}_{\kappa\lambda}(M, \overset{o}{Q}) \left[\mathfrak{u}_{\lambda}(M) - \mathfrak{u}_{\lambda}(\overset{o}{Q}) \right] ds_{M} = 0 , \qquad (4.8b)$$

$$\lim_{R_{\varepsilon} \to 0} \int_{\mathcal{L}_{\varepsilon}'} \mathfrak{U}_{\kappa\lambda}(M, \overset{\circ}{Q}) \mathfrak{t}_{\lambda}(M) \, ds_M = 0 \; . \tag{4.8c}$$

If we take the limit of equation (4.7) as $R_{\varepsilon} \to 0$ and substitute the formulae (4.8a,b,c) we obtain the second dual Somigliana relation:

$$c_{\kappa\lambda}(\overset{o}{Q})\mathfrak{u}_{\lambda}(\overset{o}{Q}) = \oint_{\mathcal{L}_o} \mathfrak{U}_{\kappa\lambda}(\overset{o}{M},\overset{o}{Q})\mathfrak{t}_{\lambda}(\overset{o}{M}) \, ds_{\overset{o}{M}} - \oint_{\mathcal{L}_o} \mathfrak{T}_{\kappa\lambda}(\overset{o}{M},\overset{o}{Q})\mathfrak{u}_{\lambda}(\overset{o}{M}) \, ds_{\overset{o}{M}} \ . \tag{4.9}$$

Remark 9.: The two line integrals in (4.9) should be taken in principal value.

REMARK 10.: The integral equation (4.9) with unknowns $\mathfrak{u}_{\lambda}(M)$ on \mathcal{L}_{u} and $\mathfrak{t}_{\lambda}(M)$ on \mathcal{L}_{t} is that of the direct method.

3. If $Q \notin (A \cup \mathcal{L}_o)$, then the line integral in the identity (4.3) is taken on \mathcal{L}_o (the surface integrals on the right side are ab ovo equal to zero) and by repeating the steps leading to (4.4) we have the third dual SOMIGLIANA formula:

$$0 = \oint_{\mathcal{L}_{\mathcal{O}}} \mathfrak{U}_{k\lambda}(\overset{\circ}{M}, Q) \mathfrak{t}_{\lambda}(\overset{\circ}{M}) \, ds_{\overset{\circ}{M}} - \oint_{\mathcal{L}_{\mathcal{O}}} \mathfrak{T}_{k\lambda}(\overset{\circ}{M}, Q) \mathfrak{u}_{\lambda}(\overset{\circ}{M}) \, ds_{\overset{\circ}{M}} \,. \tag{4.10}$$

Making use of the first dual Somigliana formula (4.6) and the dual kinematic equation (2.1) (in the latter case one has to recall that there are no body forces, consequently the particular solution is zero) one obtains the formula for the stresses $\mathfrak{s}_k = (t_{11}, t_{12}, t_{22})$ by performing the corresponding derivations

$$\mathfrak{s}_{k}(Q) = \oint_{\mathcal{L}_{o}} \mathcal{D}_{k\lambda}(\overset{\circ}{M}, Q) \mathfrak{t}_{\lambda}(\overset{\circ}{M}) \, ds_{\overset{\circ}{M}} - \oint_{\mathcal{L}_{o}} \mathcal{S}_{k\lambda}(\overset{\circ}{M}, Q) \mathfrak{u}_{\lambda}(\overset{\circ}{M}) \, ds_{\overset{\circ}{M}} \tag{4.11}$$

where the elements of $D_{k\lambda}(\stackrel{\circ}{M},Q)$ and $S_{k\lambda}(\stackrel{\circ}{M},Q)$ are given by

$$D_{k\lambda}(M, Q) = \frac{\mu}{4\pi(1-\nu)R^2} \hat{D}_{k\lambda}(M, Q),$$
 (4.12a)

$$\hat{\mathbf{D}}_{k\lambda}(M,Q) = \begin{bmatrix} 6r_2 - 4r_2^3/R^2 & -2r_1 + 4r_1r_2^2/R^2 \\ -2r_1 + 4r_1r_2^2/R^2 & 2r_2 - 4r_1^2r_2/R^2 \\ 2r_2 - 4r_1^2r_2/R^2 & -6r_1 + 4r_1^3/R^2 \end{bmatrix}$$
(4.12b)

and

$$S_{k\lambda}(M, Q) = \frac{1}{8\pi(1-\nu)R^2} \hat{S}_{k\lambda}(M, Q),$$
 (4.13a)

$$\hat{\mathbf{S}}_{11} = \frac{1}{R^2} (n_1 r_1 + n_2 r_2) \left[16 \frac{r_2^3}{R^2} - 4(5 - 2\nu) r_2 \right] - n_2 \left[4 \frac{r_2^2}{R^2} - 2(3 - 2\nu) \right] , \quad (4.13b)$$

$$\hat{S}_{12} = n_1 \left[4 \frac{r_1^2}{R^2} - 2(1 - 2\nu) \right] - \frac{1}{R^2} n_2 r_1 \left[16 \frac{r_2^3}{R^2} - 4(1 + 2\nu) r_2 \right] - \frac{1}{R^2} n_1 r_2 \left[16 \frac{r_1^2 r_2}{R^2} - 4(1 - 2\nu) r_2 \right] , \qquad (4.13c)$$

$$\hat{S}_{21} = \hat{S}_{12} , \qquad (4.13d)$$

$$\hat{S}_{22} = \frac{1}{R^2} n_1 r_2 \left[16 \frac{r_1^3}{R^2} - 4(3 - 2\nu) r_1 \right] + \frac{1}{R^2} n_2 r_1 \left[16 \frac{r_1 r_2^2}{R^2} - 4(1 - 2\nu) r_2 \right] - n_2 \left[4 \frac{r_2^2}{R^2} + 2(1 - 2\nu) \right] , \qquad (4.13e)$$

$$\hat{S}_{31} = \hat{S}_{22} , \qquad (4.13f)$$

$$\hat{S}_{32} = \frac{1}{R^2} (n_1 r_1 + n_2 r_2) \left[16 \frac{r_1^3}{R^2} - 4(5 - 2\nu) r_1 \right] - n_1 \left[4 \frac{r_1^2}{R^2} - 2(3 - 2\nu) \right] .$$
 (4.13g)

We remark that the normal is taken at $\stackrel{o}{M}$.

5. Somigliana formulae in dual system - outer region

By the outer region A_e we mean the region outside the contour \mathcal{L}_0 . We shall assume that the stresses are constants at infinity. These are denoted by

$$t_{11}(\infty), t_{12}(\infty) = t_{21}(\infty) \text{ and } t_{22}(\infty).$$

We shall also assume that there is no rigid body rotation at infinity, that is,

$$\varphi_3(\infty) = 0. (5.1)$$

Observe that the strains obtainable from the stresses at infinity via Hook's law are compatible for they satisfy the compatibility condition (2.3). The corresponding stress functions are of the form

$$\tilde{\mathfrak{u}}_{\lambda}(Q) = \epsilon_{\alpha 3\rho} \xi_{\alpha} t_{\lambda \rho}(\infty) + c_{\lambda}(\infty) \tag{5.2}$$

where $c_{\lambda}(\infty)$ is a constant vector to which there belong no stresses. Further let

$$\tilde{\mathfrak{u}}_3(Q) = -\varphi_3(\infty) = 0. \tag{5.3}$$

When deriving the dual Somigliana formula for the outer region A_e , we shall follow the line of thought of the previous section with an emphasis placed on the difference. It is assumed again that u_k^* is the elastic state described by the fundamental solutions (3.11) and (3.12). Further, u_k is also an elastic state arbitrary at finite but it is to meet the conditions

$$\mathfrak{u}_{\kappa} = \tilde{\mathfrak{u}}_{\lambda} \text{ and } \mathfrak{u}_3 = \tilde{\mathfrak{u}}_3 = 0$$

at infinity. Depending on the location of the point Q, we distinguish three cases in the same way as we did for the inner region A_i . It is assumed that the origin O is within the region A_i .

1. If $Q \in A_e$, we shall consider the triple connected region A'_e bounded by the contours \mathcal{L}_0 , $\mathcal{L}_{\varepsilon}$ and the circle \mathcal{L}_R with radius ${}_eR$ and center at O. Here $\mathcal{L}_{\varepsilon}$ is the contour of the neighborhood A_{ε} of Q with radius R_{ε} while ${}_eR$ is sufficiently large to involve both \mathcal{L}_0 , and $\mathcal{L}_{\varepsilon}$. In addition, A_{ε} is to lie wholly in A'_e . Now we apply the dual Somigliana identity to the region A'_e and take the limit of the resulting equation

$$\oint_{\mathcal{L}_{o}} \left[\mathfrak{T}_{k\lambda}(\overset{\circ}{M}, Q) \mathfrak{u}_{\lambda}(\overset{\circ}{M}) - \mathfrak{U}_{k\lambda}(\overset{\circ}{M}, Q) \mathfrak{t}_{\lambda}(\overset{\circ}{M}) \right] ds_{\overset{\circ}{M}}$$

$$+ \oint_{\mathcal{L}_{\varepsilon}} \left[\mathfrak{T}_{k\lambda}(\overset{\circ}{M}, Q) \mathfrak{u}_{\lambda}(\overset{\circ}{M}) - \mathfrak{U}_{k\lambda}(\overset{\circ}{M}, Q) \mathfrak{t}_{\lambda}(\overset{\circ}{M}) \right] ds_{\overset{\circ}{M}}$$

$$+ \oint_{\mathcal{L}_{R}} \left[\mathfrak{T}_{k\lambda}(\overset{\circ}{M}, Q) \mathfrak{u}_{\lambda}(\overset{\circ}{M}) - \mathfrak{U}_{k\lambda}(\overset{\circ}{M}, Q) \mathfrak{t}_{\lambda}(\overset{\circ}{M}) \right] ds_{\overset{\circ}{M}} = 0$$
(5.4)

as $R_{\varepsilon} \longrightarrow 0$ and ${}_{e}R \longrightarrow \infty$. As regards the sum of the first two integrals observe, that the limit is formally the same as that of the integrals in (4.4):

$$\oint_{\mathcal{L}_o} \dots + \lim_{R_{\varepsilon} \longrightarrow 0} \oint_{\mathcal{L}_{\varepsilon}} \dots = \mathfrak{u}_k(Q) + \oint_{\mathcal{L}_o} [\mathfrak{T}_{k\lambda}(\overset{\circ}{M}, Q)\mathfrak{u}_{\lambda}(\overset{\circ}{M}) - \mathfrak{U}_{k\lambda}(\overset{\circ}{M}, Q)\mathfrak{t}_{\lambda}(\overset{\circ}{M})] ds_{\overset{\circ}{M}}.$$
(5.5)

For the limit of the third integral we obtain

$$\lim_{eR \longrightarrow \infty} \oint_{\mathcal{L}_R} \dots = -\tilde{\mathfrak{u}}_k(Q) . \tag{5.6}$$

By making use of the results (5.5) and (5.6) we shall find from (5.4) for the first dual Somigliana identity on the outer region that

$$\mathfrak{u}_k(Q) = \tilde{\mathfrak{u}}_k(Q) + \oint_{\mathcal{L}_0} \mathfrak{U}_{k\lambda}(\overset{o}{M},Q) \mathfrak{t}_{\lambda}(\overset{o}{M}) \, ds_{\overset{o}{M}} - \oint_{\mathcal{L}_0} \mathfrak{T}_{k\lambda}(\overset{o}{M},Q) \mathfrak{u}_{\lambda}(\overset{o}{M}) \, ds_{\overset{o}{M}} \ . \ (5.7)$$

REMARK 11.: Derivation of the relation (5.7) requires long formal transformations. First one has to approximate $\mathfrak{U}_{k\lambda}$ and $\mathfrak{T}_{k\lambda}$ with one series in terms of ${}_{e}R$ to the power 1,0,-1,-2 etc. This transformation relies upon the use of the relations:

$$x_{\alpha}(\overset{\circ}{M}) = {}_{e}Rn_{\alpha}(\overset{\circ}{M}), \qquad \qquad r_{\alpha}(\overset{\circ}{M},Q) = x_{\alpha}(\overset{\circ}{M}) - \xi_{\alpha}(Q) \qquad \qquad (5.8a)$$

$$\frac{1}{R} = \frac{1}{eR} \left(1 + \frac{n_{\alpha}(M)\xi_{\alpha}(Q)}{eR} - \frac{1}{2} \frac{\xi_{\alpha}(Q)\xi_{\alpha}(Q)}{eR^2} + \cdots \right)$$
 (5.8b)

$$\ln \frac{1}{R} = \ln \frac{1}{eR} + \frac{n_{\alpha}(M)\xi_{\alpha}(Q)}{eR} - \frac{1}{2} \frac{\xi_{\alpha}(Q)\xi_{\alpha}(Q)}{eR^2} + \cdots$$
 (5.8c)

$$\frac{r_{\alpha}r_{\beta}}{eR^{2}} \approx n_{\alpha}n_{\beta} + 2n_{\alpha}n_{\beta}\frac{n_{\psi}\xi_{\psi}}{eR} - \frac{1}{eR}\left(\xi_{\alpha}n_{\beta} + n_{\alpha}\xi_{\beta}\right) + \cdots \qquad (5.8d)$$

Further one has also to utilize the following:

(a) For the outward unit normal and unit tangent in terms of φ , we may write

$$n_a = (\sin \varphi, \cos \varphi), \qquad \tau_\alpha = (-\cos \varphi, \sin \varphi)$$
 (5.9a)

(φ is the polar angle).

(b) For $_eR \longrightarrow \infty$ – see (3.17), (2.15), (2.14) and (2.2) –

$$\mathfrak{t}_{\lambda}(\stackrel{o}{M}) = -\frac{du_{\lambda}}{ds} = \tau_{\kappa} e_{\kappa\lambda} = \tau_{\kappa} \frac{1}{2\mu} \left(t_{\kappa\lambda}(\infty) - \nu t_{\psi\psi}(\infty) \delta_{\kappa\lambda} \right) \tag{5.9b}$$

and

$$ds_{\stackrel{o}{M}} = {}_{e}Rd\varphi . {} (5.9c)$$

(c) Since the stresses (consequently the strains as well) tend to constant value as ${}_eR \longrightarrow \infty$ the coefficients of ${}_eR$ always assume the form: an expression constant at infinity and multiplied by

$$\int_0^{2\pi} \sin^n \varphi \cos^k \varphi \, d\theta$$

where the powers n and k are natural numbers and depend on the term considered, but the integral is of zero value.

- (d) The structure of the terms being the coefficients of ${}_{e}R$ to the power zero is similar, but they involve ξ_{α} and the trigonometric integrals are not necessarily equal to zero.
- (e) It holds that

$$\oint_{\mathcal{L}_R} \mathfrak{T}_{\kappa\lambda}(\stackrel{\circ}{M}, Q) \, ds_{\stackrel{\circ}{M}} = -\delta_{\kappa\lambda} \; . \tag{5.9d}$$

(The same relation holds for any simply connected contour provided that Q is an inner point.)

For keeping the extent of the paper below a reasonable limit we have omitted the transformations leading to (5.7).

2. If $Q = \overset{\circ}{Q} \in \partial A = \mathcal{L}_o$, we shall consider the double connected region A'_e bounded by \mathcal{L}'_o , $\mathcal{L}'_{\varepsilon}$ and \mathcal{L}_R where \mathcal{L}'_o is the part of \mathcal{L}_o that is left after the removal of A_{ε} and $\mathcal{L}'_{\varepsilon}$ is the part of $\mathcal{L}_{\varepsilon}$ that lies within A_e . Applying again the dual Somigliana identity to A'_e and taking the limit as as $R_{\varepsilon} \longrightarrow 0$ and ${}_eR \longrightarrow \infty$, we get the second dual Somigliana relation for the outer region A_e :

$$c_{\kappa\lambda}(\overset{o}{Q})\mathfrak{u}_{\lambda}(\overset{o}{Q}) = \tilde{\mathfrak{u}}_{\kappa}(Q) + \oint_{\mathcal{L}_{o}} \mathfrak{U}_{\kappa\lambda}(\overset{o}{M},\overset{o}{Q})\mathfrak{t}_{\lambda}(\overset{o}{M}) ds_{\overset{o}{M}} - \oint_{\mathcal{L}_{o}} \mathfrak{T}_{\kappa\lambda}(\overset{o}{M},\overset{o}{Q})\mathfrak{u}_{\lambda}(\overset{o}{M}) ds_{\overset{o}{M}}.$$

$$(5.10)$$

REMARK 12.: The integral equation (5.10) with unknowns $\mathfrak{u}_{\lambda}(M)$ on \mathcal{L}_{u} and $\mathfrak{t}_{\lambda}(M)$ on \mathcal{L}_{t} is that of the direct method for outer regions.

REMARK 13.: We have omitted again the details since the limit of the integral on \mathcal{L}_R is the same as that for $Q \in A_e$ while the other terms can be derived letter by letter in the same way as for the integral equation (4.9).

3. It is obvious on the basis of all that has been said above that for $Q \in A_i$ the third dual Somigliana relation for the outer region is of the form

$$0 = \tilde{\mathfrak{u}}_{k}(Q) + \oint_{\mathcal{L}_{o}} \mathfrak{U}_{\kappa\lambda}(\overset{\circ}{M}, Q) \mathfrak{t}_{\lambda}(\overset{\circ}{M}) \, ds_{\overset{\circ}{M}} - \oint_{\mathcal{L}_{o}} \mathfrak{T}_{\kappa\lambda}(\overset{\circ}{M}, Q) \mathfrak{u}_{\lambda}(\overset{\circ}{M}) \, ds_{\overset{\circ}{M}} . \quad (5.11)$$

Let

$$\tilde{\mathfrak{s}}_k = (t_{11}(\infty), t_{12}(\infty), t_{22}(\infty)) \ .$$
 (5.12)

By repeating the line of thought leading to (4.11) we obtain the formula for the stresses at the internal points of the outer region A_e :

$$\mathfrak{s}_{k}(Q) = \tilde{\mathfrak{s}}_{k}(Q) + \oint_{\mathcal{L}_{o}} \mathcal{D}_{k\lambda}(\overset{o}{M}, Q) \mathfrak{t}_{\lambda}(\overset{o}{M}) \, ds_{\overset{o}{M}} - \oint_{\mathcal{L}_{o}} \mathcal{S}_{k\lambda}(\overset{o}{M}, Q) \mathfrak{u}_{\lambda}(\overset{o}{M}) \, ds_{\overset{o}{M}}$$
 (5.13)

where $D_{k\lambda}(\stackrel{\circ}{M},Q)$ and $S_{k\lambda}(\stackrel{\circ}{M},Q)$ are given by (4.12a),...,(4.13g).

6. Examples

We have applied the usual and well known procedure – see for instance [13] – for the solution of the boundary integral equation of the direct method (4.9). The program was written in Fortran 90.

In what follows we detail the main features of the algorithm.

We have used partially discontinuous quadratic elements by mapping the element onto the interval $\eta \in [-1, 1]$. The corresponding shape functions are Lagrange polynomials

$$N^{1}(\eta) = \frac{1}{(\eta^{1} - \eta^{2})(\eta^{1} - \eta^{3})} (\eta - \eta^{2})(\eta - \eta^{3}) ,$$

$$N^{2}(\eta) = \frac{1}{(\eta^{2} - \eta^{3})(\eta^{2} - \eta^{1})} (\eta - \eta^{3})(\eta - \eta^{1}) ,$$

$$N^{3}(\eta) = \frac{1}{(\eta^{3} - \eta^{1})(\eta^{3} - \eta^{2})} (\eta - \eta^{1})(\eta - \eta^{2})$$
(6.1)

with local nodal points η^1 , η^2 and η^3 where $\eta^1=-1$ and $-1<\eta^2<\eta^3<1$ are regarded as previously fixed parameters if the discontinuity occurs at $\eta=1$ while $\eta^3=1$ and $-1<\eta^1<\eta^2<1$ are regarded again as previously fixed parameters if the discontinuity occurs at $\eta=-1$. For $\eta^1=-1$ $\eta^2=0$ and $\eta^3=1$ the above polynomials give the usual isoparametric approximation.

Let n_{bn} be the number of nodal points. Further let n_{be} be the number of boundary elements. The elements are denoted by $\mathcal{L}_e - e = 1, \dots, n_{be}$.

Let

$$\mathbf{u}_{j} = \begin{bmatrix} \mathbf{u}_{1}^{j} \\ \mathbf{u}_{2}^{j} \end{bmatrix} \quad \text{and} \quad \mathbf{t}_{j} = \begin{bmatrix} \mathbf{t}_{1}^{j} \\ \mathbf{t}_{2}^{j} \end{bmatrix} \quad j = 1, \dots, n_{bn}$$
 (6.2)

be the stress functions and the displacement derivative $-du_{\lambda}/ds$ at the nodal point j. The matrices of the stress functions \mathbf{u} and that of the displacement derivatives \mathbf{t}

are defined by

$$\mathbf{u}^{T} = \left[\underbrace{u_{1}^{1} u_{2}^{1}}_{\mathbf{u}_{1}^{T}} | \underbrace{u_{1}^{2} u_{2}^{2}}_{\mathbf{u}_{2}^{T}} | \dots | \underbrace{u_{1}^{n_{bn}} u_{2}^{n_{bn}}}_{\mathbf{u}_{n_{bn}}^{T}} \right], \tag{6.3a}$$

$$\mathbf{t}^T = \left[\underbrace{\mathbf{t}_1^1 \ \mathbf{t}_2^1}_{\mathbf{t}_1^T} \middle| \underbrace{\mathbf{t}_2^1 \ \mathbf{t}_2^2}_{\mathbf{t}_2^T} \middle| \dots \middle| \underbrace{\mathbf{t}_1^{n_{bn}} \ \mathbf{t}_2^{n_{bn}}}_{\mathbf{t}_{n_{bn}}^T} \right]. \tag{6.3b}$$

Let there be constructed a function a(j, e) giving the local node number of the node on element e with global node number j. For our latter considerations we introduce the integrals

$$\hat{\mathbf{h}}_{ij} = \left[\sum_{e \in j} \int_{\mathcal{L}_e} \mathfrak{T}_{\kappa\lambda}(Q_i, \eta) N^{a(j,e)}(\eta) J(\eta) \, d\eta \right]$$
(6.4)

and

$$\mathbf{b}_{ij} = \left[\sum_{e \in j} \int_{\mathcal{L}_e} \mathfrak{U}_{\kappa\lambda}(Q_i, \eta) N^{a(j,e)}(\eta) J(\eta) \, d\eta \right]$$
 (6.5)

where the summation is taken over those elements containing the nodal point with number j, Q_i is the i-th nodal point (collocation point) and $J(\eta)$ is the Jacobian. With the notations $(6.2), \ldots, (6.5)$,

$$\mathbf{c}_{ii} = [c_{\kappa\lambda}(Q_i)] \tag{6.6}$$

and

$$\mathbf{h}_{ij} = \begin{cases} \hat{\mathbf{h}}_{ii} + \mathbf{c}_{ii} & \text{ha } i = j\\ \hat{\mathbf{h}}_{ij} & \text{ha } i \neq j \end{cases}$$
 (6.7)

it follows from the second dual Somigliana formula (4.9) taken at the collocation point $\overset{o}{Q} = Q_i$ that

$$\begin{bmatrix} \mathbf{h}_{i1} & \mathbf{h}_{i2} & \cdots & \mathbf{h}_{in_{bn}} \end{bmatrix} \begin{bmatrix} \mathbf{u}_{1} \\ \mathbf{u}_{2} \\ \cdots \\ \mathbf{u}_{n_{bn}} \end{bmatrix} = \begin{bmatrix} \mathbf{b}_{i1} & \mathbf{b}_{i2} & \cdots & \mathbf{b}_{in_{bn}} \end{bmatrix} \begin{bmatrix} \mathbf{t}_{1} \\ \mathbf{t}_{2} \\ \cdots \\ \mathbf{t}_{n_{bn}} \end{bmatrix},$$

$$i = 1, \dots, n_{bn} \quad (6.8)$$

After uniting these equations we have

$$\begin{bmatrix} \mathbf{h}_{11} & \mathbf{h}_{12} & \cdots & \mathbf{h}_{1n_{bn}} \\ \mathbf{h}_{21} & \mathbf{h}_{22} & \cdots & \mathbf{h}_{2n_{bn}} \\ \vdots & \vdots & \vdots & \vdots \\ \mathbf{h}_{n_{bn}1} & \mathbf{h}_{n_{bn}2} & \cdots & \mathbf{h}_{n_{bn}n_{bn}} \end{bmatrix} \begin{bmatrix} \mathbf{u}_{1} \\ \mathbf{u}_{2} \\ \vdots \\ \mathbf{u}_{n_{bn}} \end{bmatrix} = \begin{bmatrix} \mathbf{b}_{11} & \mathbf{b}_{12} & \cdots & \mathbf{b}_{1n_{bn}} \\ \mathbf{b}_{21} & \mathbf{b}_{22} & \cdots & \mathbf{b}_{2n_{bn}} \\ \vdots & \vdots & \vdots \\ \mathbf{b}_{n_{bn}1} & \mathbf{b}_{n_{bn}2} & \cdots & \mathbf{b}_{n_{bn}n_{bn}} \end{bmatrix} \begin{bmatrix} \mathbf{t}_{1} \\ \mathbf{t}_{2} \\ \vdots \\ \mathbf{t}_{n_{bn}} \end{bmatrix}$$

$$\begin{bmatrix} \mathbf{t}_{1} \\ \mathbf{t}_{2} \\ \vdots \\ \mathbf{t}_{n_{bn}} \end{bmatrix}$$

$$(6.9)$$

or in a more compact form

$$\mathbf{H}\mathbf{u} = \mathbf{B}\mathbf{t} . \tag{6.10}$$

After solving the above system of linear equations we have the nodal values of the unknown stress functions \mathfrak{u}_{λ} on \mathcal{L}_{u} and the nodal values of the unknown displacement derivatives \mathfrak{t}_{λ} on \mathcal{L}_{t} .

In the knowledge of the nodal values stresses at the internal points are computed by using (4.11). Stresses on \mathcal{L}_u are computed element by element by substituting the local approximation of the stress functions into (2.5).

Since there belong no stresses to the constant stress functions they are determined with the accuracy of a constant vector. Consequently

$$t_{\lambda} = -\frac{du_{\lambda}}{ds} = -\varphi_3 \frac{dx^{\kappa}}{ds} \epsilon_{3\kappa\lambda}$$

where φ_3 is the rigid body rotation which is to be constant if there are no stresses and strains. Therefore it can be set to zero. If this is the case then $\mathbf{t} = \mathbf{0}$ and if we take the constant stress functions as $u_k = 1$ $(k = 1, ..., n_{bn})$, then we have

$$\sum_{j=1}^{2n_{bn}} H_{ij} = 0 \quad \text{or, which is the same thing,} \quad H_{ii} = -\sum_{\substack{j=1 \ (i \neq j)}}^{2n_{bn}} H_{ij} \qquad i = 1, 2, \dots, 2n_{bn} ,$$
(6.11)

where H_{ij} is an element of the matrix **H**. By using this property one can avoid the numerical integration of strongly singular integrals.

If the region under consideration is an outer one, then there are some changes in the final equation system. Let the matrix $\tilde{\mathbf{u}}$ be defined by

$$\tilde{\mathbf{u}}^T = \left[\underbrace{\tilde{\mathbf{u}}_1^1 \, \tilde{\mathbf{u}}_2^1}_{\tilde{\mathbf{u}}_1^T} \middle| \underbrace{\tilde{\mathbf{u}}_1^2 \, \tilde{\mathbf{u}}_2^2}_{\tilde{\mathbf{u}}_2^T} \middle| \dots \middle| \underbrace{\tilde{\mathbf{u}}_1^{n_{bn}} \, \tilde{\mathbf{u}}_2^{n_{bn}}}_{\tilde{\mathbf{u}}_{n_{bn}}^T} \right] \tag{6.12}$$

where $\tilde{\mathbf{u}}_j$ is the matrix that involves $\tilde{\mathbf{u}}_{\kappa}$ at the nodal point Q_j $(j = 1, ..., n_{bn})$. With this notation the equation system to be solved for the unknown nodal values takes the form

$$\mathbf{H}\mathbf{u} = \mathbf{\tilde{u}} + \mathbf{B}\mathbf{t}.\tag{6.13}$$

Computation of strongly singular integrals can be avoided if we use the relation

$$H_{ii} = -\sum_{\substack{j=1\\(i\neq j)}}^{2n_{bn}} H_{ij} + 1 \qquad i = 1, 2, \dots, 2n_{bn} .$$

$$(6.14)$$

Equation (6.14) can be established in the same way as (6.11). c_{ρ} in $\tilde{\mathbf{u}}_{j}$ – see (5.2) – is set to zero.

Three examples are presented. The region under consideration including its matter, is the same for the first two cases. $r_0 = 10 [\text{mm}], \ \mu = 8 \cdot 10^4 [\text{MPa}], \ \nu = 0.3$

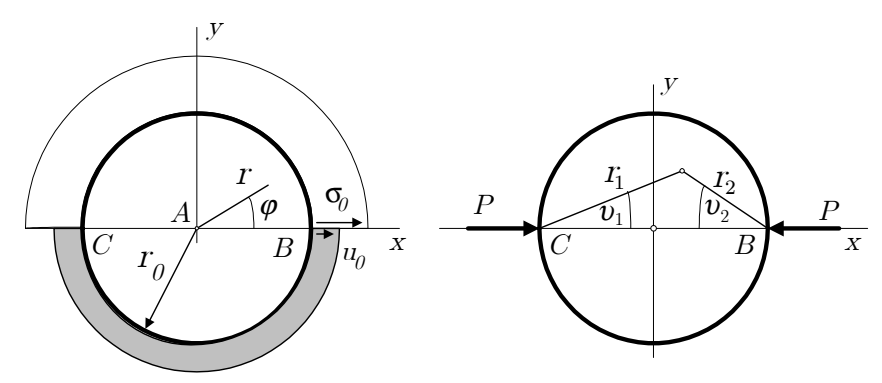


Figure 3.

Problem 1. On arc BC the radial stress (normal stress) is $\sigma_o = 100$ [MPa] (there are no shear stresses). On arc CB the radial displacement is $u_o = (1 - 2\nu)\sigma_o r_o/2\mu$ (there is no tangential displacement). One can check with ease that these values determine a homogeneous state of stress of the region. The exact solutions are given by the equations

$$\mathcal{F}_{1} = \mathcal{F}_{x} = \sigma_{o}y = \sigma_{o}r\sin\varphi , \qquad \mathcal{F}_{2} = \mathcal{F}_{y} = -\sigma_{o}x = -\sigma_{o}r\cos\varphi ,$$

$$\sigma_{xx} = \sigma_{yy} = \sigma_{o} , \qquad \tau_{xy} = 0 ,$$

$$u_{x} = \frac{1 - 2\nu}{2\mu}\sigma_{o}x = \frac{1 - 2\nu}{2\mu}\sigma_{o}r\sin\varphi ,$$

$$u_{y} = \frac{1 - 2\nu}{2\mu}\sigma_{o}y = \frac{1 - 2\nu}{2\mu}\sigma_{o}r\cos\varphi$$

where r and φ are polar coordinates. On arc BC and CB

$$u_x = \mathcal{F}_x = \sigma_{\text{o}} r_{\text{o}} \sin \varphi , \qquad \qquad u_y = \mathcal{F}_y = -\sigma_{\text{o}} r_{\text{o}} \cos \varphi$$

and

$$-\mathfrak{t}_x = \frac{du_x}{ds} = \frac{1 - 2\nu}{2\mu} \sigma_0 \sin \varphi \; , \qquad \qquad -\mathfrak{t}_y = \frac{du_y}{ds} = \frac{1 - 2\nu}{2\mu} \sigma_0 \cos \varphi$$

are the boundary conditions. The contour was divided into 16 equidistant elements. The table below contains the numerical results for the stresses

x [mm]	y [mm]	σ_{xx} [MPa]	τ_{xy} [MPa]	σ_{yy} [MPa]
-7.50	0.00	99.99927	0.0001113	99.99983
-5.00	0.00	99.99912	0.0000478	99.99988
-2.50	0.00	99.99917	0.0000182	99.99983
0.00	0.00	99.99918	0.0000000	99.99982
2.50	0.00	99.99917	0.0000182	99.99983
5.00	0.00	99.99912	0.0000478	99.99988
7.50	0.00	99.99927	0.0001112	99.99983
7.50	5.00	99.98317	0.0048330	100.00853
5.00	7.50	100.00854	0.0048269	99.98308
9.00	1.00	99.96938	0.0122755	100.02786

Problem 2. The region is subjected to a pair of compressive forces with magnitude 100.0 N/mm. Consequently the boundary conditions on the arcs AB and BC are

$$\mathcal{F}_x = P = -100, \qquad \mathcal{F}_y = 0$$

and

$$\mathcal{F}_x = 0$$
, $\mathcal{F}_y = 0$,

respectively. With the notations of Figure 4

$$\begin{split} \sigma_{xx} &= \frac{2P}{\pi} \left[\frac{\cos^3 \vartheta_1}{r_1} + \frac{\cos^3 \vartheta_2}{r_2} \right] - \frac{P}{\pi r_o} \;, \\ \tau_{xy} &= -\frac{2P}{\pi} \left[\frac{\sin \vartheta_1 \cos^2 \vartheta_1}{r_1} - \frac{\sin \vartheta_2 \cos^2 \vartheta_2}{r_2} \right] \;, \\ \sigma_{yy} &= \frac{2P}{\pi} \left[\frac{\sin^2 \vartheta_1 \cos \vartheta_1}{r_1} + \frac{\sin^2 \vartheta_2 \cos \vartheta_2}{r_2} \right] - \frac{P}{\pi r_o} \end{split}$$

are the exact solutions [14]. Figures 4 to 6 represent the exact and the numerical solutions. The latter is denoted by diamonds. In this case the contour was divided into 40 equidistant elements. The pairs of elements that meet at A and B are partially discontinuous.

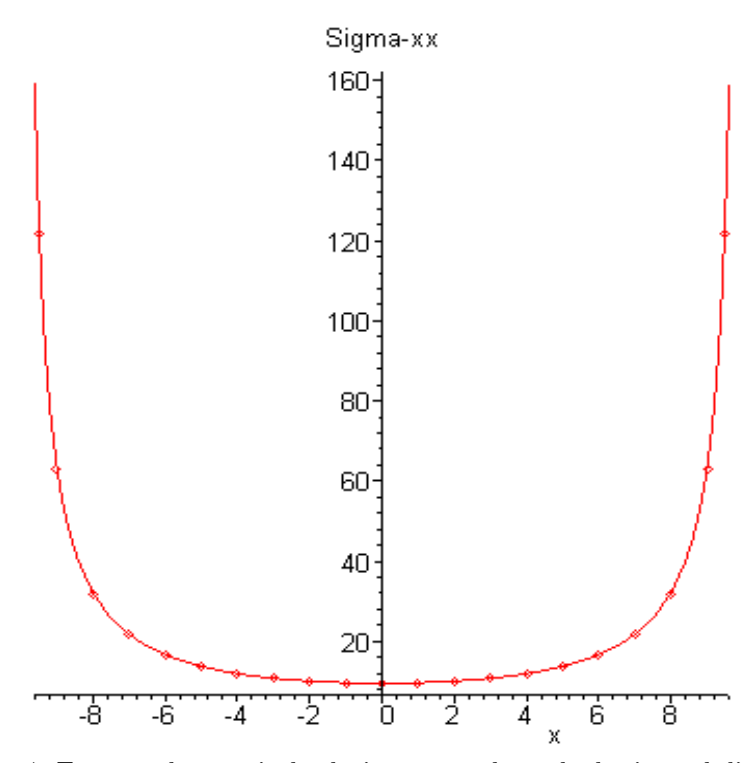


Figure 4. Exact and numerical solution – σ_{xx} along the horizontal diameter

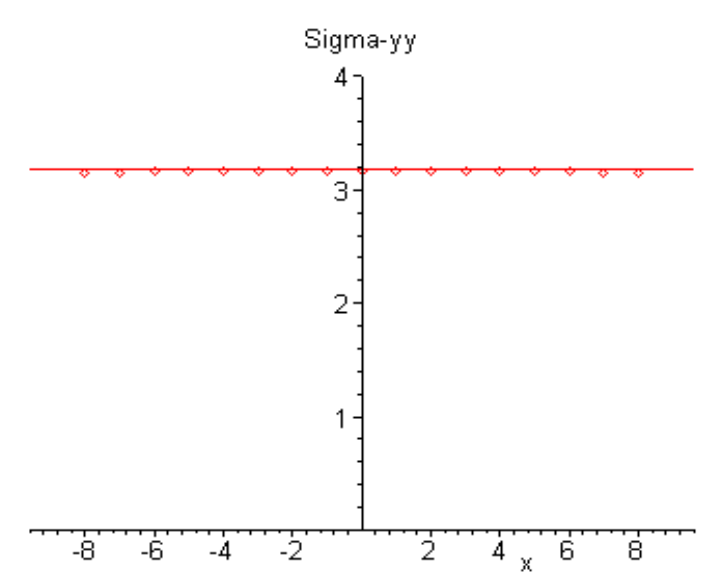


Figure 5. Exact and numerical solution – σ_{yy} along the horizontal diameter

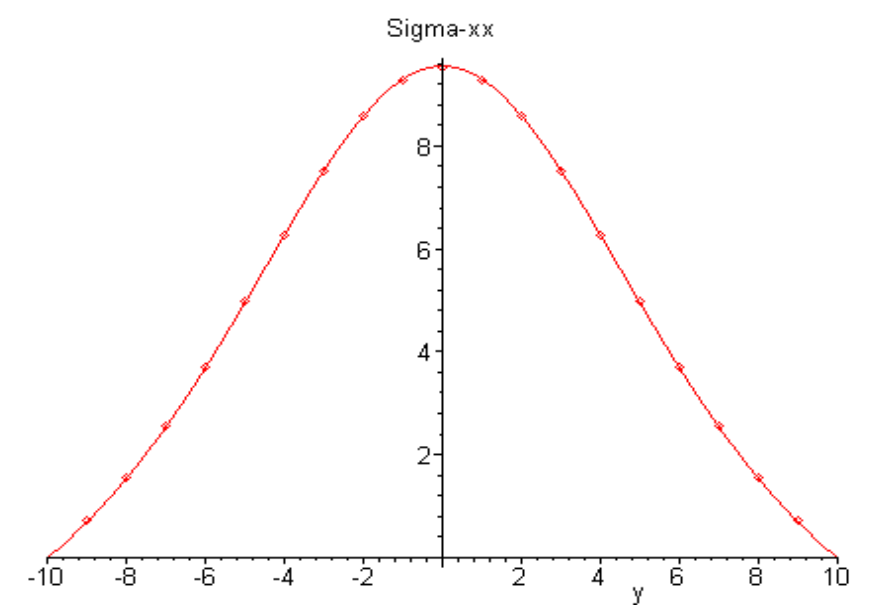


Figure 6. Exact and numerical solution – σ_{xx} along the vertical diameter

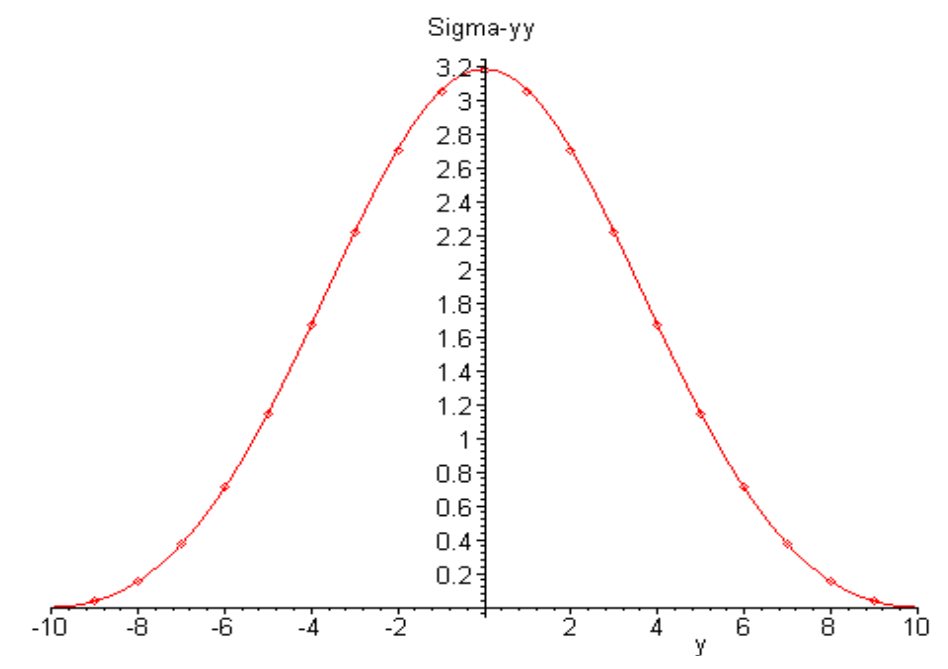


Figure 7. Exact and numerical solution – σ_{yy} along the vertical diameter

Problem 3. Though the contour \mathcal{L}_o and the material are the same as in the previous examples the region under consideration is the outer one for which a constant stress state $\sigma_{xx}(\infty) = 100 [\text{MPa}]$, $\sigma_{xy}(\infty) = \sigma_{yx}(\infty) = \sigma_{yy}(\infty) = 0$ is prescribed at infinity.

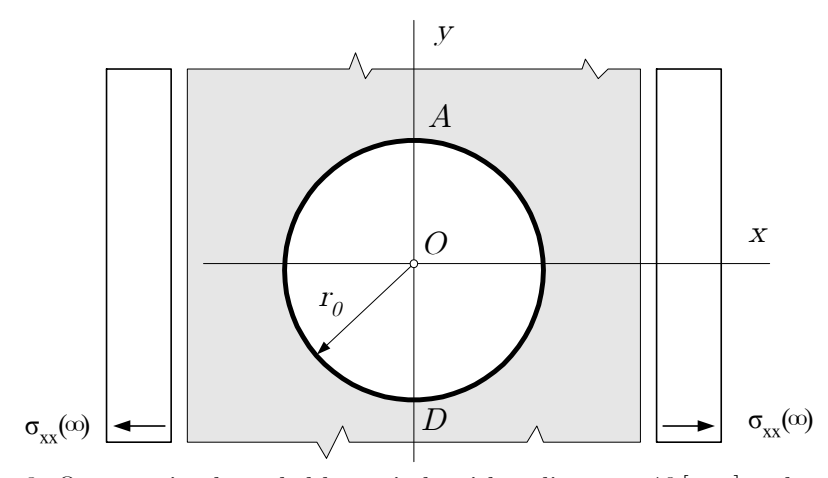


Figure 8. Outer region bounded by a circle with radius $r_o=10\,[\mathrm{mm}]$ and centered at O

It is well known that the formulae

$$\begin{split} \sigma_{rr} &= \frac{\sigma_{xx}(\infty)}{2} \left[\left(1 - \frac{r_o^2}{r^2} \right) + \left(1 + \frac{3r_o^4}{r^4} - \frac{4r_o^2}{r^2} \right) \cos 2\varphi \right] ,\\ \sigma_{\varphi\varphi} &= \frac{\sigma_{xx}(\infty)}{2} \left[\left(1 + \frac{r_o^2}{r^2} \right) - \left(1 + \frac{3r_o^4}{r^4} \right) \cos 2\varphi \right] ,\\ \sigma_{r\varphi} &= \frac{\sigma_{xx}(\infty)}{2} \left[\left(1 - \frac{3r_o^4}{r^4} + \frac{2r_o^2}{r^2} \right) \sin 2\varphi \right] \end{split}$$

written in polar coordinates give the exact solution to this problem [15], [14]. The table below shows both the stresses we computed and the exact solution on the y axis. The contour was divided into 16 equidistant element.

x [mm]	y [mm]	σ_{xx} [MPa]	τ_{xy} [MPa]	σ_{yy} [MPa]
0.00	10.00	300.0395	0.0000000	0.001035
		300.0000	0.0000000	0.000000
0.00	11.00	243.7623	0.0000000	21.51840
		243.7743	0.0000000	21.51494
0.00	12.00	207.0554	0.0000000	31.82829
		207.0602	0.0000000	31.82870
0.00	13.00	182.1018	0.0000000	36.23794
		182.1049	0.0000000	36.23823
0.00	14.00	164.5539	0.0000000	37.48413
		164.5564	0.0000000	37.48438
0.00	15.00	151.8498	0.0000000	37.03671
		151.8518	0.0000000	37.03704

7. Concluding remarks

In accordance with our aims we have clarified what the supplementary conditions of single valuedness are for a class of mixed boundary value problems in the dual system of plane elasticity assuming multiply connected domains.

The fundamental solutions for the stress functions of order one have also been constructed. In the knowledge of the fundamental solutions we have established the dual Somigliana relations both for inner regions and for outer ones, which involve the equations of the direct method. It has been shown that the system matrix **H** has the same properties as in the primal system that is the sum of the elements in a row is equal to zero (inner region) or to one (outer region). A program has been developed in Fortran 90 for the numerical solution by using partially discontinuous quadratic boundary elements. The three examples illustrate the applicability of the algorithm.

Two advantages of the algorithm are worthy of mention (a) calculation of stresses requires the knowledge of the first derivatives of stress functions (b) concentrated forces can be handled. It is, however a disadvantage that the supplementary conditions of single valuedness should be taken into account on multiply connected domains. The present program has not been capable of handling multiply connected domains.

It can be shown, though the proof is not presented here, that the integrand in the boundary integral equations is divergence free. Therefore it is possible to develop the boundary contour method in a dual system as well [16].

Acknowledgement. The support provided by the Hungarian National Research Foundation (projects No. T022022 and No. T031998) is gratefully acknowledged.

REFERENCES

- JASWON, M. A., MAITI, M. and SYMM, G. T.: Numerical biharmonic analysis and some applications, Int. J. Solids Structures, 3, (1967), 309–332.
- 2. Jaswon M. A. and Symm, G. T.: Integral Equation Methods in Potential Theory and Elastostatics, Academic Press, London NewYork San Francisco, 1977.
- 3. Frajeis de Veubeke, B. M.: Stress Function Approach, In Proc. World Cong. on Finite Element Methods in Structural Mechanics, Bournemouth, U.K., pp. J1-J51, 1975.
- 4. Frajeis de Veubeke, B. M. and Millard, A.: Discretization of stress fields in finite element method, J. Franklin Inst., 302, (1976), 389–412.
- 5. E. Bertoti, E.: Indeterminacy of first order stress functions and the stress and rotation based formulation of linear elasticity, Computational Mechanics, 14, (1994), 249–265.
- E. Bertoti, E.: Stress and rotation-based hierarchic models for laminated composites, International Journal for Numerical Methods in Engineering, 39, (1996), 2647–2671.
- 7. HEISE, U.: Application of the singularity method for the formulation of plane elastostatical boundary value problems as integral equations, Acta Mechanica, 31, (1978), 33–69.
- 8. Heise, U.: Systematic compilation of integral equations of the Rizzo type and of Kupradze's functional equations for boundary value problems of plane elastostatics, Journal of Elasticity, 10, (1980), 23–56.
- 9. SZEIDL, G.: Dual Problems of Continuum Mechanics (Derivation of Defining Equations, Single Valuedness of Mixed Boundary Value Problems, Boundary Element Method for Plane problems), Habilitation Thesis of the Miskolc University, Faculty of Mechanical Engineering, University of Miskolc, Department of Mechanics, November 26, 1997. (in Hungarian)
- Eringen, A. C.: Mechanics of Continua, John Wiley & Sons. Inc., New York London Sydney, 1951.
- 11. Lurie, A. I.: On the theory of systems of linear differential equations with constant coefficients, Transactions of the Leningrad Industrial Institute, Number 6., Section of Physics and Mathematics, 6(3), (1937), 31–36.
- 12. HÖRMANDER, L.: Linear Partial Differential Operators, Springer-Verlag, Berlin, 1964.
- 13. Banarjee, P. K. and Butterfield, R.: Boundary Element Methods in Engineering Science, Mir, Moscow, 1984. (Russian translation)
- 14. Muskhelisvili, N. I.: Some Fundamental Problems of Mathematical Theory of Elasticity, Publisher NAUKA, Moscow, 6^{th} edition, 1966. (in Russian)
- 15. TIMOSHENKO, S. and GOODIER, J. N.: Theory of Elasticity, McGraw-Hill, New York Toronto London, 1951.
- Phan, A. V., Mukherjee, S. and Mayer, J. R. R.: The boundary contour method for two-dimensional linear elasticity with quadratic boundary elements, Computational Mechanics, 20, (1997), 310–319.

BOUNDED SOLUTIONS OF PLANE ELASTICITY PROBLEMS IN A SEMI-PLANE

VASYL VIHAK AND ANDRIY RYCHAHIVSKYY
Pidstryhach Institute for Applied Problems of Mechanics and Mathematics
79053 Lviv, Ukraine
dept11@iapmm.lviv.ua

[Received: July 12, 2001]

Abstract. By using the method of direct integration for solving the differential equations of plane elasticity in a semi-plane, continuous and integrable solutions are found for the boundary value problems when tractions, displacements or mixed boundary conditions are imposed on the boundary. Single-valued relations are established between the tractions and displacements on the boundary of the semi-plane. To ensure the correctness of the solutions, the necessary integral equilibrium conditions for the tractions and a compatibility condition for the displacements are formulated.

Mathematical Subject Classification: 74B05

Keywords: Plane problems of elasticity, semi-plane, relations between tractions and displacements, integral conditions

1. Introduction

As is well known, the biharmonic Airy and Love functions are widely used [1,2,3] to solve two-dimensional quasi-static boundary value problems of elasticity in infinite regions by which we mean plane problems in a plane, semi-plane, and infinite strip or axisymmetric problems in a space, semi-space, and infinite layer. By applying for their construction the most powerful, as Gakhov aptly indicated in his famous treatise [4], method of integral transforms [4,5], one can ascertain that the biharmonic functions mentioned exist in the original space and belong to the class of continuous and bounded functions, if the equilibrium conditions are satisfied by the loads. The reason for this is that the integrals, in terms of which these functions are determined, are non-convergent. This phenomenon is due to the discontinuity of the integrands for s = 0, where s is the parameter of the integral transformation. We consider the Airy function for a plane elasticity problem in the semi-plane $D = \{x \in (-\infty, \infty), y \in [0, \infty)\}$ as an example. This function can be given in the form

$$\varphi = \frac{1}{2\pi} \int_{-\infty}^{\infty} \frac{1}{s^2} \left[\bar{p} + \left(\bar{p} + i \frac{|s|}{s} \bar{q} \right) |s| y \right] \exp(-|s| y + i s x) ds, \quad i = \sqrt{-1}.$$

Here \bar{p} and \bar{q} are the integral Fourier transforms [4,5] of the normal and shear tractions p(x) and q(x) imposed on the boundary of the semi-plane. The correctness of the representation above can be checked by inserting the formulae for stresses, which

will be derived below, into the expressions giving the stresses in terms of the Airy function. The previous formula shows that the integrand has a pole of order two if s = 0. However, we are able to remove it by forcing the tractions p and q to satisfy the static equilibrium conditions

$$\int_{-\infty}^{\infty} p dx = \int_{-\infty}^{\infty} x p dx = \int_{-\infty}^{\infty} q dx = 0.$$
 (1.1)

In view of the definition [4,5]

$$(\bar{p}, \bar{q}) \stackrel{def}{=} \int_{-\infty}^{\infty} (p, q) \exp(-isx) dx,$$

conditions (1.1) are equivalent to the following ones in the transformed space:

$$\bar{p}(0) = \bar{p}'(0) = \bar{q}(0) = 0.$$
 (1.2)

It is proved in the well-known treatise [6] by Muskhelishvili that fulfillment of the static equilibrium conditions $(1.1)_{1,3}$ by the external forces is necessary for the displacements to be bounded.

Note that the static equilibrium conditions, i.e., making the resultant vector and the moment of the external forces about a given point equal to zero, are natural preconditions the loads should meet in the theory of elasticity if the region under consideration is a finite one. However, when we consider infinite regions, e.g., a semiplane or semi-space, in many cases the infinitely remote parts of the body are unloaded though the resultant vector and moment of the total load are different from zero. It is obvious that this leads to the violation of conditions (1.1). The vivid example for such a problem is that of a semi-plane subjected to the pressure p = const, $x \in [-a, a]$, $a < \infty$; p = 0, $x \in (-\infty, -a) \cup (a, \infty)$, and q = 0, $x \in (-\infty, \infty)$ on its boundary.

As a matter of fact, when one establishes the problem of finding continuous and bounded solutions for the stresses and displacements in infinite regions under the supplementary conditions of integrability of the functions in question in their domain of definition, – these conditions, among others, follow from the requirement that the strain energy should also be bounded – then in order that correct solutions [7] of these problems could exist it is necessary that the tractions and body forces are self-equilibrated as is the case for bounded regions. Besides, we shall require that the correct solution of the boundary value problem of the classical elasticity theory should be within the framework of an appropriate mathematical model: the stress tensor should be symmetric and the model should adequately reflect the properties of continua, i.e., integral equilibrium conditions deduced below for the stresses and the integral compatibility conditions for the displacements and strains should all be satisfied.

Making use of the method of direct integration of equilibrium equations, the paper presents a correct solution of a plane elasticity problem in a semi-plane provided that tractions are imposed on the boundary. Single-valued relationships are set up between the tractions and displacements on the region's boundary. Utilizing these relations and the solution in terms of stresses, we can easily find solutions for such problems when displacements are prescribed on the boundary as well as under mixed boundary conditions. It is proved that the solution of a plane problem in a semi-plane is correct if the tractions satisfy the equilibrium conditions (1.1) and one component of the displacement vector satisfies the so-called integral compatibility condition.

2. Solution of the problem if tractions are imposed on the boundary

In the absence of body forces the plane strain state in a homogeneous and isotropic semi-plane $D = \{x \in (-\infty, \infty), y \in [0, \infty)\}$ is governed by [1,2]

the equilibrium equations:

$$\frac{\partial \sigma_x}{\partial x} + \frac{\partial \sigma_{xy}}{\partial y} = 0, \qquad \frac{\partial \sigma_{xy}}{\partial x} + \frac{\partial \sigma_y}{\partial y} = 0, \tag{2.1}$$

the compatibility equation in terms of stresses:

$$\Delta \sigma = 0, \quad \sigma = \sigma_x + \sigma_y, \quad \Delta = \frac{\partial^2}{\partial x^2} + \frac{\partial^2}{\partial y^2},$$
 (2.2)

the physical relations ($e_z = 0$):

$$2Ge_x = (1 - \nu)\sigma_x - \nu\sigma_y , \qquad \sigma_z = \nu\sigma , \qquad (2.3a)$$

$$2Ge_y = (1 - \nu)\sigma_y - \nu\sigma_x , \qquad Ge_{xy} = \sigma_{xy} , \qquad (2.3b)$$

and the Cauchy compatibility equations (relations):

$$e_x = \frac{\partial u}{\partial x}, \quad e_y = \frac{\partial v}{\partial y}, \quad e_{xy} = \frac{\partial u}{\partial y} + \frac{\partial v}{\partial x}.$$
 (2.4)

Here (x, y) are dimensionless coordinates; σ_i (i = x, y, z), σ_{xy} , and e_i (i = x, y, z), e_{xy} denote the components of the stress tensor and strain tensor, respectively; G and ν are the shear modulus and Poisson's ratio; u and v are dimensionless displacements (referred to l).

Let us assume that both the tractions

$$\sigma_y(x, 0) = -p(x), \quad \sigma_{xy}(x, 0) = q(x)$$
 (2.5)

imposed on the boundary of the semi-plane and the stresses vanish if $|x|,y\to\infty$. Under this condition the Fourier transforms of the solution

$$\bar{\sigma}_{x} = \bar{\sigma} - \bar{\sigma}_{y}, \quad \bar{\sigma} = -2\left(\bar{p} + i\frac{|s|}{s}\bar{q}\right)\exp(-|s|y),$$

$$\bar{\sigma}_{y} = -\left[\bar{p} + (\bar{p} + i\frac{|s|}{s}\bar{q})|s|y\right]\exp(-|s|y),$$

$$\bar{\sigma}_{xy} = \left[\bar{q} - (\bar{q} - i\frac{|s|}{s}\bar{p})|s|y\right]\exp(-|s|y)$$
(2.6)

can be obtained from the differential equations (2.1), (2.2) – see [8] for details – by the method of direct integration. Formulae (2.6) can easily be transformed back into the original space [4,5].

As the solutions of equations (2.1)–(2.5) are sought in the class of functions derivable continuously – see equations (2.1), (2.2), and (2.4) – the tractions p(x) and q(x) should be continuous and absolutely integrable functions. The continuity requirements for the tractions on the boundary are also caused by the fact that – as an analysis of the solutions found by Muskhelishvili [6] shows – the stresses are unbounded at the point of the boundary where the normal tractions have a discontinuity of the first kind. In addition, the shear stress does not fulfill the symmetry condition. If we suppose that the shear traction is discontinuous, the violation of the symmetry law is obvious at the point of discontinuity. Moreover, as follows from the second equilibrium equation (2.1) for such a case, discontinuity of the shear traction on the line y = 0 leads the mathematical model of the problem out of the classical theory into the theory of generalized functions [9]. This follows from the fact that the derivative

$$\left. \frac{\partial \sigma_y}{\partial y} \right|_{y=0} = -\frac{dq}{dx}$$

should be considered in a generalized sense. Therefore, when the discontinuity of the tractions p(x) and q(x) violates the symmetry of the stress tensor, in order that the solution could be correct under given piecewise continuos tractions on the boundary, we should expand our mathematical model to the so called micropolar or unsymmetric theory of elasticity [2].

Integrability of the corresponding functions and the existence of the double integrals [10] which involve the components of the stress tensor demand that these functions should belong to the class L(D), i.e., the class of absolutely integrable functions in their domain of definition D. By integrating the equilibrium equations (2.1) and taking the boundary conditions (2.5) into account, one can prove that the components of the stress tensor should satisfy the integral equilibrium conditions

$$2\int_{0}^{\infty} \sigma_{x} dy = \int_{-\infty}^{\infty} q \operatorname{sign}(x - \eta) d\eta, \qquad \int_{-\infty}^{\infty} \sigma_{y} dx = \int_{-\infty}^{\infty} \sigma_{y} x dx = 0,$$
$$2\int_{0}^{\infty} \sigma_{x} y dy = -\int_{-\infty}^{\infty} p|x - \eta| d\eta, \quad \int_{-\infty}^{\infty} \sigma_{xy} dx = 0, \quad 2\int_{0}^{\infty} \sigma_{xy} dy = -\int_{-\infty}^{\infty} p \operatorname{sign}(x - \eta) d\eta$$

as necessary conditions. Making use of the boundary conditions (2.5), it is easy to obtain the equilibrium conditions (1.1) the tractions should meet from the conditions we have set up above for σ_y and σ_{xy} provided that y = 0.

After the stresses (2.6) have been found, the strains are determined by relations (2.3). Then integrating any two of the three equations (2.4), one can find the displacements. The easiest way for such a procedure is to give the displacements in terms of the longitudinal strains e_i (i = x, y). Consequently, under the condition that the displacements vanish at the infinitely remote points of the semi-plane, we find from

equations $(2.4)_{1.2}$ the displacements

$$2u = \int_{-\infty}^{\infty} e_x \operatorname{sign}(x - \eta) \, d\eta, \quad 2v = v_1 + \int_{0}^{\infty} e_y \operatorname{sign}(y - \xi) \, d\xi, \quad v_1 = v(x, 0), \quad (2.7)$$

whence the conditions

$$\int_{-\infty}^{\infty} e_x \, \mathrm{d}x = 0, \quad \text{and} \quad v_1 = -\int_{0}^{\infty} e_y \, \mathrm{d}y$$
 (2.8)

follow if $x \to \pm \infty$ and y = 0, respectively. The first one expresses the compatibility condition for the strain e_x , and the second one determines the displacement v_1 of the boundary of the semi-plane in terms of the strain e_y .

Inserting equations (2.7) into equation $(2.4)_3$, we obtain the initial compatibility equation

$$2e_{xy} = \frac{\partial}{\partial y} \int_{-\infty}^{\infty} e_x \operatorname{sign}(x - \eta) \, d\eta + \frac{\partial}{\partial x} \left[v_1 + \int_{0}^{\infty} e_y \operatorname{sign}(y - \xi) \, d\xi \right]. \tag{2.9}$$

Differentiating with respect to x and y, we get that the latter equation implies the well-known compatibility equation

$$\frac{\partial^2 e_{xy}}{\partial x \partial y} = \frac{\partial^2 e_x}{\partial y^2} + \frac{\partial^2 e_y}{\partial x^2} \tag{2.10}$$

under the necessary equivalence condition

$$2\frac{\mathrm{d}v_1}{\mathrm{d}x} = 2e_{xy}(0) - \int_{-\infty}^{\infty} \frac{\partial e_x(0)}{\partial y} \operatorname{sign}(x - \eta) \,\mathrm{d}\eta, \qquad (2.11)$$

whence

$$2v_1 = \int_{-\infty}^{\infty} \left[e_{xy}(0) \operatorname{sign}(x - \eta) - \frac{\partial e_x(0)}{\partial y} |x - \eta| \right] d\eta.$$
 (2.12)

For the sake of brevity here and in the sequel we employ the notational convention $e_{xy}(0) = e_{xy}(x, 0)$, etc. Observe that the equivalence condition (2.11) has been obtained by an appropriate integration of equation (2.10) with the purpose of reducing it to equation (2.9) and by further comparison of the two expressions obtained.

It follows from expressions $(2.8)_2$ and (2.12) that the strain e_y should satisfy the compatibility condition

$$2\int_{0}^{\infty} e_y \,dy = -\int_{-\infty}^{\infty} \left[e_{xy}(0)\operatorname{sign}(x-\eta) - \frac{\partial e_x(0)}{\partial y} |x-\eta| \right] \,d\eta.$$
 (2.13)

By integrating equation $(2.4)_3$ and taking the solution (2.7) for the displacement u into account, we obtain the integral compatibility condition for the shear strain

$$\int \int_{D} e_{xy} \, \mathrm{d}x \mathrm{d}y = \int_{-\infty}^{\infty} x e_{x}(0) \, \mathrm{d}x.$$
 (2.14)

For our analysis to be complete, we also give the two integral compatibility conditions for the displacement vector components. These are easily obtainable by integrating formulae (2.7) and utilizing conditions (2.8):

$$\int_{-\infty}^{\infty} u dx = -\int_{-\infty}^{\infty} x e_x dx, \quad \int_{0}^{\infty} v dy = -\int_{0}^{\infty} y e_y dy.$$
 (2.15)

Consequently, in the case of a plane problem of mechanics of deformable solids in a semi-plane the strains and displacements should satisfy the integral compatibility conditions (2.8), (2.13)–(2.15).

Using the physical relations (2.3) for the longitudinal strains and the solution (2.6) for the stresses and taking the conditions (2.8) into account, we can express the displacements (2.7) in terms of the tractions imposed on the boundary:

$$4Gu = \frac{1}{\pi} \int_{-\infty}^{\infty} \left[\left(\bar{p} + i \frac{|s|}{s} \bar{q} \right) |s|y - (1 - 2\nu)\bar{p} - 2(1 - \nu)i \frac{|s|}{s} \bar{q} \right] \exp(-|s|y + isx) \frac{\mathrm{d}s}{is},$$

$$(2.16a)$$

$$4Gv = \frac{1}{\pi} \int_{-\infty}^{\infty} \left[\left(\bar{p} + i \frac{|s|}{s} \bar{q} \right) y + 2(1 - \nu) \frac{1}{|s|} \bar{p} + (1 - 2\nu) \frac{i}{s} \bar{q} \right] \exp(-|s|y + isx) \, ds \,.$$
(2.16b)

These formulae show that the integrands have a singularity of the first order at s = 0. In other words, for the integrals (2.16) and simultaneously the solutions of the problem (2.1)–(2.5) – including the solutions for the displacements as well – to exist in the form of continuous and bounded functions the singularity of the integrals (2.16) should be removed. If we require that $\bar{p}(0) = \bar{q}(0) = 0$, then the singularity is removed. This condition is equivalent to making the resultant vector of the tractions (1.1) equal zero.

It can also be proved that vanishing of the resultant moment (1.1) of the traction p is necessary for fulfilling the integral condition (2.14) and the existence of the integrals (2.15). Fulfillment of conditions (1.1) is sufficient for the validity of conditions (2.8) and (2.13).

Therefore, it follows from the equilibrium equations (2.1) and the compatibility ones that for the solution of the plane elasticity problem (2.1)–(2.5) to exist in the class of continuous and integrable functions, the tractions imposed on the boundary should satisfy the equilibrium conditions (1.1), i.e., they should be self-equilibrated. In the opposite case neither the stresses nor the strains are integrable and the displacements

do not belong to the class of bounded functions. In other words, solutions of elasticity problems when the tractions on the boundary or the body forces are given in the form of the Dirac delta-function should be considered only as Green's functions [11]. The latter represent some generalized functions [9] (from a mathematical point of view), which have a physical sense on a par with given "good" functions in the form of an integral convolution. In our case, this is the convolution with self-equilibrated tractions on the boundary of the semi-plane. On the basis of formulae (2.6) and (2.16) they can be presented in a final form similar to that in [5].

It should be emphasized that according to our investigations the stresses (2.16) in a semi-plane subjected to tractions being not self-equilibrated are the asymptotic solution of a plane elasticity problem in an infinite strip under the same tractions exerted on one side of the boundary and the Winkler conditions on the opposite one, the latter tending to infinity. If this is the case, both the displacements and the elastic strain energy are unbounded and thus lose their physical sense.

3. Solution of the problem if displacements are imposed on the boundary

Let us assume that the field equations (2.1)–(2.4) are associated with the boundary conditions

$$u(x, 0) = u_1(x), \quad v(x, 0) = v_1(x),$$
 (3.1)

where the functions $u_1(x)$ and $v_1(x)$ are continuous together with their first derivatives, absolutely integrable and vanish if $|x| \to \infty$. Using formulae (2.16), we can give the displacements on the boundary in terms of the tractions p and q:

$$-2Gis\bar{u}_1 = (1-2\nu)\bar{p} + 2(1-\nu)i\frac{|s|}{s}\bar{q}, \qquad (3.2a)$$

$$2G|s|\bar{v}_1 = 2(1-\nu)\bar{p} + (1-2\nu)i\frac{|s|}{s}\bar{q}$$
(3.2b)

or vice versa:

$$\bar{p} = \frac{2G}{3 - 4\nu} \left[(1 - 2\nu)is\bar{u}_1 + 2(1 - \nu)|s|\bar{v}_1 \right], \tag{3.3a}$$

$$\bar{q} = \frac{2G}{3 - 4\nu} \left[(1 - 2\nu)is\bar{v}_1 - 2(1 - \nu)|s|\bar{u}_1 \right]. \tag{3.3b}$$

Inserting expressions (3.3) into formulae (2.6), we have the solution of problem (2.1)–(2.4) under the boundary conditions (3.1). Since relations (3.2) and (3.3) are one-to-one, the solution of problem (2.1)–(2.4), (3.1) has been reduced to the solution of problem (2.1)–(2.5). By using the integral Fourier transformation of generalized

functions [12], these relations can also be presented in the original space:

$$2Gu_{1} = -\frac{1}{2}(1 - 2\nu) \int_{-\infty}^{\infty} p \operatorname{sign}(x - \eta) d\eta + \frac{2}{\pi}(1 - \nu) \int_{-\infty}^{\infty} q \ln|x - \eta| d\eta, \quad (3.4a)$$

$$2Gv_1 = -\frac{1}{2}(1 - 2\nu) \int_{-\infty}^{\infty} q \operatorname{sign}(x - \eta) d\eta - \frac{2}{\pi}(1 - \nu) \int_{-\infty}^{\infty} p \ln|x - \eta| d\eta; \quad (3.4b)$$

$$p = \frac{2G}{3 - 4\nu} \left[(1 - 2\nu) \frac{\mathrm{d}u_1}{\mathrm{d}x} - \frac{2}{\pi} (1 - \nu) \int_{-\infty}^{\infty} \frac{v_1}{(x - \eta)^2} \mathrm{d}\eta \right], \tag{3.5a}$$

$$q = \frac{2G}{3 - 4\nu} \left[(1 - 2\nu) \frac{\mathrm{d}v_1}{\mathrm{d}x} + \frac{2}{\pi} (1 - \nu) \int_{-\infty}^{\infty} \frac{u_1}{(x - \eta)^2} \,\mathrm{d}\eta \right].$$
 (3.5b)

If the functions p(x) and q(x) are even, we see from (3.4) that the displacement u_1 depends on the traction q only, and the displacement v_1 – on p. In the absence of one traction, i.e., if q = 0, $p \neq 0$ or p = 0, $q \neq 0$ it follows from (3.3) or (3.5) that the displacements on the boundary are interdependent and the non-zero tractions can be given in terms of the displacements in a very simple form

$$p = -\frac{2G}{1 - 2\nu} \frac{\mathrm{d}u_1}{\mathrm{d}x}, \quad q = -\frac{2G}{1 - 2\nu} \frac{\mathrm{d}v_1}{\mathrm{d}x}$$

Note that the second integrals in the expressions (3.4) giving the displacements can be determined by integrations by parts:

$$\int_{-\infty}^{\infty} (p, q) \ln|x - \eta| d\eta = \lim_{\eta \longrightarrow \infty} \ln|x - \eta| \int_{-\infty}^{\eta} (p, q) d\eta_1 + \int_{-\infty}^{\infty} \frac{d\eta}{x - \eta} \int_{-\infty}^{\eta} (p, q) d\eta_1,$$

whence it follows that, by forcing the functions $\int_{-\infty}^{\eta} (p, q) d\eta_1$ to satisfy the Hölder conditions, the Cauchy integrals in the above expressions exist in the sense of the Cauchy principal value [6], and the limits are equal to zero if conditions (1.1) are satisfied. If the tractions p and q are not self-equilibrated, these limits are equal to infinity, which confirms again the above assertion concerning the absence of a correct solution for problem (2.1)–(2.5) when conditions (1.1) are violated.

As regards the existence of a correct solution of problem (2.1)–(2.5), the tractions p and q should satisfy conditions (1.1), and there exist relations – see (3.5) – between the tractions and displacements u_1 and v_1 . In addition one has to check whether additional conditions should be prescribed on these displacements so that an unambiguous solution of problem (2.1)–(2.4), (3.1) can exist. Inserting the expressions for tractions (3.5) into conditions (1.1) (or expressions (3.3) into conditions (1.2)), we easily ascertain that they are satisfied identically by the resultant vector. However,

for condition (1.1) or condition (1.2)₂ in the transformed space to be satisfied by the resultant moment the equality $\bar{u}_1(0) = 0$ should be fulfilled. In the original space, the latter is equivalent to the additional compatibility condition:

$$\int_{-\infty}^{\infty} u_1 \, dx = 0. \tag{3.6}$$

Consequently, for a solution of problem (2.1)–(2.4), (3.1) to exist in the class of continuous and integrable functions, it is also necessary that the displacement u_1 of the boundary of the semi-plane should satisfy the integral compatibility condition (3.6). This fact does not mean that there exist no solution of the elasticity equations mentioned if the boundary condition $u(x, 0) = u_1(x)$ violates the integral condition (3.6). However, such a violation leads to dissatisfying the necessary condition (1.1) for the resultant moment. This makes the fulfillment of conditions (2.14) and (2.15) impossible; the solution becomes an incorrect one for the mechanics of deformable solids because it does not satisfy the conditions of compatibility of continua. However, the integral compatibility condition (3.6) is not an unexpected one typical only of the problem under consideration. As the research in connection with the existence of solutions for some other one- and two-dimensional elasticity problems for which displacements are imposed on the boundary (e.g. a two-dimensional non-axisymmetric problem in a hollow cylinder) has shown, the displacements cannot be given in an arbitrary way – they should satisfy some integral condition.

4. Solution of the problem if mixed conditions are imposed on the boundary

Let us consider finally the solution to the problem (2.1)–(2.4) in a semi-plane, when the mixed boundary conditions

$$(q \neq 0)$$
 $\sigma_u(x, 0) = -p(x),$ $u(x, 0) = u_1(x),$ (4.1)

or

$$(p \neq 0)$$
 $\sigma_{xy}(x, 0) = q(x),$ $v(x, 0) = v_1(x)$ (4.2)

are imposed on the boundary. If equations (4.1) are the boundary conditions, then, by making use of the relation (3.2a), we determine the Fourier transform of the unknown shear traction q on the boundary in terms of the given functions p and u_1 :

$$\bar{q} = \frac{1}{2(1-\nu)} \left[(1-2\nu)i \operatorname{sign} s \bar{p} - 2G|s|\bar{u}_1 \right].$$
 (4.3)

Inserting expression (4.3) into formulae (2.6) we obtain the solution of the boundary value problem (2.1)–(2.4) for the case of mixed boundary conditions (4.1). In a similar manner we can also get the solution for the case of the mixed boundary conditions (4.2): from the relation (3.2b) we determine the transform \bar{p} in terms of the prescribed functions on the boundary q and v_1 and insert that expression into formulae (2.6).

It is obvious that for the correctness of the solutions the functions imposed on the boundary of the semi-plane should satisfy the integral conditions (1.1) and (3.6).

The paper does not intend to seek solutions for the problem (2.1)–(2.4) in a semiplane under such mixed boundary conditions when tractions are prescribed on a part of the boundary, and the displacements are prescribed on the complementary part, or if different versions of the conditions (4.1) and (4.2) are imposed on separate parts of the boundary.

5. Conclusions

Using the method of direct integration, continuous and integrable solutions are found for the equations of plane elasticity in a semi-plane provided the tractions are imposed on the boundary. Making use of the one-to-one relations set up between the tractions and the displacements taken on the boundary of the semi-plane, boundary value problems of the plane theory of elasticity with displacement or mixed boundary conditions are reduced to the solution of the problem when the tractions are prescribed on the boundary. Integral equilibrium conditions for the tractions and a compatibility condition for the displacements are established to ensure the correctness of the solutions we have constructed.

REFERENCES

- 1. Lurie, A. I.: Theory of Elasticity, Nauka, Moscow, 1970. (in Russian)
- NOWACKI, W.: Teoria Sprezystosci, Panstwowe Wydawnictwo Naukowe, Warszawa, 1970. (in Polish)
- 3. Hahn, H. G.: Elastizitätstheorie. Grundlagen der Linearen Theorie und Anwendungen auf Eindimensionale, Ebene und Räumliche Probleme, B.G. Teubner, Stuttgart, 1985. (in German)
- 4. Knyazyev, P. N.: Integral Transforms, Vys. Shkola, Minsk, 1969. (in Russian)
- 5. SNEDDON, I. N.: Fourier Transforms, McGraw-Hill Book Company, New York, 1951.
- Muskhelishvili, N. I.: Some Basic Problems of the Mathematical Theory of Elasticity, Noordhoff, Groningen, 1953.
- ARSENIN, V. YA.: Methods of Mathematical Physics and Special Functions, Nauka, Moscow, 1974. (in Russian)
- 8. VIHAK, V. M.: Direct method of integration of the equations for plane elasticity and thermoelasticity problems, Dopovidi NANU, 12, (1998), 62-67. (in Ukrainian)
- 9. KECH, V. and TEODORESCU, P.: Introduction to the Theory of Generalized Functions with Application in Engineering, Mir, Moscow, 1978. (in Russian)
- FICHTENHOLTZ, G. M.: The Course of Differential and Integral Calculus, Nauka, Moscow, 1969. (in Russian)
- 11. Butkovskyi, A. G.: Characteristics of a System with Distributed Parametres, Nauka, Moscow, 1979. (in Russian)
- 12. Brychkov, Yu. A. and Proudnikov, A. P.: Integral Transforms of Generalized Functions, Nauka, Moscow, 1977. (in Russian)

A LAGRANGIAN FOR THE LARGE DEFLECTIONS OF A RHOMBIC PLATE

JI-HUAN HE

Shanghai Institute of Applied Mathematics and Mechanics, Shanghai University 149 Yanchang Road, Shanghai 200072, China

jhhe@mail.shu.edu.cn

[Received: May 18, 2001]

Abstract. The inverse problem of the variational calculus is discussed in the present paper. We shall show step by step how to find a Lagrangian for the large deflections of a rhombic plate from the nonlinear partial differential equation proposed by Banerjee.

Mathematical Subject Classification: 74K20, 74B20 Keywords: Variational representation, skew plate

1. Introduction

It is well known from the literature [1] that a system of differential equations has a variational representation if it is self-adjoint, but it is very difficult to identify the variational model in a traditional way. If the system of equations is not self-adjoint there is no simple way to find an equivalent variational model.

For example, first let us consider the following equation

$$\frac{u''}{u'} + a = 0, \quad u'(x) \neq 0, \tag{1.1}$$

which is clearly self-adjoint [1]. As we have just mentioned, it is difficult to find an equivalent variational model in the traditional way. By applying the semi-inverse method [2, 3, 4, 5], however, we can easily obtain the corresponding variational functional.

Let us assume that the Lagrangian of equation (1.1) can be expressed as

$$L(x, u, u') = u' \ln u' + F(x, u) , \qquad (1.2)$$

where F is an unknown function to be determined. Therefore we obtain the following Euler equation

$$-\left(\ln u'\right)' - \left(\frac{u'}{u'}\right)' + \frac{\partial F}{\partial u} = 0, \qquad (1.3)$$

or

$$-\frac{u''}{u'} + \frac{\partial F}{\partial u} = 0. \tag{1.4}$$

If we set

$$\frac{\partial F}{\partial u} = -a\,, (1.5)$$

274 Ji-Huan He

then equation (1.4) coincides with the original equation (1.1). It follows from equation (1.5) that the unknown function F has the form

$$F = -au. (1.6)$$

Consequently, we have obtained the following functional for equation (1.1):

$$J(u) = \int (u' \ln u' - au) \, dx. \qquad (1.7)$$

However, if equation (1.1) is written in the form

$$u'' + au' = 0, (1.8)$$

then it is clearly not self-adjoint.

According to He's semi-inverse method [2, 3, 4, 5], a Lagrangian assumes the form

$$L(x, u, u') = F(x, u) u'^{2},$$
 (1.9)

where F is an unknown function. The corresponding Euler equation can be written as

$$\frac{\partial F}{\partial u}u'^2 - 2\left(Fu'\right)' = 0, \qquad (1.10)$$

from where by performing the derivation we have

$$\frac{\partial F}{\partial u}u'^2 - 2\left(\frac{\partial F}{\partial u}u'^2 + \frac{\partial F}{\partial x}u' + Fu''\right) = 0, \qquad (1.11)$$

and

$$u'' + \frac{\partial F}{F \partial x} u' + \frac{\partial F}{2F \partial u} u'^2 = 0. \tag{1.12}$$

If we assume that

$$\frac{\partial F}{F\partial x} = a$$
 and $\frac{\partial F}{2F\partial u} = 0$, (1.13)

then equation (1.12) coincides with equation (1.8). In addition it immediately follows from equations (1.13) that the unknown functional has the form

$$F = Ce^{ax}, (1.14)$$

where C is a nonzero constant. In other words, the variational representation for equation (1.8) can be expressed as

$$J(u) = \int Ce^{ax}u'^2 dx. \tag{1.15}$$

In the present paper, we shall propose a straightforward approach to the inverse problem of the calculus of variations, and seek a Lagrangian for the differential equation which describes the large deflections of rhombic plates [6]. We should remark that we shall neglect the question of boundary conditions.

2. Mathematical formulae for small displacement theory

Consider a rhombic plate made of an elastic, isotropic material and having a uniform thickness h. Let the size of each side of the skew plate be sufficiently large compared to h. The origin of the rectangular Cartesian coordinate system (x, y) is located at one of the corners of the skew plate.

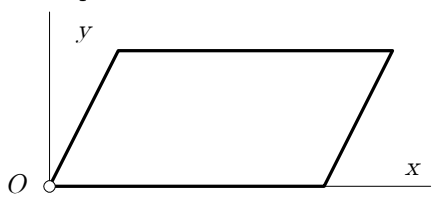


Figure 1. Skew plate

Following Banerjee's hypothesis [7], the differential equation which describes the large deflection of plates is a complex nonlinear 4th order partial differential equation [6,7]:

$$\nabla^{4}w - \frac{12A}{h^{2}} (w_{xx} + vw_{yy}) - \frac{6\lambda}{h^{2}} (3w_{xx}w_{x}^{2} + 3w_{yy}w_{y}^{2} + w_{xx}w_{y}^{2} + w_{yy}w_{x}^{2} + 4w_{xy}w_{x}w_{y}) = \frac{q}{D}, \quad (2.1)$$

where E is the modulus of elasticity, D is the flexural rigidity, h is the thickness of the plate, q is the load intensity, v is the Poisson ratio of the plate material, $\lambda = v^2$, A is a constant, w is the deflection normal to the middle plane of the plate.

First we shall consider the biharmonic equation

$$\nabla^4 w = 0. (2.2)$$

The Lagrangian of equation (2.2) can be found with ease:

$$L_1(w) = \frac{1}{2} \left(\nabla^2 w \right)^2. \tag{2.3}$$

To proceed, we regard the equation

$$w_{xx} + vw_{yy} = 0, (2.4)$$

for which obviously

$$L_2(w) = -\frac{1}{2} \left(w_x^2 + v w_y^2 \right)$$
 (2.5)

is the Lagrangian. Now we consider the Lagrangian

$$L_3(w) = -\frac{1}{2}w_x^2 + w_y^2 \tag{2.6}$$

276 Ji-Huan He

since the corresponding Euler equation reads

$$(w_x w_y^2)_x + (w_y w_y^2)_y = 0$$
 (2.7)

or which is the same

$$w_{xx}w_y^2 + w_{yy}w_x^2 + 4w_xw_yw_{xy} = 0. (2.8)$$

It is obvious that the left side of equation (2.8) is involved in equation (2.1).

Now we take the following Lagrangian

$$L_4(w) = w \left(w_{xx} w_x^2 + w_{yy} w_y^2 \right). {(2.9)}$$

The corresponding Euler equation reads

$$ww_{xx}w_{x}^{2} + (ww_{x}^{2})_{xx} - 2(ww_{xx}w_{x})_{x} + ww_{yy}w_{y}^{2} + (ww_{y}^{2})_{yy} - 2(ww_{yy}w_{y})_{y} = 0. (2.10)$$

By a simple manipulation, equation. (2.10) can be transformed into the form

$$3w_{xx}w_x^2 + 3w_{yy}w_y^2 = 0. (2.11)$$

which is again a part of equation (2.1). Making use of equations (2.3), (2.5) (2.6) and (2.7), we obtain

$$L(w) = L_1(w) - \frac{12A}{h^2} L_2(w) - \frac{6\lambda}{h^2} \left(L_3 + \frac{3}{4} L_4 \right)$$

$$= \frac{1}{2} \left(\nabla^2 w \right)^2 + \frac{6A}{h^2} \left(w_x^2 + v w_y^2 \right) + \frac{3\lambda}{h^2} w_x^2 w_y^2 - \frac{9\lambda}{2h^2} w \left(w_{xx} w_x^2 + w_{yy} w_y^2 \right).$$
(2.12)

as the Lagrangian of equation (2.1). It can easily be checked by determining the Euler equation of the functional (2.12) that the former really coincides with equation (2.1).

3. Conclusion

We have found a Lagrangian for the Banerjee equation which describes the large deflections of a rhombic plate. However, the paper has dealt neither with the issue of the boundary conditions nor with the effect the skew angle in the rhombic has on the solutions. As regards the issue how to involve boundary conditions in the model, we refer the reader to paper [8]. At the same time we remark that the singularities due to discontinuous distributions of bending moments can be taken into account by applying the method proposed in the book by Washizu [9].

Acknowledgement. The author is grateful to the unknown reviewer for his helpful comments.

REFERENCES

1. Santilli, R. M.: Foundations of Theoretical Mechanics I: The Inverse Problem in Newtonian Mechanics, Springer-Verlag, 1978.

- HE, J. H.: Semi-inverse method of establishing generalized variational principles for fluid mechanics with emphasis on turbomachinery aerodynamics, Int. J. Turbo & Jet-Engines, 14(1), (1997), 23-28.
- 3. HE, J. H.: Semi-inverse method and generalized variational principles with multivariables in elasticity, Applied Math. Mech., 21, (2000), 721-731.
- HE, J. H.: Generalized Hellinger-Reissner principle, ASME J. Appl. Mech., 67, (2000), 326-331.
- 5. HE, J. H.: A classical variational model for micropolar elastodynamics, International Journal of Nonlinear Sciences and Numerical Simulation, 1(2), (2000), 133-138.
- RAY. A,K., BANERJEE, B. and BHATTACHARJEE, B.: Large deflection of rhombic plate

 A new approach, International Journal of Nonlinear Mechanics, 27(6), (1992), 1007-1014.
- BANERJEE, B.: Large deflections of polygonal plates under non-stationary temperature,
 J. Thermal Stresses, 7, 1984, 285-292.
- HE, J. H.: Coupled variational principles of piezoelectricity, Int. J. Engineering Sciences, 39(3), (2000), 323-341.
- 9. Washizu, K.: Variational Methods in Elasticity and Plasticity, (3rd ed.), Pergamon Press, Oxford, 1982.

Notes for Contributors to the Journal of Computational and Applied Mechanics

Aims and scope. The aim of the journal is to publish research papers on theoretical and applied mechanics. Special emphasis is given to articles on computational mechanics, continuum mechanics (mechanics of solid bodies, fluid mechanics, heat and mass transfer) and dynamics. Review papers on a research field and materials effective for teaching can also be accepted and are published as review papers or classroom notes. Papers devoted to mathematical problems relevant to mechanics will also be considered.

Frequency of the journal. Two issues a year (approximately 80 pages per issue).

Submission of Manuscripts. Submission of a manuscript implies that the paper has not been published, nor is being considered for publication elsewhere. Papers should be written in standard grammatical English. Two copies of the manuscript should be submitted on pages of A4 size. The text is to be 130 mm wide and 190 mm long and the main text should be typeset in 10pt CMR fonts. Though the length of a paper is not prescribed, authors are encouraged to write concisely. However, short communications or discussions on papers published in the journal must not be longer than 2 pages. Each manuscript should be provided with an English Abstract of about 50–70 words, reporting concisely on the objective and results of the paper. The Abstract is followed by the Mathematical Subject Classification – in case the author (or authors) give the classification codes – then the keywords (no more than five). References should be grouped at the end of the paper in numerical order of appearance. Author's name(s) and initials, paper titles, journal name, volume, issue, year and page numbers should be given for all journals referenced.

The journal prefers the submission of manuscripts in LATEX. Authors should prefer the standard LATEX article style and are not recommended to define their own LATEX commands. Visit our home page for further details concerning the issue how to edit your paper.

For the purpose of refereeing, two copies of the manuscripts should initially be submitted in hardcopy to an editor of the journal. The eventual supply of an accepted-for-publication paper in its final camera-ready form (together with the corresponding files on an MS–DOS diskette) will ensure more rapid publication. Format requirements are provided by the home page of the journal from which sample LaTeX files can be downloaded:

http://www.uni-miskolc.hu/home/web/pumns/mechanics

These sample files can also be obtained directly (via e-mail) from a member of the Editorial Board, Gy. Szeidl (mechszgy@gold.uni-miskolc.hu), upon request.

Twenty offprints of each paper will be provided free of charge and mailed to the correspondent author.

The Journal of Computational and Applied Mechanics is abstracted in Zentralblatt für Mathematik and in the Russian Referativnij Zhurnal.

Responsible for publication: Rector of the Miskolc University

Published by the Miskolc University Press under the leadership of Dr. József PÉTER

Responsible for duplication: works manager Mária KOVÁCS

Number of copies printed: 200

Put to the Press on December 4, 2001 Number of permission: TU 02-01-ME

 $HU\ ISSN\ 1586-2070$

A Short History of the Publications of the University of Miskolc

The University of Miskolc (Hungary) is an important center of research in Central Europe. Its parent university was founded by the Empress Maria Teresia in Selmecbánya (today Banska Štiavnica, Slovakia) in 1735. After the first World War the legal predecessor of the University of Miskolc moved to Sopron (Hungary) where, in 1929, it started the series of university publications with the title Publications of the Mining and Metallurgical Division of the Hungarian Academy of Mining and Forestry Engineering (Volumes I.-VI.). From 1934 to 1947 the Institution had the name Faculty of Mining, Metallurgical and Forestry Engineering of the József Nádor University of Technology and Economic Sciences at Sopron. Accordingly, the publications were given the title Publications of the Mining and Metallurgical Engineering Division (Volumes VII.-XVI.). For the last volume before 1950 – due to a further change in the name of the Institution – Technical University, Faculties of Mining, Metallurgical and Forestry Engineering, Publications of the Mining and Metallurgical Divisions was the title.

For some years after 1950 the Publications were temporarily suspended.

After the foundation of the Mechanical Engineering Faculty in Miskolc in 1949 and the movement of the Sopron Mining and Metallurgical Faculties to Miskolc, the Publications restarted with the general title *Publications of the Technical University of Heavy Industry* in 1955. Four new series - Series A (Mining), Series B (Metallurgy), Series C (Machinery) and Series D (Natural Sciences) - were founded in 1976. These came out both in foreign languages (English, German and Russian) and in Hungarian.

In 1990, right after the foundation of some new faculties, the university was renamed to University of Miskolc. At the same time the structure of the Publications was reorganized so that it could follow the faculty structure. Accordingly three new series were established: Series E (Legal Sciences), Series F (Economic Sciences) and Series G (Humanities and Social Sciences). The seven series are formed by some periodicals and such publications which come out with various frequencies.

Papers on computational and applied mechanics were published in the

Publications of the University of Miskolc, Series D, Natural Sciences.

This series was given the name Natural Sciences, Mathematics in 1995. The name change reflects the fact that most of the papers published in the journal are of mathematical nature though papers on mechanics also come out.

The series

Publications of the University of Miskolc, Series C, Fundamental Engineering Sciences

founded in 1995 also published papers on mechanical issues. The present journal, which is published with the support of the Faculty of Mechanical Engineering as a member of the Series C (Machinery), is the legal successor of the above journal.



Journal of Computational and Applied Mechanics

Volume 2, Number 2 (2001)

Contents

Contributed Papers

Heon Meen BAE, László BARANYI, Mizuyasu KOIDE, Tsutomu TAKAHASHI and Masataka SHIRAKASI: Suppression of Kármán vortex excitation of a circular cylinder by a second cylinder set downstream in	
	175–188
István ECSEDI: Relations for the torsion of nonhomogeneous cylindrical bars	189–194
Akbar Khodaparast HAGHI: Simultaneous moisture and heat transfer in porous system	195–204
Imre KOZÁK: Time rates of tensors in continuum mechanics under arbitrary time dependent transformations, Part I. Material time rates	205-221
Enno SAKS and Mati HEINLOO: Stresses and displacements in a semidigger mouldboard and a ploughshare	223-236
György SZEIDL: Boundary integral equations for plane problems in terms of stress functions of order one	237–261
Vasyl VIHAK and Andriy RYCHAHIVSKYY: Bounded solutions of plane elasticity problems in a semi-plane	263-272
Classroom Note	
Ji-Huan HE: A Lagrangian for the large deflections of a rhombic plate	273-277